Characterization of High-Affinity Nitrate and Nitrite Transporters in *Arabidopsis thaliana*

by

Zorica Kotur

BSc. University of Novi Sad, Serbia, 2002

MSc. University of Hannover, Germany, 2005

A THESIS SUBMITTED IN PARTIAL FULLFILMENT OF

THE REQUIREMENTS FOR THE DEGREE OF

DOCTOR OF PHILOSOPHY

in

The Faculty of Graduate and Postdoctoral Studies

(Botany)

THE UNIVERSITY OF BRITISH COLUMBIA

(Vancouver)

September 2013

Abstract

Nitrite is a potential nitrogen source in the environment. Algae and fungi posses nitrite-specific transporters, whereas plant counterparts have not been identified. Because nitrate transporters can take up nitrite, I used nitrate uptake-defective Arabidopsis mutants to eliminate the masking effect of nitrate transporters and measured $^{13}NO_2^-$ influx to characterize nitrite uptake. The *Atnar2.1-2* mutant, lacking a functional high-affinity nitrate transport system, is capable of nitrite influx that is constitutive and thermodynamically active. This provides strong evidence for a nitrite-specific transporter that enables *Atnar2.1-2* mutants, which are incapable of sustained growth on low nitrate, to maintain significant growth on low nitrite.

To accommodate the variable nitrate concentration in soil solution, plants have high- and low-affinity uptake systems (HATS and LATS, respectively). AtNRT2.1, the major inducible HATS transporter, requires expression of a second polypeptide AtNAR2.1 to be functional. Immunological and transient protoplast expression methods revealed that an intact two-component complex of AtNRT2.1 and AtNAR2.1 is localized in the plasma membrane, has a size of ~150kDa, and half-life of 35h. Based on the absence of monomeric AtNRT2.1 in protein isolates, and lack of the oligomer in mutants of *NRT2.1* or *NAR2.1,* I propose that this complex, rather than monomeric AtNRT2.1, is the form active in inducible HATS nitrate transport. After the large central cytosolic loop from the *Aspergillus nidulans* iHATS (NRTA) was introduced into AtNRT2.1, instead of its smaller loop, interaction with AtNAR2.1 was abolished. This observation shows that the central loop of AtNRT2.1 is required for interaction with AtNAR2.1.

The Arabidopsis NRT2 family has 6 other members in addition to AtNRT2.1. By using heterologous expression in the yeast-two-hybrid system, *Xenopus* oocytes and leaf protoplasts, I have shown that, with the exception of AtNRT2.7, all NRT2s interact with AtNAR2.1 and are capable of nitrate transport.

Plants also have a constitutive high-affinity transport system (cHATS) with proposed role of upregulation of many nitrate-inducible genes, including *AtNRT2.1*. For the first time in

plants, a gene required for cHATS was isolated. *Atnrt2.5* mutants exhibit ~60% reduction of the cHATS activity compared to WT plants at low nitrate concentrations, suggesting that *AtNRT2.5* encodes the saturable cHATS transporter.

Preface

Chapter 1 was published entirely in the New Phytologist.
Zorica Kotur, Yaeesh M. Siddiqi and Anthony D.M. Glass (2013). Characterization of nitrite uptake in *Arabidopsis thaliana* - evidence for a nitrite-specific transporter. New Phytologist (DOI: 10.1111/nph.12358). Dr. Yaeesh Siddiqi and Dr Anthony Glass helped with radioactive N processing.

Chapter 2 was published except for the work presented in Table 2-4, Figures 2-9 and 2-10.
Zhenhua Yong, Zorica Kotur and Anthony D.M. Glass (2010). Characterization of an intact two-component high-affinity nitrate transporter from Arabidopsis roots. Plant Journal 63: 739-748.
Dr Zhenhua Yong has produced Western blots in Figures 2-3 to 2-7.

Chapter 3 was published entirely in the New Phytologist.
Zorica Kotur, Nenah Mackenzie, Sunita Ramesh, Steve D Tyerman, Brent N Kaiser, Anthony D.M. Glass (2012). Nitrate transport capacity of the *Arabidopsis thaliana* NRT2 family members and their interactions with AtNAR2.1. New Phytologist 194: 724-731.
Nenah Mackenzie measured isotope ratio on Isotope Ratio Mass Spectrometer, and Sunita Ramesh harvested oocytes from *Xenopus laevis*.

For **Chapter 4** Dr Sheila Unkles and Dr Ye Wang made NRT2.1 with modified loop from *Aspergillus nidulans*, and transformed *A. nidulans* double Δ*nrta nrtb* mutant with that construct, while Dr Mamoru Okamoto prepared pATP and pATP2. Figure 4-1 adapted from Unkles *et al.* (2001) with permission.

All experiments presented in the **Chapter 5** were performed by me, while Dr Anthony Glass helped with the radioactive N processing.

Table of contents

List of tables

List of figures

Abbreviations

ABRC- Arabidopsis Biological Resource Center

ANOVA- analysis of variance

ATP- adenosine tri phosphate

BN-PAGE- blue native polyacrylamide gel electrophoresis

bp- base pairs

CCCP- carbonyl cyanide m-chlorophenyl hydrazone

cHATS- constitutive high affinity transport system

cLATS- constitutive low affinity transport system

cRNA- complementary ribonucleic acid

DW- dry weight

ECL- enhanced chemiluminescence

EDTA- ethylenediaminetetraacetic acid

EGTA- ethylene glycol tetraacetic acid

EMS- ethyl methanesulfonate

ER- endoplasmic reticulum

FNT- formate nitrite transporters

FW- fresh weight

GOGAT- glutamine-2-oxoglutarate aminotransferase

GS- glutamine synthetase

HATS- high affinity transport system

HPLC- high pressure liquid chromatography

iHATS- inducible high affinity transport system

iLATS- inducible low affinity transport system

kDa- kilo Dalton

Km- nitrate or nitrite concentration required to reach ½ of Vmax

LATS- low affinity transport system

MES- 2-(N-morpholino)ethanesulfonic acid

MFS- major facilitator superfamily

MS- Murashige and Skoog

NASC- Nottingham Arabidopsis Stock Centre

NiR- nitrite reductase

NNP- nitrate nitrite porters

NR- nitrate reductase

OSMO- osmotic medium

PEG- poly ethylene glycol

PM- plasma membrane

PVDF- polyvinylidene difluoride

PVP- polyvinylpyrrolidone

rpm- revolutions per minute

RT- reverse transcriptase

SD- standard deviation

SDS-PAGE- sodium dodecyl sulfate polyacrylamide gel electrophoresis

SE- standard error

SHAM- salicylhydroxamic acid

TCA- trichloroacetic acid

TMR- transmembrane region

TRIS- tris(hydroxymethyl) aminomethane

v/v- volume per volume

Vmax- maximum nitrate or nitrite uptake rate

w/v- weight per volume

WT- wild type

YFP- yellow fluorescent protein

Y2H- yeast two-hybrid

Acknowledgements

I would like to express enormous gratitude to my supervisor Dr Anthony D. M. Glass for his help in all aspects of my research, guidance and patience during my PhD work in his lab. I would also like to thank my supervisory committee, Dr Beverley R. Green and Dr Lacey A. Samuels for their help, revisions and patience. Furthermore, I would like to thank Dr Brent N. Kaiser and Dr Steve D. Tyerman, and their lab members from the University of Adelaide for accepting me in their labs for 2 months and helping with the work on *Xenopus* oocytes. I would also like to thank Dr Yaeesh M. Siddiqi from UBC for his helpful advice and assistance with ^{13}N work. I would also like to thank Dr Sheila Unkles for her help with *Aspergillus nidulans* work. I gratefully acknowledge the assistance of the University of British Columbia (TRIUMF) cyclotron facility for provision of ^{13}N. In addition, I would like to thank Arabidopsis Biological Resource Center and John Innes Centre for provision of pSAT and pGreen vectors, respectively, and to UBC BioImaging facility for assistance with fluorescence microscopy. I would like to thank ABRC, NASC and GABI-KAT for provision of Arabidopsis T-DNA insertional mutants. Sincere gratitude goes to Dr. Nelly Panté lab at UBC for assistance with *Xenopus* oocytes work.

I would gratefully like to acknowledge financial support from my supervisor Anthony DM Glass (NSERC Grant), University of British Columbia graduate fellowship, UBC research travel award and Australian Research Council Linkage Grant to Dr Brent N. Kaiser.

I would like to thank the kind and helpful members of ADM Glass's, AL Samuels', BR Green's, CJ Douglas', GO Wasteneyes' and ML Berbee's labs.

I would like to thank all the staff of the Department of Botany for making my experience at UBC productive and enjoyable.

I would like to thank my family for their understanding and adjusting to the graduate student way of life.

Introduction

Nitrogen importance and availability

Nitrogen (N) is a macro nutrient essential for plant cells as a constituent of cell building blocks such as amino acids and nucleic acids. Although 78% of the atmosphere is elemental nitrogen (N_2), it cannot be used by plants. Atmospheric N is made available for plants by N_2-fixing bacteria and symbiotic rhizobacteria that convert N_2 to ammonia, and as fertilizers produced using the industrial Haber-Bosch process. Most of the N in soil (>90 %) is in organic form that has to be decomposed into plant-available N (Haynes, 1986). Available forms that are readily taken up by plant roots are amino acids, ammonium, nitrate and nitrite. Ammonium and amino acids accumulate in rice paddies (Sahrawat, 2005; Satoshi, 2011), forest soils (Schimel and Chapin, 1996; Hofmockel *et al.*, 2010; Metcalfe *et al.*, 2011) and cold arctic soils (Nadelhoffer *et al.*, 1992; Henry and Jefferies, 2002). Nitrate is the major inorganic form on most aerated warm cultivated soils, because ammonium coming from fertilizers is quickly oxidized to nitrate by nitrification (Glass *et al.*, 1999). Nitrate ions are not well adsorbed to soil particles due to their negative charge, and are, therefore, prone to leaching. In addition, some nitrate is lost due to dentrification under low oxygen conditions (reviewed in Cameron *et al.*, 2013). Modern agricultural production relies on excessive N-fertilizer use. This N is used with low efficiency because a significant portion of the applied fertilizers is lost from the soil due to leaching and denitrification (reviewed in Glass, 2003; Cameron *et al.*, 2013), leading to an increase in world N fertilizer consumption of approximately 10 times over the past few decades. N-fertilizer consumption reached more than 100 million tonnes in 2010 (Fig. 1). Meanwhile consumption of phosphate and potassium fertilizers increased only 3 to 4 fold (Fig. 1). This excessive use of N fertilizers leads to numerous environmental issues like pollution and eutrophication of water bodies, contamination of underground water and green house gas emissions (Adetunji, 1994; Boesch *et al.*, 1997; Rouse *et al.*, 1999; Liu and Zhang, 2011; Cameron *et al.*, 2013).

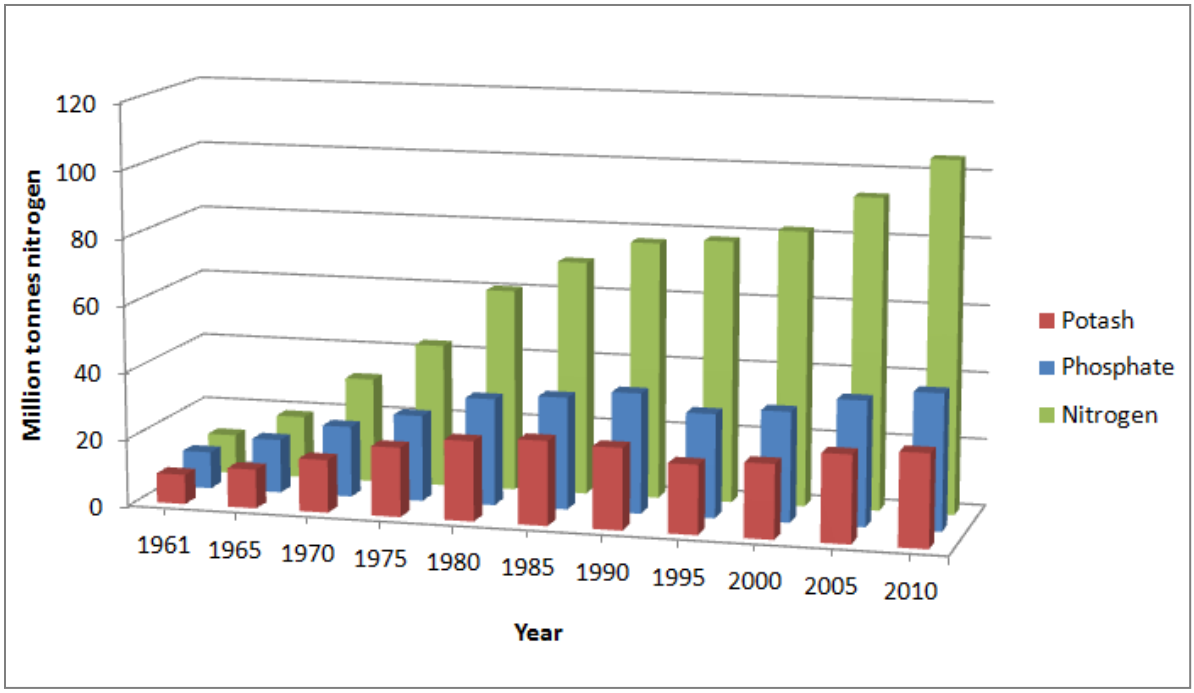

Figure 1. Fertilizer consumption in the world from 1961 to 2010.
Graph plotted based on statistics from the International Fertilizer Industry Association (IFA) database (http://www.fertilizer.org/ifa/HomePage/STATISTICS).

Although soil nitrite concentrations are typically low compared to nitrate, under some conditions they may become elevated (Riley *et al.*, 2001). NO_2^- is produced as a result of the oxidation of NH_4^+ by bacteria such as *Nitrosomonas* and accumulates in aerated soil at elevated pH due to disruption of the second step of nitrification (Chapman and Liebig, 1952). It is also produced from nitrate in soils and aquatic systems through plant and microbial reduction of nitrate by the enzyme nitrate reductase. While the reduction of nitrate to nitrite can occur anaerobically, the large energy requirement for nitrite reduction to ammonium results in disruption of this second step of nitrate assimilation whenever environmental conditions limit metabolism (Broadbent and Clark, 1965). Thus, for example, low Fe availability, and low light may lead to nitrate reduction and subsequent nitrite excretion by phytoplankton (Collos, 1982). Significant nitrite can also accumulate at lower pH values in water-logged, poorly aerated soils (Lee, 1979). For example, anoxic conditions in rice paddy fields often cause significant increases in NO_2^- concentration, as a consequence of incomplete denitrification (Samater *et al.*, 1998).

Nitrate uptake - physiological aspects

Nitrate fluctuates greatly over a wide range of concentrations. A study of 77 world-wide agricultural soils revealed huge variations in nitrate concentration in the soil solution, from micromolar to 50 mM (Wolt, 1994). Plants have developed different transport systems that effectively adapt to changes of N availability in the environment. Uptake of nitrate at high external concentrations is accomplished mainly by Low Affinity Transport Systems (LATS), while at concentrations below 0.5 mM nitrate uptake is achieved through High Affinity Transport Systems (HATS) (reviewed in Crawford and Glass, 1998; Forde, 2000; Wang *et al.*, 2012). Evidence from numerous physiological studies suggests that LATS is linear in plants, as shown in tobacco cell suspensions (Guy *et al.*, 1988), barely roots (Siddiqi *et al.*, 1989; Aslam *et al.*, 1992), roots of spruce (Kronzucker *et al.*, 1995), Arabidopsis (Touraine and Glass, 1997) and *Camellia sinensis* (Yang *et al.*, 2013). It was shown in Arabidopsis that LATS has two components: constitutive and inducible LATS (Tsay *et al.*, 1993; Huang *et al.*, 1999). Based on physiological evidence, it is accepted that the HATS system also has two components: inducible and constitutive, iHATS and cHATS, respectively (reviewed in Glass and Siddiqi, 1995; Crawford and Glass, 1998; Wang *et al.*, 2012). The latter transport system is present in plants even before they have been exposed to external nitrate. cHATS in barley was measured using a sensitive $^{13}NO_3^-$ technique in N-starved plants by Siddiqi *et al.* (1990). The authors found that the nitrate fluxes were saturable at 0.2 mM KNO_3, exhibiting 27 fold lower Vmax and 4 fold lower Km than plants induced with nitrate, therefore iHATS has a much higher capacity and lower affinity for nitrate than the cHATS. Both cHATS and iHATS are induced by nitrate, although the uptake rate due to iHATS is induced to a much greater extent than cHATS uptake (Siddiqi *et al.*, 1990). Similarly in spruce, Kronzucker *et al.* (1995) found that cHATS nitrate influx was 4 times lower than nitrate influx in induced plants. Both inducible and constitutive high affinity nitrate transport follows Michaelis-Menten saturable kinetics (Doddema and Telkamp, 1979; Siddiqi *et al.*, 1989; Aslam *et al.*, 1992; Kronzucker *et al.*, 1995). Based on the evidence of transient plasma membrane depolarization after exposure to nitrate, nitrate uptake into roots is considered to be a metabolically active process of symport where 2 protons and one nitrate ion are transported across the membrane against the electrochemical gradient (Crawford and Glass, 1998; Fig. 2).

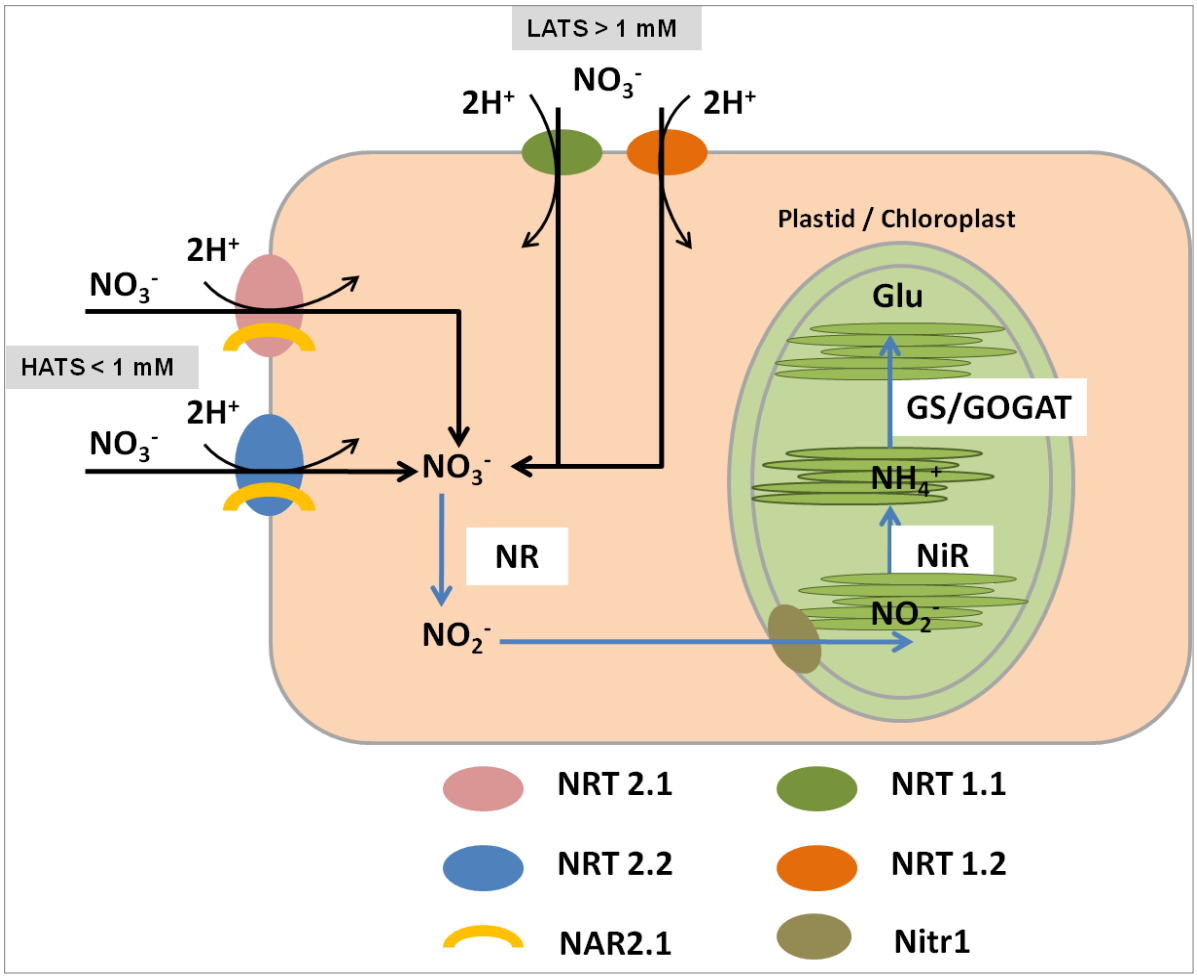

Figure 2. Schematic presentation of the major *Arabidopsis thaliana* nitrate transporters and assimilatory enzymes. HATS: high affinity transport system; LATS: low affinity transport system; NR: nitrate reductase; NiR: nitrite reductase; GS/GOGAT: glutamine synthetase/ glutamine-2-oxoglutarate aminotransferase.

Nitrate uptake – molecular aspects

The first identified eukaryotic gene involved in nitrate transport at low external concentration was *NRTA* (*CRNA*) from *Aspergillus nidulans* (Unkles *et al.*, 1991). Following *NRTA*, other genes encoding eukaryotic HATS nitrate transporters were cloned from *Chlamydomonas reinhardtii* (Quesada *et al.*, 1994), barley (Trueman *et al.*, 1997), *Nicotiana plumbaginofolia* (Quesada *et al.*, 1997; Krapp *et al.*, 1998), soybean (Amarasinghe *et al.*, 1998), *A. thaliana* (Filleur and Daniel-Vedele, 1999; Zhuo *et al.*, 1999), tomato (Ono *et al.*, 2000), rice (Araki and Hasegawa, 2006; Miller *et al.*, 2007; Cai *et al.*, 2008), wheat (Zhao *et al.*, 2004; Cai *et*

al., 2007; Yin *et al.*, 2007), *Physcomitrella patens* (Tsujimoto *et al.*, 2007) and *Lotus japonicus* (Criscuolo *et al.*, 2012). iHATS transport in Arabidopsis is achieved through the activity of *AtNRT2.1* and *AtNRT2.2* (Filleur *et al.*, 2001; Li *et al.*, 2007; Fig. 2). Addition of nitrate to the external solution induces expression of *AtNRT2.1* and *AtNRT2.2* in previously N-starved plants, increasing mRNA levels 6 and 4 fold, respectively (Okamoto *et al.*, 2003). In addition to these Major Facilitator Superfamily (MFS) transporters, it was first shown in *C. reinhardtii* that expression of a non-related, small protein NAR2.1 is required for functional iHATS nitrate uptake (Quesada *et al.*, 1994; Zhou *et al.*, 2000a). The first higher plant orthologs were cloned from barley by Tong *et al.* (2005). The authors demonstrated that HvNRT2.1 required co-expression of a *NAR2*-like gene in *Xenopus* oocytes for functional nitrate transport (Tong *et al.*, 2005). Function of the Arabidopsis orthologue was characterized later by the use of knock out mutants of the *AtNAR2.1* (also named *AtNRT3.1*) by Okamoto *et al.* (2006), Orsel *et al.* (2006) and Wirth *et al.* (2007). All *nar2* mutants showed very limited growth on low nitrate media, while LATS nitrate uptake was unaffected. In addition, Wirth *et al.* (2007) failed to detect AtNRT2.1 protein in the membrane of *Atnar2.1* mutants, even though the *AtNRT2.1* gene was expressed at high level. A two-component nitrate uptake system was also described in rice, where a knock down line *Osnar2.1* had notably impaired nitrate transport, and nitrate uptake into *Xenopus* oocytes. The authors demonstrated that OsNAR2.1 interacts with OsNRT2.1, OsNRT2.2 and OsNRT2.3a (Ming *et al.*, 2011).

Low-affinity nitrate transport in plants is encoded by *NRT1* genes, and in *Arabidopsis thaliana* NRT1.1 and NRT1.2 are the major contributors to inducible LATS and constitutive LATS, respectively (Tsay *et al.*, 1993; Huang *et al.*, 1999; Fig. 2).

Regulation of nitrate uptake

Once in the root cell, nitrate can be reduced to nitrite (by the enzyme nitrate reductase- NR) and ammonium (by the enzyme nitrite reductase- NiR), which is quickly assimilated into amino acids by glutamine synthetase and glutamine-2-oxoglutarate aminotransferase (GS/ GOGAT cycle) (Lea *et al.*, 1990). Depending on the external concentration, nitrate is often loaded into xylem and assimilated in leaves, or stored in vacuoles (Andrews, 1986; Cooper and Clarkson, 1989; Grignon *et al.*, 2001). Nitrate uptake is a highly regulated process,

where nitrate serves as a signal that increases the expression of nitrate assimilation genes when plants are exposed to N-limiting conditions (discussed above), but under conditions of extended high N-availability, nitrate uptake rate is quickly down-regulated, as determined by plant N demand (Touraine and Gojon, 2001). Split-root experiments demonstrated that the uptake rate is largely regulated by signals from leaves, as exposing half of the root to low nitrate increases uptake in the other half of the root that is exposed to high nitrate (Laine *et al.*, 1998; Cerezo *et al.*, 2001; Gansel *et al.*, 2001). In addition, uptake of nitrate is subject to diurnal regulation by photosynthetic products that stimulate nitrate uptake (Clement *et al.*, 1978; Delhon *et al.*, 1995; Lejay *et al.*, 2003). Expression of nitrate HATS is repressed by exposure to ammonium and some amino acids (Lee and Drew, 1989; Zhuo *et al.*, 1999; Vidmar *et al.*, 2000; Nazoa *et al.*, 2003). Kronzucker *et al.* (1999) found that provision of ammonium decreased influx and increased efflux of nitrate in barley within minutes of ammonium supply. However many studies have documented that treatment with the GS inhibitor MSX blocked down-regulation of influx, suggesting that it is the end-product of ammonium assimilation (probably glutamine), not ammonium itself that is responsible for down-regulating influx, at least at the transcriptional level (Lee and Rudge, 1986; Lee *et al.*, 1992; Muller and Touraine, 1992; Rodgers and Barneix, 1993). The mechanisms underlying this feedback repression of nitrate uptake are not clear, and are the subject of ongoing research (reviewed in Gojon *et al.*, 2009). Girin *et al.* (2007) have identified a 150 bp- cis element located upstream of the *AtNRT2.1* TATA box, required for gene up-regulation by nitrate and down-regulation by reduced N forms. In a recent study monitoring genome-wide expression responses of Arabidopsis genes shortly after exposure to nitrate, the authors found that the first nitrate response includes genes involved in translation, while the changing expression of the genes involved in N metabolism was detected after 9 min of nitrate treatment, and genes responding at later time points were part of hormone signaling pathways (Krouk *et al.*, 2010).

Nitrite uptake – physiological and molecular aspects

The presence of NO_2^- in nutrient solution can have adverse effects on plant growth (Phipps and Cornforth, 1970; Lee, 1979; Samater *et al.*, 1998; Zsoldos *et al.*, 2001; Ezzine *et al.*, 2011). Its toxicity is, however, more pronounced at high concentrations and low pH

(Bancroft *et al.*, 1979), possibly as a result of free nitrous acid (the conjugate acid of NO_2^-) permeation, in addition to plant NO_2^- anion uptake (Zentmyer and Bingham, 1956). However, at more modest concentrations (<1 mM), it has been reported on numerous occasions that NO_2^- can also be taken up as an alternative N source if available in soil solution. Criddle *et al.* (1988) reported that wheat (*Triticum aestivum*) seedlings take up significant amount of nitrite, and Zsoldos *et al.* (1993) found that wheat seedlings take up NO_2^- faster than NO_3^-. Brinkhuis *et al.* (1989) measured high rates of NO_2^- uptake in the brown seaweed *Laminaria japonica*, with a very strong initial rate that stabilizes after 1 h. In summary, NO_2^- uptake has been examined in many species of plants, algae, fungi and bacteria.

Nitrite is an intermediate in the nitrate assimilation pathway, being reduced to NH_4^+ by nitrite reductase activity in plastids (Crawford, 1995). Given that nitrate reduction by nitrate reductase occurs in the cytosol, there is therefore an obvious requirement for nitrite transport into the chloroplasts. Recent findings indicate the existence of nitrite-specific transporters in chloroplasts of *Arabidopsis thaliana* and *Cucumis sativa* (Sustiprijatno *et al.*, 2006; Sugiura *et al.*, 2007; Ferrario-Mery *et al.*, 2008), and in chloroplasts of *Chlamydomonas reinhardtii* (Rexach *et al.*, 2000; Mariscal *et al.*, 2004).

The uptake of nitrite from the external environment may occur through nitrate–nitrite bispecific transporters, examples of which are NRT2.1/NAR2 in *C. reinhardtii* (Galvan *et al.*, 1996), NARU in *Escherichia.coli* (Jia *et al.*, 2009), NRTA and NRTB in *Aspergillus nidulans* (Wang *et al.*, 2008), or by NO_2^--specific transporters as reported in *C. reinhardtii* (Galvan *et al.*, 1996), *E. coli* (Jia and Cole, 2005; Jia *et al.*, 2009), *Hansenula polymorpha* (Serrani and Berardi, 2005), *A. nidulans* (Wang *et al.*, 2008; Unkles *et al.*, 2011), *Neurospora crassa* (Gao-Rubinelli and Marzluf, 2004) and *Nostoc* ANTH (Bhattacharya *et al.*, 2002). Nitrite transporters in *A. nidulans* NitA and *E.coli* NirC belong to a family of formate-nitrite transporters. Nitrite transport system III in *C. reinhardtii* is coded by the *NRT2.3* gene, an MFS member, and functions independently of the *NAR2-like* gene which is essential for nitrate uptake by NRT2.1 or NRT2.2 (Rexach *et al.*, 1999; Fernandez and Galvan, 2008).

Research Hypotheses

Based on the current state of knowledge on the nitrate and nitrite transport in plants, I have formulated and pursued the following hypotheses and objectives:

1. Nitrite-specific transporters have been described in fungi and algae, but solid evidence of higher plant nitrite-specific transporters is lacking. It is hard to distinguish between nitrite transport by nitrate transporters and transport by distinct nitrite transporters. I have made use of *Arabidopsis thaliana* knock-out mutants of the major nitrate transporter genes in order to separate nitrite from nitrate uptake, to test the hypothesis that nitrite transport into roots is mediated by both nitrate-nitrite bi-specific transporters as well as a nitrite-specific transporter.

2. It well established that nitrate iHATS in plant relies on a two-component system involving AtNRT2.1 and AtNAR2.1 in *Arabidopsis thaliana*. The nature of their interaction is unknown. Using native protein gel separation and immuno-blotting techniques, I have sought to isolate and characterize a putative molecular complex of AtNRT2.1 and AtNAR2.1 from plasma membranes of Arabidopsis roots.

3. There are seven members of the Arabidopsis *NRT2* family of transporters. *NRT2.1* and *NRT2.2* are well-characterized as nitrate transporters, and their interaction with AtNAR2.1 was demonstrated in plants and *Xenopus* oocytes. Using heterologous expression of all *NRT2* genes together with *NAR2.1* in yeast and *Xenopus* oocytes, as well as expression in Arabidopsis protoplasts, I have evaluated the hypothesis that all members of the *AtNRT2* family are capable of nitrate transport and that this transport depends on interaction with *NAR2.1*.

4. The physiological function of the AtNRT2.5 transporter is not known. However, while evaluating hypothesis 3, it was noted that AtNRT2.5 transport was very strongly stimulated by co-expressing AtNRT2.5 with NAR2.1. By the use of Arabidopsis T-DNA insertion mutants disrupted in *AtNRT2.5,* I have evaluated the flux characteristics of the corresponding transporter to determine the contribution of AtNRT2.5 to nitrate HATS under nitrate-induced and un-induced conditions.

5. *Aspergillus nidulans* iHATS nitrate transporter NRTA is a homolog of Arabidopsis NRT2.1, but it does not require a NAR2-like protein for function. A major difference between the two proteins is based in the size of the central cytosolic loop. The AnNRTA loop is 4 times larger than that of AtNRT2.1. The importance of the cytosolic loop for transport function of the NRT proteins was evaluated by measurement of nitrate influx in *A. nidulans* expressing AtNRT2.1 with loop modifications.

Chapter 1. Characterization of nitrite uptake in Arabidopsis-evidence for a nitrite-specific transporter

Background

Nitrite (NO_2^-) is a form of inorganic nitrogen (N) that is widely available in soil and aquatic environments under specific conditions (described in Introduction). It accumulates in aerated soil at elevated pH due to disruption of the second step of nitrification (Lee, 1979), and under environmental conditions that limit metabolism (water-logged soils). Morard *et al.* (2004) reported that tomato plants grown under anaerobic conditions are able to utilize nitrate for "nitrate respiration" and excrete nitrite. NO_2^- is also abundant in oceans at the base of the euphotic zone where it accumulates as a result of nitrification during summer and excretion by phytoplankton during winter (Meeder *et al.*, 2012). Its concentration in oceans normally ranges from 10 to 400 nM, but can reach up to 4500 nM (Lomas and Lipschultz, 2006). Nitrite availability in soil varies greatly as influenced by conditions mentioned above. Burns *et al.* (1995) reported nitrite concentrations in fertilized grassland soil in Ireland ranging from 0 to 2.7 µg N g^{-1}. Likewise, in agricultural soil in Kansas significant amounts of nitrite were found near ground water amounting to 0.16 mM (Jones and Schwab, 1993). Uwah *et al.* (2009) reported above 200 µg g^{-1} in soil samples from two areas in Nigeria, while nitrite ranged from 0.01 to 0.14 mM in Santiago del Estero, Argentina, soil samples (Lopez Pasquali *et al.*, 2007).

The presence of NO_2^- in nutrient solution can have adverse effects on plant growth (Phipps and Cornforth, 1970; Lee, 1979; Samater *et al.*, 1998; Zsoldos *et al.*, 2001; Ezzine *et al.*, 2011). However, at more modest concentrations, it has often been reported that NO_2^- can be taken up as an alternative N source (see Introduction).

Nitrite uptake by higher plants has been investigated extensively, but results are inconclusive regarding the existence of nitrite-specific transporters. Ibarlucea *et al.* (1983) found that nitrite uptake in barley (*Hordeum vulgare*) seedlings was inducible, and followed Michaelis-Menten kinetics. Jackson *et al.* (1974b) reported that addition of nitrite inhibited induction of nitrate uptake in *Triticum vulgare*, whereas the reciprocal effect on nitrite uptake was not elicited by nitrate, suggesting the possibility of a separate nitrite transport system. Similarly,

De La Haba *et al.* (1990) showed that ammonium inhibited uptake of nitrate, but had no effect on the uptake of nitrite in sunflower (*Helianthus annuus*). Other reports, however, support the idea of a dual nitrate/nitrite transport system because the two ions have similar properties and research undertaken with barley showed that nitrate and nitrite ions mutually inhibit uptake competitively (Aslam, *et al.*, 1992; Siddiqi, *et al.*, 1992).

Objective

There is no conclusive evidence of a nitrite-specific plasma membrane transporter in higher plants. It is generally postulated that nitrite uses nitrate transporters belonging to the MFS nitrate-nitrite porter family, such as AtNRT2.1 in Arabidopsis. The availability of several Arabidopsis mutants defective in high-affinity nitrate transport has enabled me to characterize nitrite uptake in Arabidopsis using $^{13}NO_2^-$ to measure nitrite influx. This approach allowed me to clearly distinguish between nitrate and nitrite uptake, and provide evidence for the existence of a nitrite-specific transporter in roots of Arabidopsis.

Materials and methods

Plant material and growth conditions

*Arabidopsis thalian*a (L.) Heynh. plants (WT ecotype Wassilewskija, and knock-out mutant lines *Atnrt2.1* (Salk_141712), *Atnrt2.2* (Salk_043543) and *Atnrt2.1-nrt2.2* (Salk_035429) (Li *et al.*, 2007), and *Atnar2.1-2* (Okamoto *et al.*, 2006) were grown hydroponically under non-sterile conditions as described previously (Zhuo *et al.*, 1999; Okamoto *et al.*, 2003). Three to four seeds were sown into 1.5 cm plastic cylinders filled with acid-washed sand and fitted into floating styrofoam platforms. The platforms floated in plastic containers filled with 7 L of nutrient solution (1 mM KH_2PO_4, 0.5 mM $MgSO_4$, 0.25 mM $CaSO_4$, 20 µM Fe-EDTA, 25 µM H_3BO_3, 2 µM $ZnSO_4$, 2 µM $MnSO_4$, 0.5 µM $CuSO_4$, 0.5 µM Na_2MoO_4, and 1 mM NH_4NO_3). Solutions were aerated continuously by means of aquarium stones and the pH of solutions was maintained around 6 by adding powdered $CaCO_3$. Nutrient solutions were completely replaced once a week. Plants were grown for four weeks, and then deprived of nitrogen for the fifth week. To induce iHATS plants were next transferred to solution containing 1 mM KNO_3 or KNO_2 for 6 hours. Growth conditions in the growth room were 8 h of light (100 µmol m^{-2} s^{-1} at plant level) and 16 h of dark, at corresponding temperatures of

24°C and 22°C, respectively, and a relative humidity ~70%. In the experiment where pH effects on nitrite uptake were measured, 5mM 2-(N-morpholino) ethanesulfonic acid (MES) was used as a buffering agent. For growth on MS agar plates, Arabidopsis seeds were sterilized in 1% bleach (plus 0.01% Tween 20) for 15 min, and left for 3 days in sterile water at 4°C to synchronize germination. Seeds were then sown on half strength solid N-free MS salts media (pH=6, 0.8 % w/v agar), supplemented with 0.25 mM KNO_2 or 0.25 mM KNO_3. The plates were kept in a vertical position and plants grown for 2.5 weeks under the same conditions as described above.

$^{13}NO_3^-$ and $^{13}NO_2^-$ isotope synthesis

^{13}N-nitrate was generated by proton irradiation of water at the cyclotron facility (Tri-University Meson Facility), University of British Columbia as described earlier (Siddiqi *et al.*, 1989). This radioactive nitrate was used as the source material to generate ^{13}nitrite following the method of McElfresh and colleagues (1979). Trace quantities of hydrogen peroxide, added to the water target to promote an oxidizing environment for the generation of $^{13}NO_3^-$, were removed by the addition of 1 ml commercial catalase enzyme (2 g/l) (Sigma Aldrich, USA) since the reduction of nitrate to nitrite by a cadmium column is compromised by the presence of hydrogen peroxide. ^{13}Nitrate was then passed twice through the cadmium column prepared according to McElfresh and colleagues (1979). This procedure generated >96% ^{13}N-nitrite as determined by passing the column eluate through an HPLC with a gamma detector in series with the column. Passage through the column resulted in replacement of the ^{13}N-nitrate peak by a peak corresponding to ^{13}N-nitrite. After the cadmium reduction, the column eluate was treated with 100 µl 2N KOH and boiled for 2 min to remove any contaminating NH_4^+. pH was brought back to neutral by addition of 10% H_2SO_4 (v/v).

$^{13}NO_2^-$ and $^{13}NO_3^-$ influx measurements

Nitrate influx, using $^{13}NO_3^-$, was measured as described earlier (Zhuo *et al.*, 1999; Okamoto *et al.*, 2003). The basic components of the solution for pre-treatment, influx, and desorption were the same as those of the growth media, except that low concentrations of KNO_3 or KNO_2 replaced NH_4NO_3 (exact concentrations are given in each figure). Prior to measuring ^{13}N influx, plants were pretreated for 5 min with solution containing the same concentration

of nitrate or nitrite as the influx solution, and then transferred for 5 min into the influx solution, which was labelled with ^{13}N. After the influx period, roots were desorbed with non-labelled solution (identical to pre-treatment solution) for 2 min to desorb the radioactive isotope from the apoplast. Plant tissue was immediately harvested, roots were spun at low speed for 20 sec to remove excess solution, and thereafter gamma emission was measured using a gamma-counter (MINAXI Auto-Gamma 5000 series, Packard Instruments). Along with plant tissue samples, samples of influx solutions were counted using the gamma counter, and values used for calculation of ^{13}N content in tissue. Each sample was counted twice to correct for possible ^{18}F contamination. Root tissue was weighed after measuring emission to calculate influx rates.

Temperature coefficient determination and use of metabolic inhibitor

Temperature coefficient (Q_{10}) was determined by incubating 6-week old *Atnar2.1-2* plants in uptake medium, containing 100 µM KNO_2 labeled with ^{13}N-nitrite, at 10 and 23°C, according to standard procedure for 5-min influx measurement, as described above. Q_{10} values were calculated from the equation $Q_{10}=(R2/R1)^{(10/T2-T1)}$, where R1 and R2 are influx rates at 10°C (T1) and 23°C (T2). Detailed protocols are described in Glass *et al.* (1990).

To evaluate the effect of metabolic inhibition on nitrite uptake, 10 µM of the protonophore carbonyl cyanide m-chlorophenyl hydrazone (CCCP) (Sigma Aldrich, USA) was included in the pre-treatment and influx solution containing 100 µM KNO_2. $^{13}NO_2^-$ influx was measured according to the procedure described above.

Statistical analysis

All treatments included at least five replicates, and experiments were repeated at least twice. ANOVA calculations and multiple *t* test comparisons were done using GraphPad Prism 6 program (GraphPad Software Inc., USA). The same program was used for direct fitting of curves using the Michaelis-Menten equation or linear fitting.

Results

Kinetics of nitrite uptake in WT and mutants defective in nitrate transport

We have used WT and previously characterized mutants defective in high-affinity nitrate transport, to examine nitrite uptake in the low concentration (i.e. high-affinity) range. WT

and all mutant genotypes were capable of significant ^{13}N-nitrite influx in this concentration range. WT had the highest influx, while *nrt2.1* mutants showed lower capacities for nitrite uptake (Fig. 1-1); double mutant *Atnrt2.1-nrt2.2* mutant had the lowest influx, followed by *Atnrt2.1*. Direct fit of ^{13}N-nitrite influx data using the Michaelis-Menten equation provided high r^2 values (Table 1-1), and allowed estimation of kinetics parameters Km and Vmax (Table 1-1).

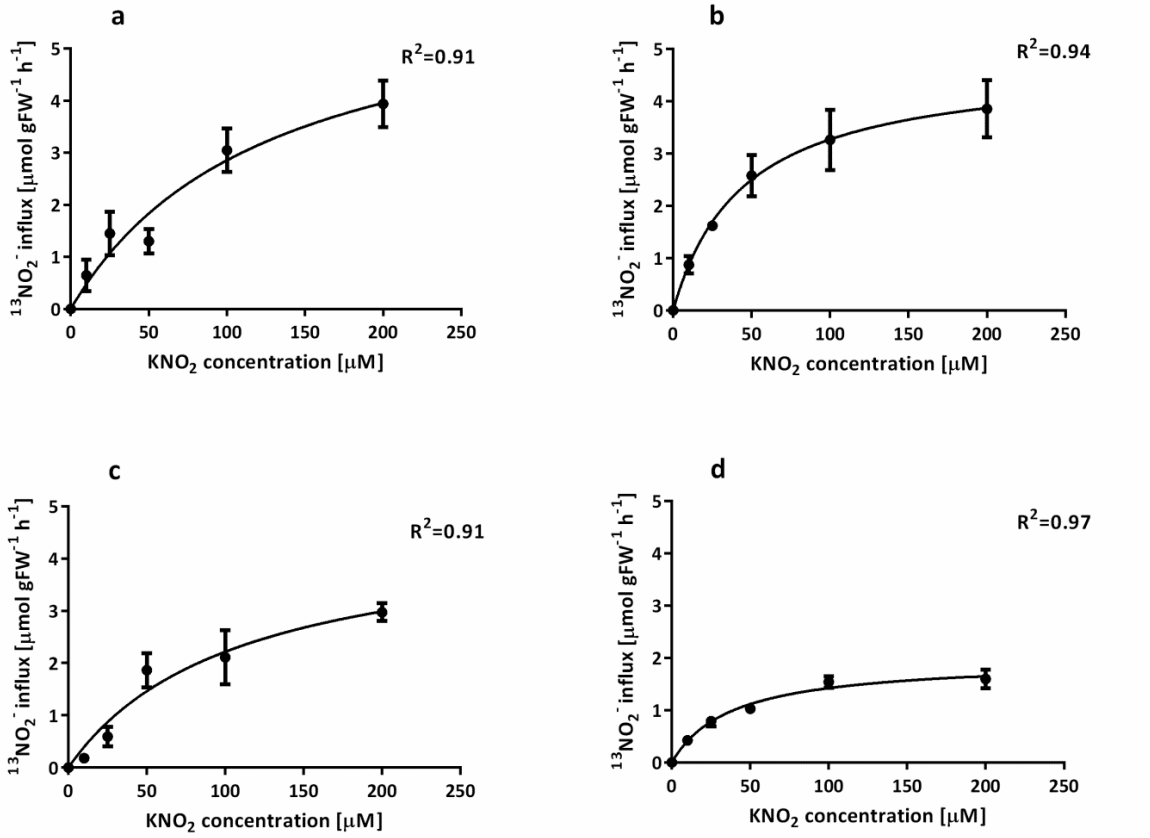

Figure 1-1. $^{13}NO_2^-$ influx at different concentrations of KNO_2, in different genotypes of *Arabidopsis thaliana* a. wild type (WT), b. *Atnrt2.2*, c. *Atnrt2.1*, d. *Atnrt2.1-nrt2.2*, fitted line is a direct Michaelis-Menten fit (± standard deviation of 5 replicates).

Table 1-1. Estimates of K_m and V_{max} parameters for NO_2^- influx in *Arabidopsis thaliana* genotypes based on direct fit using the Michaelis-Menten equation (mean ± standard error, n=5 to 10).

Genotype	**Km [µM]**	**Vmax [µmol gFW^{-1} h^{-1}]**
Wild type	125.5 ± 32.6	6.44 ± 0.86
Atnrt2.2	44.85 ± 7.2	4.73 ± 0.27
Atnrt2.1	106.8 ± 27.3	4.58 ± 0.57
Atnrt2.1-nrt2.2	37.9 ± 5	1.96 ± 0.09
Atnar2.1-2	185 ± 49	1.89 ± 0.27

High-affinity nitrate influx into roots of the *Atnar2.1-2* mutant is virtually absent at low external nitrate concentration, exhibiting 5% or less of WT flux and demonstrating a linear pattern of concentration response (Okamoto *et al.*, 2006; Orsel *et al.*, 2006). By contrast, $^{13}NO_2^-$ influx in the *Atnar2.1-2* mutant in the concentration range from 10 to 250 µM was substantial, and followed Michaelis-Menten kinetics (Fig. 1-2), with Km=185±45 µM and Vmax=1.89±0.27 µmol gFW^{-1} h^{-1}. We have also measured $^{13}NO_3^-$ and $^{13}NO_2^-$ influx at 100 µM nitrate and nitrite, respectively, in mutants and WT in the same experiment to reduce potential variation in plant growth and other variables that, in separate experiments, might make direct comparisons more difficult. Compared to WT, nitrate influx in the *Atnrt2.1-nrt2.2* double mutant was reduced by 52%, while nitrite influx was reduced by only 15 % of WT values. Nitrate influx in the *Atnar2.1-2* mutant was only 5 % of WT values, while nitrite influx remained at 60% of WT (Table 1-2).

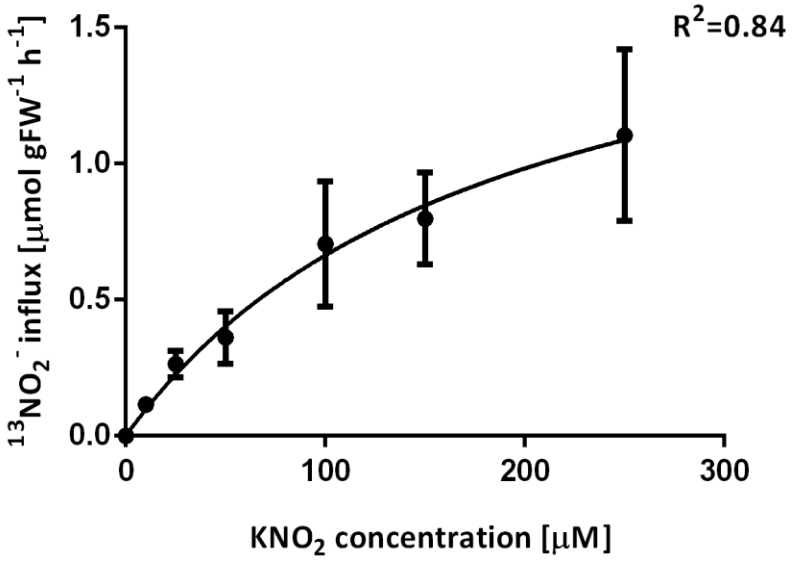

Figure 1-2. $^{13}NO_2^-$ influx at different concentrations of KNO_2, in *Atnar2.1-2* mutant of *Arabidopsis thaliana*; fitted line is a direct Michaelis-Menten fit (± standard deviation of 10 replicates)

Table 1-2. Influx of $^{13}NO_3^-$ and $^{13}NO_2^-$ at concentration of 100 µM KNO_3 and KNO_2 in different *Arabidopsis thaliana* genotypes (± standard error of 5 replicates; different letters indicate significant difference P<0.05, *t* tests within a treatment)

	$^{13}NO_3^-$ Influx [µmol g^{-1} FW h^{-1}]	**% reduction of WT**	**$^{13}NO_2^-$ Influx [µmol g^{-1} FW h^{-1}]**	**% reduction of WT**
Wild type (WT)	5.25 ± 0.39a	0	3.69 ± 0.40a	0
Atnrt2.1-2.2	2.69 ± 0.07b	48	3.20 ± 0.55a	15
Atnar2.1-2	0.24 ± 0.05c	95	1.90 ± 0.37b	40

Effect of induction by nitrite/nitrate and pH on $^{13}NO_2^-$ influx of *Atnar2.1-2* mutant

$^{13}NO_2^-$ influx of the *Atnar2.1-2* mutant was measured at 100 µM KNO_2 after N-starved plants were induced for 3 to 12 h with 1mM KNO_2 or KNO_3. There was no significant effect of induction by either nitrite or nitrate on influx of $^{13}NO_2^-$ (Fig. 1-3). Because nitrous acid is an uncharged molecule that might diffuse across the plasma membrane, we evaluated the effects of pH on $^{13}NO_2^-$ influx in the *Atnar2.1-2* mutant from 100 µM KNO_2. Nitrite influx increased substantially as pH was lowered from 6 to 4. Above pH 6 (from 6 to 8) there was no

significant effect on influx (Fig. 1-4). Standard pH of the nutrient solution used in all experiments was around 6.5.

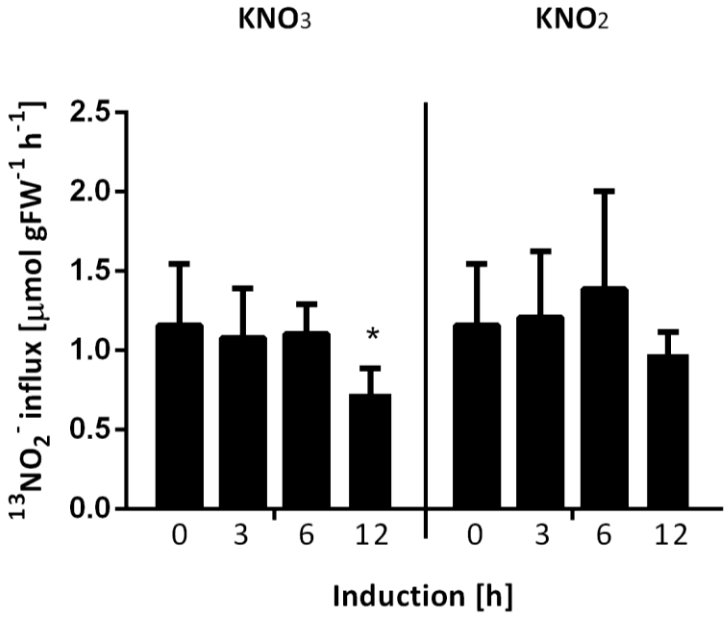

Figure 1-3. Induction of $^{13}NO_2^-$ influx in *Atnar2.1-2* mutant of *Arabidopsis thaliana* by 1mM nitrate or nitrite (± standard deviation of 5 replicates). Asterisk represents a statistically significant difference within a treatment at $P<0.05$.

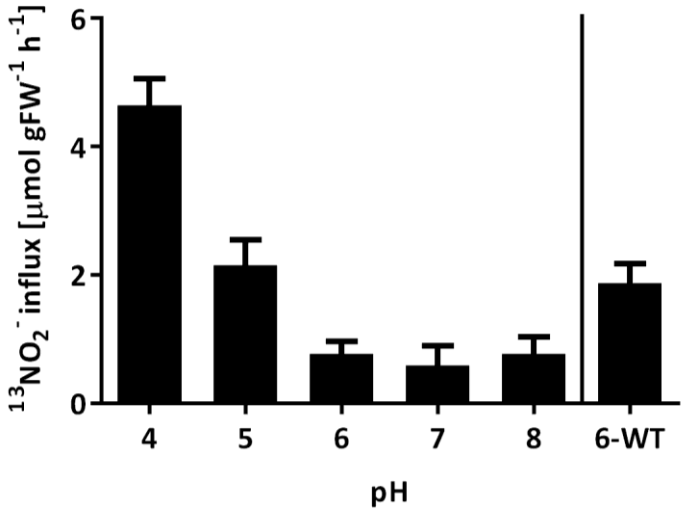

Figure 1-4. Effect of pH on $^{13}NO_2^-$ influx from 100 µM KNO_2 in *Atnar2.1-2* mutant of *Arabidopsis thaliana* (± standard deviation of 5 replicates)

Nitrate as a competitor of $^{13}NO_2^-$ influx

Based upon previously reported competitive inhibition of nitrite uptake by nitrate and vice versa, it has been suggested that nitrate and nitrite use the same transporters for entry through the plasma membrane. To determine the effect of nitrate addition on nitrite influx, we have used $^{13}NO_2^-$ to measure nitrite influxes in WT and the *Atnar2.1-2* mutant in the presence and absence of nitrate. Fig. 1-5a shows Lineweaver-Burk plots of nitrite influx based on 4 different concentrations of nitrite in WT, with and without 250 µM KNO_3. The intersection of plot lines at the Y-axis indicates competitive inhibition of nitrite uptake by nitrate. By contrast, Lineweaver-Burk plots of nitrite influx in the *Atnar2.1-2* mutant are parallel, and almost aligned (Fig. 1-5b), showing virtually no effect of nitrate on nitrite influx in this mutant.

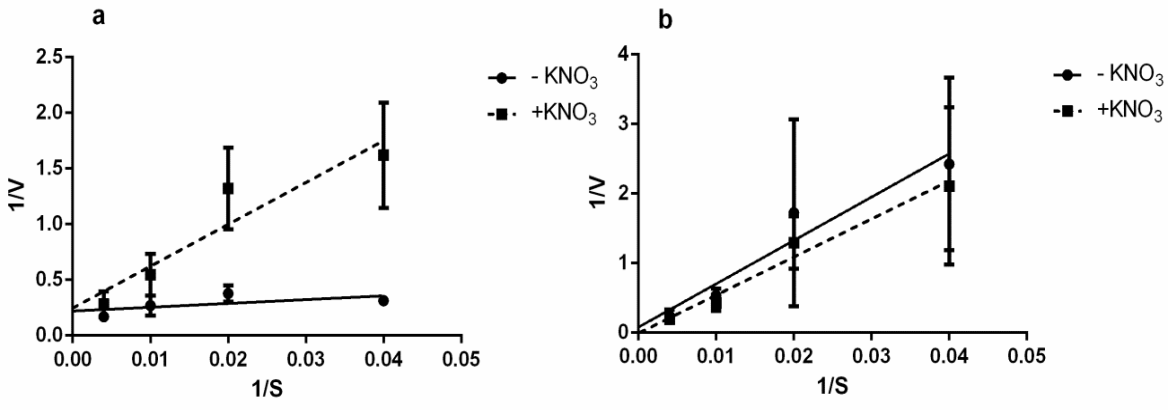

Figure 1-5. Competition of nitrate with nitrite uptake in WT and *Atnar2.1-2*
a. Lineweaver-Burk plots of $^{13}NO_2^-$ influx (V is influx rate - µmol gFW^{-1} h^{-1}) from different concentrations (S is substrate concentration - µM) of KNO_2 in *Arabidopsis thaliana* wild type (WT) in the presence and absence of 250 µM KNO_3; **b.** Lineweaver-Burk plots of $^{13}NO_2^-$ influx (V - µmol gFW^{-1} h^{-1}) from different concentrations (S - µM) of KNO_2 in *Atnar2.1* in the presence and absence of KNO_3. Values are means of 5 replicates ± SD.

Effect of temperature, ammonium and metabolic inhibitor on $^{13}NO_2^-$ influx

It is now accepted that iHATS nitrate uptake is thermodynamically active. We have used ^{13}N labeled nitrite to determine the effect of temperature reduction and a metabolic inhibitor on influx in *Atnar2.1-2* plants. Plants were grown and induced according to the standard procedure, and subjected to the following conditions: reduced temperature during the influx

period, 6 h pretreatment with 1 mM $NH_4H_2PO_4$ or 10 µM CCCP (a protonophore) for 5 minutes in the pre-treatment solution with 100 µM KNO_2, prior to incubation in the tracer-labelled influx solution. Nitrite uptake rates were lower at lower temperature, and were used to calculate Q_{10} coefficients (Table 1-3), that varied from 1.72 to 2.14, according to the temperature range examined. The effect of short exposure to the protonophore was even more pronounced, diminishing influx of $^{13}NO_2^-$ in the *Atnar2.1*-2 mutant from 3.86 µmol g^{-1} FW h^{-1} in control, to 1.25 µmol g^{-1} FW h^{-1} in CCCP-treated plants (Table 1-4). Six hours of ammonium treatment decreased nitrite influx dramatically, from 3.8 to 0.8 µmol gFW^{-1} h^{-1}.

Table 1-3. Calculated temperature coefficient (Q_{10}) values for influx of $^{13}NO_2^-$ in *Arabidopsis thaliana Atnar2.1-2* mutant, at 100 µM KNO_2, plants induced for 6 h with 1 mM KNO_3

Temperature range	**Q_{10} factor**
10-16 ˚C	1.72
10-23 ˚C	2.14

Table 1-4. Effect of ammonium treatment and protonophore carbonyl cyanide m-chlorophenyl hydrazone (CCCP) addition on influx of $^{13}NO_2^-$ in *Arabidopsis thaliana Atnar2.1-2*, at 100 µM KNO_2, plants induced for 6 h with 1 mM KNO_3 (±standard error of 5 replicates)

Treatment	**Influx [µmol gFW^{-1} h^{-1}]**
Control	3.86 ± 0.36
CCCP	1.25 ± 0.08
Ammonium (6 h)	0.84 ± 0.15

Comparison of nitrate and nitrite as N sources for growth of WT and *Atnar2.1-2*

A prediction arising from the presence of an independent nitrite transporter is that at low concentrations, growth of *Atnar2.1-2* on nitrite should be superior to that on nitrate. Figure 1-6a, 1-6b and 1-6c confirm this prediction. Fig 1-6b shows that on low nitrate *Atnar2.1-2* established virtually no growth, whereas growth on nitrite was substantial, though less than that of WT (Fig 1-6a). Fresh weights of *Atnar2.1-2* grown on 250 µM nitrate or nitrite were 15% and 45%, of WT values, respectively (Fig. 1-6c).

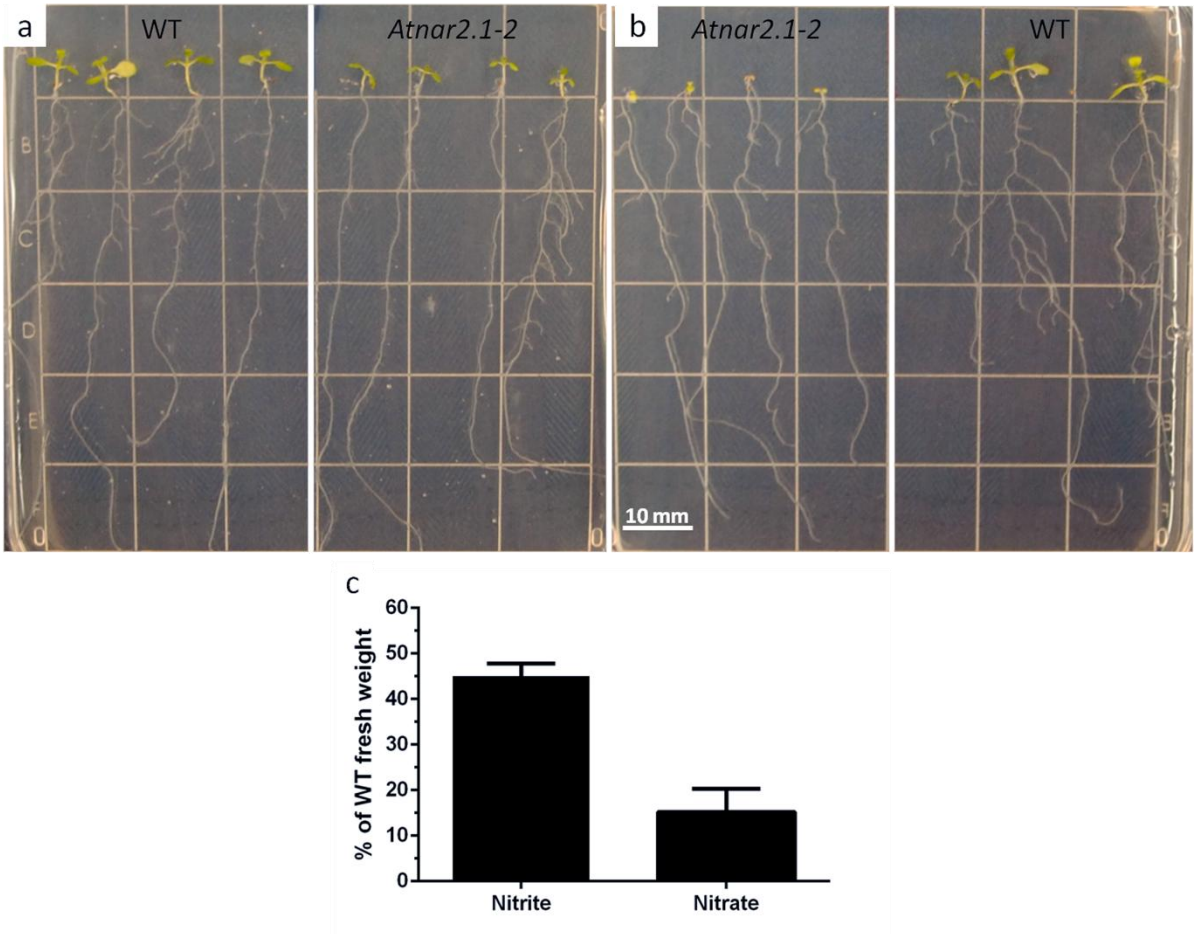

Figure 1-6. Growth of *Arabidopsis thaliana* wild type (WT) and *Atnar2.1-2* mutant on ½ strength Murashige and Skoog (MS) media plates supplemented with 0.25 mM KNO_2 (**a**) and 0.25 mM KNO_3 (**b**); **c**. Fresh plant weight of *Atnar2.1-2* mutant grown on 0.25 mM KNO_2 and 0.25 mM KNO_3 expressed as % of WT; average ± SD of 15 replicates.

Discussion

Nitrite is an important nitrogen source reported to be utilized by many organisms, including bacteria (Bhattacharya *et al.*, 2002; Jia *et al.*, 2009), fungi (Schloemer and Garret, 1974; Wang *et al.*, 2008), phytoplankton (Gabas *et al.*, 1981; Cresswell and Syrett, 1982; Sivasubramanian and Rao, 1988; Abdel-Basset and Ali, 1995), algae (Brinkhuis *et al.*, 1989; Galvan *et al.*, 1991) and flowering plants (Criddle *et al.*, 1988; Zsoldos *et al.*, 1993; Jackson *et al.*, 1974a). A recent study by R. Wang *et al.* (2007) showed that nitrite is also a potent signal for nitrogen metabolism transcriptome regulation in Arabidopsis roots, uniquely inducing significant numbers of nitrate-inducible genes (in WT Arabidopsis) that were not induced in NR mutants. It was concluded, therefore, that a significant number of the genes (apparently induced by nitrate) were actually induced in response to nitrite, produced as a result of nitrate reduction. Nevertheless, the importance of nitrite as a nutrient for plants has been overlooked, and it has mainly been studied as a toxic agent (Lee, 1979; Samater *et al.*, 1998; Zsoldos *et al.*, 2001; Ezzine *et al.*, 2011). The toxicity associated with nitrite is prevalent under conditions of low pH and high concentrations (Zsoldos *et al.*, 1995; Ezzine *et al.*, 2011), conditions that favour conversion of NO_2^- to nitrous acid (HNO_2). However, these conditions are not widespread in the environment and therefore its importance as a plant nutrient requires greater emphasis.

Physiological measurements of nitrate/nitrite competition at the uptake level have suggested that nitrate and nitrite share the same transport system, based upon observed competitive inhibition of nitrate uptake by nitrite (and vice versa) in barley (Aslam *et al*,. 1992; Siddiqi *et al.*, 1992). Therefore it might be considered that a distinct (unique) nitrite transporter would be redundant. Yet in particular cases (e.g. *C. reinhardtii* and *A. nidulans*) where it was possible to completely eliminate nitrate uptake, growth on nitrite was still possible and subsequent studies identified specific genes encoding nitrite transporters that were incapable of nitrate carriage (Rexach *et al.*, 1999; Wang *et al.*, 2008). In *A. nidulans* the responsible nitrite transporter (NitA) is a member of the FNT group which is distinct from the NrtA and NrtB nitrate transporters that belong to the Nitrate-Nitrite Porter (NNP) family, as do the Arabidopsis high-affinity nitrate transporters (AtNRT2.1 and AtNRT2.2). Unfortunately, nitrate uptake in the Arabidopsis *Atnrt2.1-nrt2.2* double mutants is not completely eliminated

(retaining roughly 40% of WT nitrate influx, as shown in Table 2 and in Filleur *et al.*, 2001 and Li *et al.*, 2007), so these mutants would not provide the appropriate context in which to identify a unique nitrite transporter. In place of Arabidopsis *nrt2* mutants, we selected to employ *Atnar2.1* mutants, in which nitrate influx is reduced to ~3-5% of WT values (Okamoto *et al.*, 2006; Orsel *et al.*, 2006). In previous biochemical studies of high-affinity nitrate influx by AtNRT2.1, it was demonstrated that in T-DNA mutants of *AtNAR2.1*, despite the presence of *AtNRT2.1* mRNA, the corresponding protein was absent from plasma membrane (PM) preparations (Wirth *et al.*, 2007). Therefore this mutant proved to be the most suitable genotype for further investigations of nitrite influx as there are no functional nitrate transporters to mask the contribution of a putative nitrite-specific transporter(s).

Fig. 1-1a shows that nitrite influx in WT is substantial, of the order of that reported for nitrate influx. Mutants disrupted in NRT2.2 (Fig.1-1b), NRT2.1 (Fig 1-1c) and NRT2.1/NRT2.2 (Fig. 1-1d) exhibit reduced nitrite influx that is quantitatively consistent with substantial nitrite transport via the high-affinity nitrate transporters. This inference is supported by the form of the Lineweaver-Burk plot (Fig. 1-5a) in which it is demonstrated that in WT plants nitrate reduced nitrite influx competitively.

The highest level of nitrite influx reduction was observed in the *Atnar2.1-2* mutant, in which virtually all high-affinity nitrate influx is eliminated (Fig. 1-2). It is noteworthy that in this mutant $^{13}NO_2^-$ influx conforms to a rectangular hyperbola, and the r^2 for regression was significantly higher than for a linear fit to the data. As these experiments (Fig. 1-1 and 1-2) were done separately for each genotype, we measured influx at a single concentration in order to examine different genotypes side by side, to better compare uptake of nitrite versus nitrate in WT, double and *Atnar2.1-2* mutants. Because of the short half-life of ^{13}N ($t_{0.5}$=9.96 min) it is not possible to accommodate large numbers of treatments. Reduction of both nitrite and nitrate influx was the highest in *Atnar2.1-2* mutant (Table 1-2). Nevertheless, while *Atnar2.1-2* plants retained only 5% of WT nitrate influx, nitrite influx was retained at 60% of WT (Table 1-2). This finding signifies the existence of an additional transport mechanism for nitrite, independent of the *AtNAR2.1* gene. Likewise, in *A. nidulans* the *NitA* gene encodes a nitrite specific transporter that appears to function independently of any NAR2-like polypeptide (Unkles *et al.*, 2011), and also the nitrite transport system III in *C. reinhardtii*

(coded by *CrNRT2.3*) which is independent of the *CrNAR2* gene (Rexach *et al.*, 1999). Nitrite fluxes that were lower in *Atnar2.1-2* than in the double mutant *Atnrt2.1-nrt2.2* (Table 1-2) suggest that despite the presence of a nitrite-specific transporter, in WT plants nitrite may be absorbed by both nitrate-nitrite transporters and this nitrite-specific transporter. However, since soil nitrate concentration typically exceeds that of nitrite, the former might be competitively inhibited, whereas the latter could function independently of nitrate. This may be an important consideration with respect to the induction of nitrite-inducible genes (R. Wang *et al.*, 2007).

Incubation of *Atnar2.1-2* plants in nitrate or nitrite for 0, 3, 6 or 12 hours prior to influx experiments, demonstrated that the putative HATS nitrite-specific transporter is not up-regulated by those treatments, i.e. it is not inducible (Fig. 1-3). This provides another difference between nitrite influx via AtNRT2.1, whose expression is increased several fold by exposure to nitrate (Zhuo *et al.*, 1999; Cerezo *et al.*, 2001; Okamoto *et al.*, 2003), and the putative nitrite-specific transporter. Incubation in 1mM nitrate for 12 h decreased nitrite influx significantly, possibly due to feedback by ammonium or other nitrogen metabolites that might act as signals for uptake regulation, similarly to the regulation of the nitrate HATS (Zhuo *et al.*, 1999; Vidmar *et al.*, 2000; Nazoa *et al.*, 2003).

Nitrite influx in *Atnar2.1-2* mutants increased between pH 6 and 4 (Fig. 1-4). In part, this effect might be explained by permeation of HNO_2 (pKa=3.4) across the plasma membrane at low pH. Yet despite a 100-fold increase of nitrous acid concentration between pH 6 and pH 4 ^{13}N influx increased only 6-fold. At pH values above 6 more than 99.9 % of NO_2^- is in the anionic form and hence its entry across the plasma membrane is a metabolically-dependent flux, demanding the participation of membrane transporters. In all other experiments influx media were maintained at pH ~ 6.5, ensuring that virtually no HNO_2 permeation would contribute to measured ^{13}N influx. Nevertheless under low pH conditions (e.g. in forest soils) nitrous acid permeation may be significant.

Due to their similar characteristics, nitrate and nitrite are known to compete for the binding site of nitrate/nitrite porters, and exhibit competitive inhibition of uptake (Aslam *et al.*, 1992; Siddiqi *et al.*, 1992). In the present experiments with Arabidopsis, we have observed similar results in WT, where the addition of 250 µM nitrate decreased and inhibited nitrite influx

competitively (Fig. 1-5a), suggesting that both ions are using the same transporter, most probably AtNRT2.1, the major contributor to iHATS nitrate uptake (Li *et al.*, 2007). By contrast, in the *Atnar2.1-2* mutant, lacking either NRT2.1 or NRT2.2 activity, nitrate was without effect on nitrite influx (Fig. 1-5b), suggesting the operation of a nitrite-specific transporter that is incapable of nitrate transport.

Studies of the energetics of nitrate uptake revealed active transport mechanisms, suggested to take the form of a symport of two protons with one NO_3^- (reviewed in Crawford and Glass, 1998). The temperature coefficient (Q_{10}) is a quotient defining the ratio of a reaction at t^{o}C/t-10^{o}C. The observed values (Table 1-3), that are significantly higher than 1, suggest that nitrite influx at pH 6.5 is thermodynamically active, unlike passive processes that have Q_{10} values close to 1. Clarkson and Warner (1979) reported that nitrate uptake in ryegrass is very sensitive to temperature. Likewise, Glass *et al.* (1990) have reported high Q_{10} values for nitrate uptake in barley. In addition, the 3-fold reduction of nitrite influx into roots of *Atnar2.1-2* plants in the presence of the protonophore CCCP, known to disrupt the proton gradient and inhibit ATP synthesis, is consistent with the metabolic dependence of influx rather than the result of a passive permeation of nitrous acid (Table 1-4). Ammonium is well documented to inhibit nitrate uptake. For example Lee and Drew (1989) reported that inhibition was evident within 3 min of ammonium application due to direct effects on nitrate transport. In addition, ammonium may reduce nitrate influx through effects operating via glutamine at the transcriptional level (Vidmar *et al.*, 2000; Nazoa *et al.*, 2003). In the case of nitrite uptake, findings on the effects of ammonium have been controversial. De la Haba *et al.* (1990) concluded that ammonium had no effect on nitrite uptake in sunflower. Ibarlucea *et al.* (1983), on the other hand, reported that ammonium diminished nitrite uptake in barley. In the present study, 6-h ammonium treatment of *Atnar2.1-2* plants reduced nitrite influx from 3.8 to 0.8 μmol gFW^{-1} h^{-1}. This provides an additional argument against passive diffusion of nitrite or nitrous acid across the PM, and supports the proposal of a distinct nitrite transport system that is down-regulated by ammonium. The importance of the distinct nitrite transport system in Arabidopsis is evident from the comparative growth of the *Atnar2.1-2* plants on low nitrate and nitrite (Fig. 1-6a-c). It has been shown that *Atnar2.1-2* mutant is incapable of growth on low nitrate (250 μM) as sole source of N (Fig. 1-6b; Okamoto *et al.*, 2006; Orsel *et al.*, 2006). The mutant stops growing after seed N reserves are

depleted, and fails to develop the first true leaves, while cotyledons become yellow. However, this mutant grows successfully on low nitrite as a sole N source (Figure 1-6a). Although smaller than WT, young *Atnar2.1-2* plants maintain 45% of WT weight on nitrite, while reaching only 15% of WT weight on nitrate media (Fig. 1-6c).

Chapter 2. Characterization of an intact two-component high-affinity nitrate transporter from Arabidopsis roots.

Background

Inducible high-affinity nitrate transport (iHATS) in *Arabidopsis thaliana* has been shown to require expression of two genes, namely *AtNRT2.1* and *AtNAR2.1* (*AtNRT3.1*) (Filleur *et al.*, 2001; Orsel *et al.*, 2004; Okamoto *et al.*, 2006; Orsel *et al.*, 2006; Li *et al.*, 2007). Thus, iHATS in T-DNA mutants disrupted in *AtNRT2.1* was reduced by approximately 70% (Filleur *et al.*, 2001; Li *et al.*, 2007), while disruption of *AtNAR2.1* caused IHATS to be reduced by as much as 98 % (Okamoto *et al.*, 2006; Orsel *et al.*, 2006). Furthermore growth of mutants disrupted in *AtNRT2.1*, or in *AtNRT2.1/AtNRT2.2* or in *AtNAR2.1* is severely restricted at low external nitrate concentration (Okamoto *et al.*, 2006; Orsel *et al.*, 2006; Li *et al.*, 2007). By contrast, low-affinity nitrate transport (LATS) encoded by *AtNRT1.1* (Tsay *et al.*, 1993) appears not to require simultaneous expression of *AtNAR2.1*, since the same *AtNAR2.1* mutants exhibited a normal LATS function (Okamoto *et al.*, 2006; Orsel *et al.*, 2006). The requirement for the simultaneous expression of two gene products in order to sustain high-affinity nitrate transport was first demonstrated genetically in *Chlamydomonas reinhardtii* where the capacity for high-affinity transport by CrNRT2.1 or CrNRT2.2 was lost in mutants lacking *CrNAR2* (Quesada *et al.*, 1994). Further support for a two-component high-affinity nitrate influx was provided by the demonstration that nitrate transport in *Xenopus* oocytes required co-expression of CrNRT2 together with the CrNAR2 protein (Zhou *et al.*, 2000a). Likewise only when both of the barley homologues (*HvNRT2.1* and *HvNAR2.3*) were co-expressed in *Xenopus* oocytes was nitrate transport realized (Tong *et al.*, 2005). Positive results reported for the yeast two-hybrid split-ubiquitin assay further suggest that the functional high-affinity nitrate transporter may involve an intimate interaction between AtNRT2.1 and AtNAR2.1 (reviewed in Glass, 2009). Nevertheless, despite this indirect evidence, no higher order complex consisting of AtNRT2.1 and AtNAR2.1 has thus far been demonstrated. Although Wirth *et al.* (2007) identified a high-molecular weight polypeptide at ~120 kDa in WT plants using NRT2.1 antibodies, the continued strong expression of this polypeptide in the *Atnar2.1* knockout mutant eliminated it as a possible candidate for the putative higher order complex of AtNRT2.1 and AtNAR2.1.

Using a combination of green fluorescent protein fusion and immunological methods, it was demonstrated that AtNRT2.1 is mainly localized in the plasma membranes of root cortical and epidermal cells (Chopin *et al.*, 2007b; Wirth *et al.*, 2007). Wirth *et al.* (2007) suggested that several forms of this polypeptide, a 45 kDa monomer and higher molecular weight forms co-exist. Of these, the authors reported that the monomeric form was the most abundant and suggested that it was the form involved in nitrate transport. The authors attempted to cross-link AtNRT2.1 with its putative partner AtNAR2.1 by treating microsomal fractions with 1% formaldehyde prior to extraction and SDS-PAGE, but failed to detect a putative complex consisting of the two participants in high-affinity nitrate influx and concluded that NAR2.1 was not a part of the high molecular mass polypeptide at ~120 kDa. In a recent study of the two component system in barley (Ishikawa *et al.*, 2009), it was demonstrated that both HvNRT2.1 and HvNAR2.3 were localized in the PM and the authors suggested that the C-terminus of HvNRT2.1 may be involved in its binding to the central region of HvNAR2.3. Indeed an earlier paper (Kawachi *et al.*, 2006) reported that a point mutation in the mid region of AtNAR2.1 resulted in a loss of HATS activity.

Objective

The objective of this study was to identify a putative molecular complex of AtNRT2.1 and AtNAR2.1 by means of blue native PAGE (BN-PAGE) and immunological methods. In order to be able to identify AtNAR2.1 polypeptide in Western blots, I used *Atnar2.1-2* T-DNA mutant described in a previous study (Okamoto *et al.*, 2006) as recipient for a myc-tagged *AtNAR2.1* cDNA. This transformed line as well as WT and other lines were used to isolate microsomal and plasma membrane-enriched fractions. Partly solubilized protein complexes were separated on a BN-PAGE, and in the second dimension by SDS-PAGE, to resolve the putative molecular complex of AtNRT2.1 and AtNAR2.1 into its component monomers. Localization of the two-component complex of AtNRT2.1 and AtNAR2.1 was examined by *in vivo* transient expression of split YFP-labelled AtNRT2.1 and AtNAR2.1 in Arabidopsis protoplasts.

Material and methods

Preparation of the *Atnar2.1-35S:NAR2.1-myc* lines

A myc-tagged *NAR2.1* gene was cloned from Arabidopsis cDNA using high fidelity enzyme (Phusion®, Finnzymes) and the following primers:

Forward-5'-ATGGATCCATGGCGATCCAGAAGATCCTCTT-3' and reverse 5'-ATGAATTCTCAATTCAGATCCTCTTCTGAGATGAGTTTTTGTTCTTTGCTTTGCTCTATCTTGGCC-3'. Modified binary pGreenII179 vector, bearing hygromycin resistance for plants (Hellens *et al.*, 2000a; Hellens *et al.*, 2000b) was used to make the *35S:NAR2.1-myc* construct. Arabidopsis knock-out *Atnar2.1-2* line was transformed using the simplified Agrobacterium-mediated floral dip method (Clough and Bent, 1998). T0 seed was subjected to selection on ½ strength MS agar plates with 20 mgL^{-1} Hygromycin B (Invitrogen, USA). Seed collected from T1 and T2 plants was used for all experiments.

Plant Material and Growth Conditions

Arabidopsis plants (WT ecotype Columbia-0 and Wassilewskija, and knock-out mutant lines *Atnrt2.1* (Salk_141712), *Atnrt2.1-nrt2.2* (Salk_035429), *Atnar2.1-2* and *Atnar2.1-35S:NAR2.1-myc* lines were grown hydroponically under non-sterile conditions as described previously (Zhuo *et al.*, 1999; Okamoto *et al.*, 2003). Details are provided in Chapter 1 of this thesis. Plants were grown for 4 weeks, and then deprived of nitrogen for the fifth week. To induce HATS (for protein expression and $^{13}NO_3^-$ influx analysis) plants were next transferred to solution containing 1 mM KNO_3 for 6 hours. For dry weight measurement, plants were grown in the same hydroponic nutrient solution described above except that NH_4NO_3 was replaced by 0.25 mM KNO_3 to subject plants to low nitrate conditions. Roots and shoots were separated and dried at room temperature for 2 days prior to weighing.

For growth on MS agar plates, Arabidopsis seeds were sterilized in 1% bleach (plus 0.01% v/v Tween 20) for 15 min, and left for 3 days in sterile water at 4°C for imbibition. Seeds were then sown on half strength N-free MS salts media, supplemented with 0.25 mM KNO_3 or10 mM KNO_3. The plates were kept in a vertical position and plants grown for 2 weeks under the same conditions as described above. Root length was measured using ImageJ and NeuronJ plug-in **(**Meijering *et al.*, 2004).

$^{13}NO_3^-$ influx measurements

Protocol for measuring nitrate influx using $^{13}NO_3^-$ was described in Chapter 1 of this thesis. The basic components of the solution for the pre-treatment, influx, and desorption were the same as those of the growth media, except that 0.1 mM KNO_3 replaced NH_4NO_3. Prior to measuring $^{13}NO_3^-$ influx, plants were pretreated for 5 min with solution containing 0.1 mM KNO_3, and then transferred for 5 min into the influx solution, which was labelled with $^{13}NO_3^-$.

Microsome preparation

Arabidopsis roots were homogenized in homogenizing buffer consisting of 0.33 M sucrose, 5 mM EGTA, 2 mM SHAM, 1 mM DTT, 1.5% soluble PVP, proteinase inhibitor and 25 mM Tris-Mes at pH 7.6. The homogenate was centrifuged at 10,000 × g for 20 min and the supernatant was then centrifuged at 100,000 × g for 40 min. The pelleted microsomes were dispersed in resuspension buffer, consisting of 0.33 M sucrose, 1 mM EDTA, 10 mM KCl, 1 mM DTT, protease inhibitor cocktail (Complete EDTA-free tablets, Roche, Germany) and 5 mM Tris-MES at pH 7.3, and spun again at the same speed for the same period of time. The pellet was again dispersed in resuspension buffer.

Isolation of plasma membranes

Plasma membranes were separated by two-phase partitioning according to the method described in Santoni (2007). Microsomes were loaded into a two-phase system consisting of 6.3% (w/w) of PEG 3350 (Sigma-Aldrich, USA) and Dextran T500 (Pharmacia, Sweden) in a final concentration of 0.33 mM sucrose, 3 mM KCl and 5 mM potassium phosphate (pH 7.8). The phase mixture was thoroughly mixed and centrifuged at 1,500 × g for 10 min. The top phase was removed and subjected to repartition by mixing with a new lower phase. Then the top phase, after the second partitioning, was diluted in resuspension buffer and pelleted at 100,000 × g for 40 min. The resulting plasma membrane pellets were resuspended in resuspension buffer and frozen at -80 °C until required for further analysis.

Sucrose step-gradient fractionation

Solutions having various sucrose concentrations (15%, 30%, 34% and 45%) were prepared by solubilising sucrose in sucrose gradient buffer consisting of 5 mM Tris-Mes (pH 7.3), 1 mM EDTA, 1 mM DTT, 10 mM KCl and protease inhibitor cocktail (Complete EDTA-free tablets, Roche, Germany). 45% sucrose was carefully overlayed with 38%, 30% and 15%

sucrose solutions, respectively. The microsome sample was layered over the 15% layer. The gradients were centrifuged at 80,000 × g for 2 h. Bands formed at each interphase were carefully collected and diluted with sucrose gradient buffer and spun at 100,000 × g for 40 min. The pellets were resuspended in resuspension buffer, and frozen at -80 °C until further use.

Assay for plasma membrane H^+-ATPase

Vanadate sensitive, K^+-stimulated Mg-ATPase activity (Leonard and Hodges, 1973) was determined by measuring the release of inorganic P (Ames, 1966). Reaction mixtures contained: 3 mM ATP (Tris form), 3 mM $MgSO_4$, 5 mM sodium azide, 1 mM sodium molybdate, 50 mM potassium nitrate, 50 mM potassium chloride, 0.2% Triton-X-100, 2 mM EDTA and 250 mM sucrose in 30 mM Tris-Mes buffer (pH 6.5), with or without 1 mM sodium orthovanadate. 10-30 µg of membrane protein was added in 0.45 ml reaction mixture to start the reaction and the incubation was conducted at 36°C for 30 min. After incubation the tubes were transferred to ice, 0.5 ml of ice-cold TCA-perchloric acid mixture (10% TCA w/v and 4% perchloric acid v/v) were added to stop the reaction and samples were incubated on ice for a further 30 min. The precipitate formed was then pelleted by centrifugation at 10,000 g for 5 min and supernatant samples of 0.5 ml were transferred to clean test tubes. To each sample, 1 ml of Ames reagent (6 parts 0.42% (w/v) ammonium molybdate in 1 N H_2SO_4 to 1 part 10% (w/v) ascorbic acid) was added and samples were incubated for 1 hour at room temperature. The absorbance was then measured at 800 nm. A standard curve was prepared using KH_2PO_4.

Immunoblot analysis

For SDS immunoblotting analysis, proteins were separated on denaturing 12% SDS-PAGE followed by an electrotransfer at 4 °C onto a polyvinylidene difluoride (PVDF) membrane (Hybond-P, Amersham, UK). NRT2.1 was detected using anti-NRT2.1 antiserum produced by Alpha Diagnostic Intl. (USA) against the following synthetic peptides (C)DLPDGNRATLEKAGE, (C)KNMHQGSLRFAENAK and (C)GRRVRSAATPPENTPNNV. The polyclonal antiserum was affinity purified by Alpha Diagnostic Intl. Myc tag was detected by C-terminal myc antibody (Santa Cruz Biotechnology, USA). ER and tonoplast markers were detected by polyclonal anti-BIP

(COSMO BIO, Japan) and anti-V-PPase antibody (COSMO BIO, Japan), respectively. The immunodetection was performed with an ECL system kit (GE healthcare, UK).

Blue native polyacrylamide gel electrophoresis (BN-PAGE) was carried out as described previously (Schagger *et al.*, 1994; Guo *et al.*, 2005). An equal volume of resuspension buffer containing 3% (w/v) dodecyl-β-D-maltoside was added to microsomes or PM suspension. After incubation at 4°C for 5 min, samples were combined with one tenth volume of 5% Serva blue G in 100 mM BisTris-HCl (pH 7.0), 0.5 M 6-amino N-caproic acid, 30% (w/v) glycerol, and applied to 1.5-mm-thick 5-16% acrylamide gradient gels in a Hoefer Mighty Small vertical electrophoresis unit, operated at 4°C. For direct immunoblotting analysis, the lanes from BN-PAGE were cut out and equilibrated for 1 h in 1 × gel buffer (50 mM BisTris-HCl, 0.5 M 6-amino N-caproic acid, pH 7.0) with 1% SDS (w/v) and 2.5% (v/v) β-mercaptoethanol. Then the samples were electro transferred onto PVDF membranes for immunoblotting analysis as described above.

For separation in a second-dimension using SDS-PAGE, the lanes from the first-dimension BN-PAGE were cut out and equilibrated for 1 h in SDS loading buffer and placed into a 12% acrylamide gel of the same thickness. Immunoblotting was performed using anti-myc antibody to detect the presence of NAR2.1-myc. After NAR2.1 detection, the PVDF was washed with stripping buffer (62.5 mM Tris-HCl pH 6.8, 2% SDS and 100 mM β-mercaptoethanol) at 50°C for 30 min by shaking slowly. Membranes were then washed with TBS-T three times for 10 min each. The washed PVDF membrane was used for immunodetection by anti-NRT2.1 antibody to detect NRT2.1. After immunoblotting analysis, the two films were overlayed so that the high molecular weight markers for native electrophoresis (GE healthcare, UK) lined up on both films. In order to quantify band intensity on Western blot films, image analysis software ImageJ was used (Abramoff *et al.*, 2004).

Transient expression in protoplasts

NRT2.1 and NAR2.1 were tagged with halves of YFP using pSAT vectors for bimolecular fluorescence (Citovsky *et al.,* 2006). cDNA of *AtNRT2.1* was fused in frame to the C-terminal half of YFP in pSAT4A-cEYFP-N1 (XhoI/BamHI restriction sites). cDNA of *AtNAR2.1* was fused in frame to the N-terminal half of YFP in pSAT1A-nEYFP-N1

(XhoI/BamHI restriction sites). Primers used for cloning of the *AtNRT2.1* and *AtNAR2.1* are shown in Appendix A (Table 1A). WT Arabidopsis leaf protoplasts were prepared and transformed with the constructs according to the protocol by Tiwari *et al.* (2006). Approximately 1 g of leaves was cut into <1 mm strips with a surgical blade and incubated in 25 ml of 1% (w/v) Cellulase (Onozuka R10) and 0.25% (w/v) Macerozyme R10 solution for 90 min, shaking in darkness at 40 rpm (recipes for all buffers/solutions are given in Appendix B). Protoplasts were then filtered through a 200 µM plastic mesh, diluted with 1/3 volume of 200 mM $CaCl_2$ and recovered by centrifugation at 180 g for 3 min. The protoplasts were then washed once with 25 ml of W5 solution, and resuspended in W5 at a concentration of 3×10^5 protoplasts/ml, and kept for 20 min at room temperature. Before transfection, W5 solution was removed and protoplasts resuspended in Mg-mannitol. 200 µl of protoplasts was mixed with 10 µg of high-purity plasmid DNA in a sterile 15 ml tube, and transfected by addition of an equal volume of PEG-solution. After thorough but gentle mixing, the tube was incubated at room temperature for 20 min, and an extra 10 min after addition of 0.8 ml of W5 solution. Thereafter, protoplasts were pellet by centrifugation at 180 g for 3 min, and PEG aspirated from the tube. The transfected protoplasts were resuspended in 1 ml of WI solution and incubated for 18 h in darkness and visualized using Spinning Disk Perkin-Elmer UltraView VoX Microscope (equipped with Leica DMI6000 inverted microscope and Hamamatsu 9100-02 CCD camera) and Volocity software.

RNA isolation and relative expression of *AtNRT2.1* and *AtNAR2.1*

Total RNA was isolated from roots of hydroponically-grown plants, under conditions described above for influx experiments, using TRIzol™ (Invitrogen, USA). Approximately 100 mg of previously frozen root tissue was ground using liquid nitrogen and mortar/pestle to a fine powder, transferred to an RNA-free 1.5 ml tube and mixed well with 1 ml TRIzol™ reagent. After 5 min incubation, 0.2 ml chloroform was added to the sample, mixed well by hand and incubated for 3 min at room temperature. The sample was then centrifuged for 15 min at 4°C, at 12,000 g. The top aqueous phase was moved into a fresh RNA-free tube and mixed with 0.5 ml isopropanol, incubated for 10 min at room temperature and spun for 10 min at 4°C, at 12,000 g to precipitate RNA. The RNA pellet was washed with 1 ml of 75 % (v/v) ethanol and air-dried for 10 min after removing the ethanol. RNA was dissolved in 50

µl of RNA-free water, and its concentration measured using a spectrophotometer (BioSpec1601, Shimadzu, Japan).

1 µg of total RNA was used for cDNA synthesis using M-MLV Reverse Transcriptase (Invitrogen, USA) with 20 µl reaction set-up as follows: 0.5 µg oligo $(dT)_{12-18}$, 0.5 mM dNTPs, 1x First-strand buffer, 0.01M DTT, 40 units RNAse-out™ inhibitor and 200 units of M-MLV RT. The reaction was incubated at 37°C for 50 min to synthesize the first strand cDNA, and inactivated at 70°C for 15 min. Relative gene expression was determined according to a model by Pfaffl (Pfaffl, 2001), by using the *Actin* gene expression as a reference. Sequences of primers used for DNA amplification in the real-time PCR reactions are given in Appendix A (Table 2A). Real-time PCR reactions of 20 µl were prepared using 2x iQ™ SYBR® Green Supermix, 400 nM of each primer and 1 µl of cDNA. Real-time PCR was done using the MiniOpticon™ Detection System (Bio-Rad, USA), for 40 cycles (conditions given in Appendix C). To be able to compare expression of the two genes, efficiency of PCR primers was determined according to Rasmussen (2001). Real-time PCR was done with the 3 sets of primers (*ACT2, NRT2.1* and *NAR2.1*) using increasing cDNA concentration. The slope of the linear regression line (threshold cycle vs. cDNA concentration) was used to calculate efficiency of the primers according to formula Efficiency (E) = $10^{(-1/slope)}$.

Statistical analysis

ANOVA was used to analyze data from experiments with different treatments and genotypes, and significant effects were tested by multiple *t* test comparisons with GraphPad Prism 6 program (GraphPad Software Inc., USA).

Results

Complementation of the *Atnar2.1-2* mutant with *35S:NAR2.1-myc*

I have expressed myc-tagged *AtNAR2.1* in the *Atnar2.1-2* mutant in order to facilitate immunological detection of AtNAR2.1 by anti-myc antibody in the absence of a suitable anti-NAR2.1 antibody. I have measured different parameters to confirm that the tagged AtNAR2.1 is functional and complements the *Atnar2.1-2*. Figures 2-1a and 2-1b show the growth of the wild type (WT), *Atnar2.1* mutant and the two myc lines on agar media

containing 0.25 mM and 10 mM KNO_3, respectively. The mutant showed virtually no growth at low nitrate, whereas when grown on high nitrate or NH_4NO_3 (Okamoto *et al.*, 2006) this same mutant grew like WT. Transformation with a myc-tagged *NAR2.1* cDNA (*AtNAR2.1-myc*) restored growth of the mutant to near WT rates when grown on low-nitrate media (Fig. 2-1 and 2-2). Dry weights of roots were also restored to WT values, while shoot growth increased from 6% of WT in the mutant to ~70% of WT in the restored lines (Table 2-1). As previously reported (Okamoto *et al.*, 2006), $^{13}NO_3^-$ influx was reduced by up to 98% compared to WT in the *Atnar2.1* mutant when plants were grown hydroponically as described below. Following transformation with *AtNAR2.1-myc* rates of $^{13}NO_3^-$ influx in "rescued" lines increased to approximately 60 and 70% of WT fluxes (Table 2-2). Taken together, these data indicate that AtNAR2.1-myc is functional and successfully complements the *Atnar2.1-2* mutant.

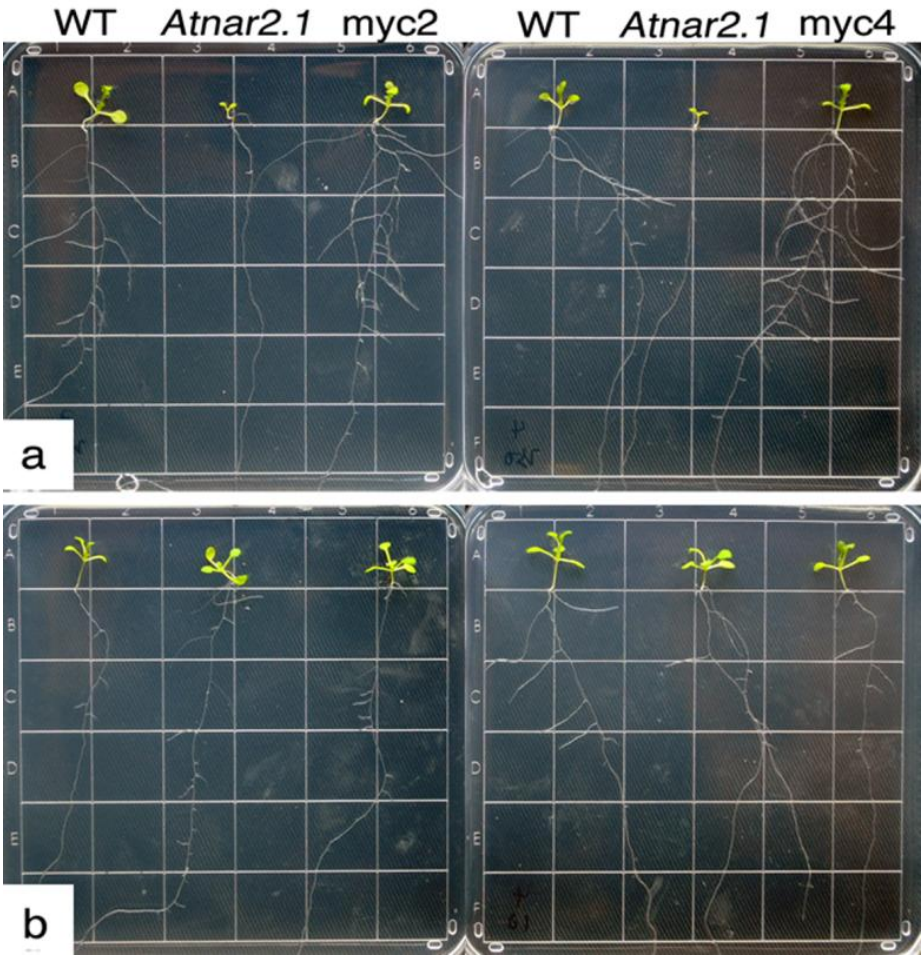

Figure 2-1. Growth of various *Arabidopsis* lines (WT-Ws, *Atnar2.1-2* mutant, and *Atnar2.1-35S:NAR2.1-myc* lines) on ½ strength MS agar containing: **a.** 0.25 mM KNO_3 and **b.** 10 mM KNO_3

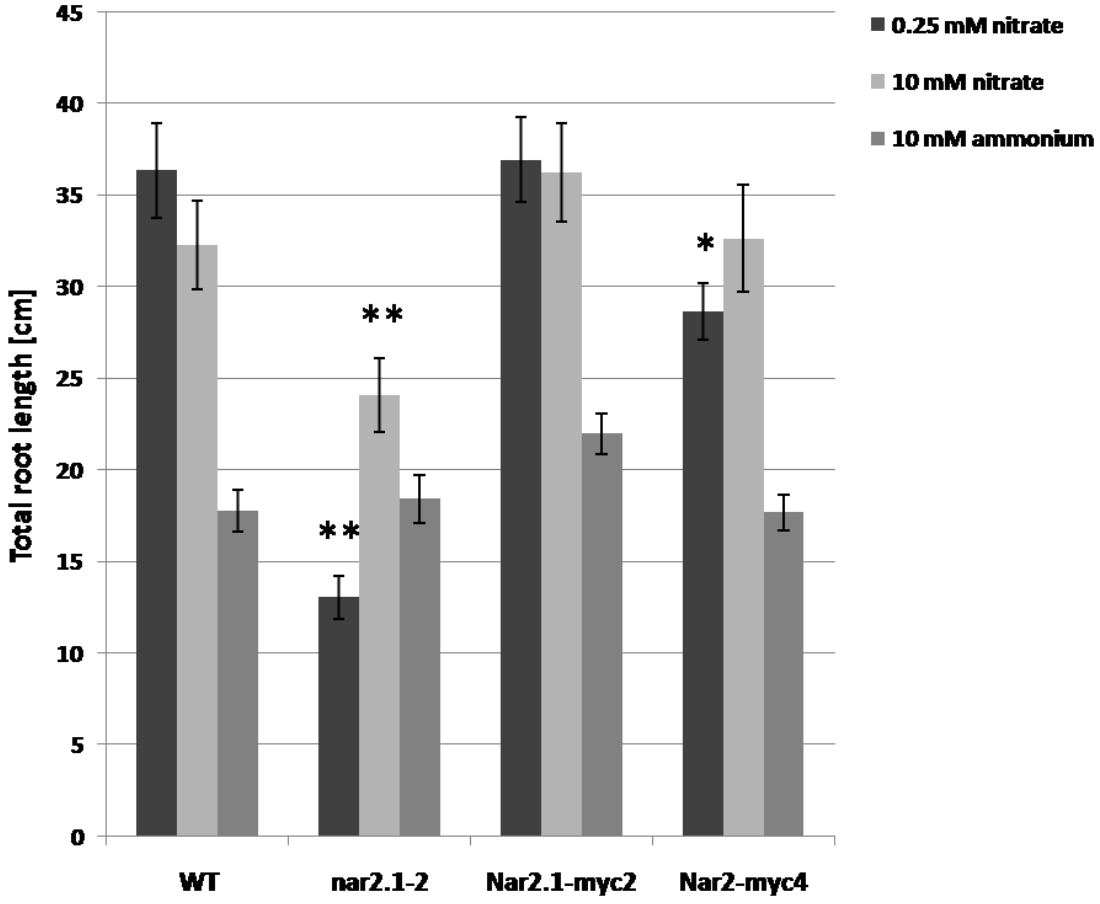

Figure 2-2. Total root length of 2-week old plants grown on ½ MS agar media supplied with different KNO_3 concentrations. Values shown are averages ± SD of 10 replicates. ANOVA was followed by *t* tests to evaluate differences among genotypes at given nitrogen levels; * $P<0.05$; ** $P<0.01$.

Table 2-1. Dry weight of plants hydroponically grown for 5 weeks at 250 µM KNO_3. Average values ± SD of 10 replicates; ANOVA followed by *t* tests of root and shoot weight between genotypes; * P<0.05.

Genotype	Root weight (mg)	% of WT	Shoot weight (mg)	% of WT
Wild type-Ws	1.40 ± 0.66	100	9.97 ± 3.47	100
Atnar2.1	0.53 ± 0.23*	38	0.64 ± 0.16*	6
Atnar2.1-NAR2.1-myc2	1.35 ± 0.32	96	6.12 ± 1.04*	61
Atnar2.1-NAR2.1-myc4	1.23 ± 0.46	87	6.76 ± 2.04*	68

Table 2-2. $^{13}NO_3^-$ influx into roots of WT, *Atnar2.1* mutant and *Atnar2.1-35S:NAR2.1-myc* lines after induction with 1 mM KNO_3 for 6 h. Influx was measured using 0.1 mM KNO_3 to characterize iHATS. Values shown are means ± SE of 6 replicates.

Genotype	Influx (µmol g FW^{-1} h^{-1})	% of WT Flux
Wild type-Ws	5.58 ± 0.37	100
Atnar2.1	0.36 ± 0.06	6
Atnar2.1-NAR2.1-myc2	3.26 ± 0.13	58
Atnar2.1-NAR2.1-myc4	3.72 ± 0.19	67

Absence of AtNRT2.1 in various mutants

Lines of various mutant plants, disrupted exclusively in *AtNRT2.1* (Li *et al.*, 2007), in both *AtNRT2.1* and *AtNRT2.2* (Filleur *et al.*, 2001; Li *et al.*, 2007) or in *AtNAR2.1* (Okamoto *et al.*, 2006) were grown and microsomal fractions prepared from roots of these plants after 4 weeks hydroponic growth on media containing 1 mM NH_4NO_3 followed by 1 week without N and 6 hours induction with 1 mM KNO_3. This treatment maximizes expression of *AtNRT2.1*, *AtNAR2.1* and inducible high-affinity $^{13}NO_3^-$ influx (Okamoto *et al.*, 2006).

Microsomal fractions were subjected to SDS-PAGE and Western blots were prepared and probed with anti-AtNRT2.1 antibody. Figure 2-3 reveals that AtNRT2.1 was present in WT microsomal fractions but was absent from the fractions isolated from the *Atnrt2.1* mutant, the double mutant (*Atnrt2.1-nrt2.2*) and from the *Atnar2.1-2* mutant.

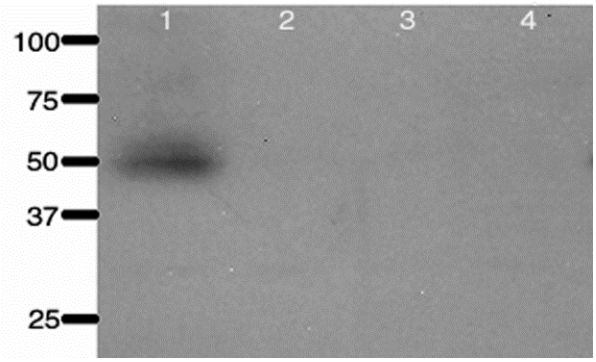

Figure 2-3. Western blot of microsomal fractions from roots of various *Arabidopsis* lines after SDS-PAGE, probed with anti-NRT2.1 antibody. Lane **1**: WT (Col). Lane **2**: *Atnrt2.1* mutant; Lane **3**: *Atnrt2.1-nrt2.2* (double mutant); Lane **4**: *Atnar2.1-2* mutant.

Plasma membrane localization of AtNRT2.1 and AtNAR2.1

AtNRT2.1, the major iHATS nitrate transporter is localized in the plasma membrane of root cortical cells (Wirth *et al*., 2007). In order to determine the localization of the putative interacting protein AtNAR2.1, roots of the rescued *A. thaliana Atnar2.1-2* mutant (*Atnar2.1-35S:NAR2.1-myc* line) containing AtNAR2.1-myc and a WT AtNRT2.1 were used as the source of plant material for isolation of membrane fractions. Plants were grown hydroponically in the same manner as for flux determination, described above. Roots of the rescued *Atnar2.1-35S:NAR2.1-myc4* line were excised from shoot tissue and used to isolate microsomes. This microsomal preparation was subjected to sucrose-gradient centrifugation followed by SDS-PAGE. Western blots were then probed with anti-myc antibodies. Figure 2-4 reveals that anti-myc antibodies recognized the presence of AtNAR2.1-myc in microsomal-, plasma membrane-, and endoplasmic reticulum (ER)/Golgi- enriched fractions but not in a tonoplast-enriched fraction. We also used two-phase partitioning in PEG/dextran to obtain a highly purified plasma membrane (PM) fraction. The identity and purity of this preparation was evaluated by determining ATPase activity in the presence and absence of 1.0 mM

vanadate, a specific inhibitor of PM H^+-ATPase activity and by use of specific antibodies. Vanadate-inhibitable ATPase activity of microsomes and PM was reduced by 70 and 80%, respectively, in the presence of 1 mM vanadate (Table 2-3). The microsomal and PEG/dextran generated PM fractions were subjected to SDS-PAGE followed by Western blotting and then probed with polyclonal antibodies against ER- and tonoplast-specific proteins to evaluate the extent of contamination by these membranes, and against AtNRT2.1 and AtNAR2.1 to verify their presence in this purified PM fraction (Fig. 2-5). The virtual absence of a reaction to anti-V-PPase (tonoplast marker) and anti-BIP (ER marker) indicated low levels of contamination by these membranes, while the reactions to anti-AtNRT2.1 and anti-myc confirm the presence of these polypeptides in this purified PM fraction. Figure 2-5 also confirms molecular masses of 48 and 26 kDa, respectively, for these polypeptides.

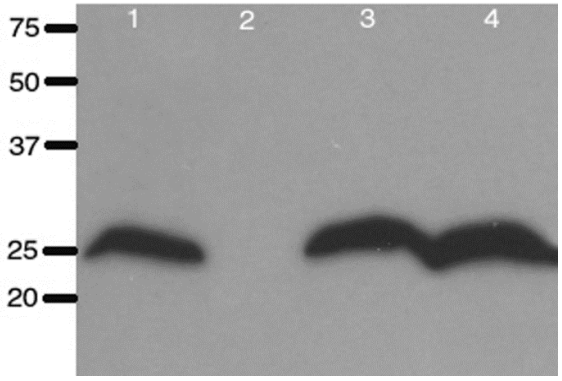

Figure 2-4. Western blot of various membrane-enriched fractions from roots of *Atnar2.1-35S:NAR2.1-myc4* line separated by sucrose gradient centrifugation, followed by SDS-PAGE and probed with anti-myc antibody to localize AtNAR2.1-myc. Lane **1**: microsomes; Lane **2**: tonoplast; Lane **3**: plasma membrane; Lane **4**: endoplasmic reticulum/Golgi.

Table 2-3. ATPase activity of microsomes and PEG/dextran-purified PM. Values shown are means ± SE of 6 replicates.

Membrane fraction	ATPase activity (µmol Pi mg^{-1} hr^{-1})		% inhibition
	Without vanadate	With 1 mM vanadate	
Microsomes	19.43±1.69	5.93±0.71	70
PM	45.56±0.83	8.95±0.32	80

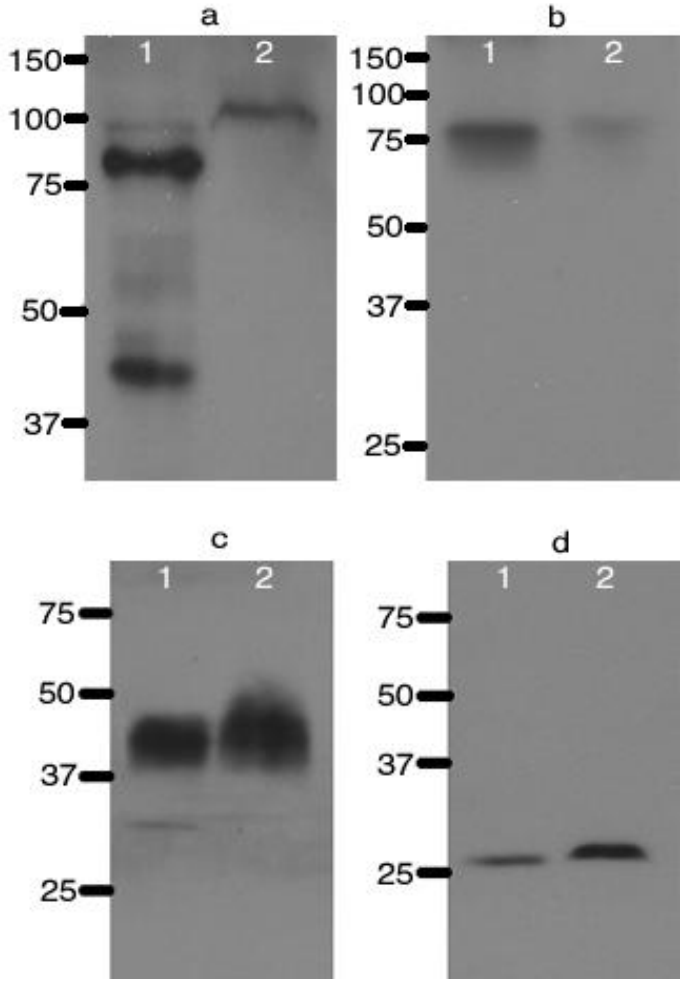

Figure 2-5. Evaluation of PM purity and confirmation of the presence of AtNRT2.1 and AtNAR2.1-myc in microsomes and plasma membrane fractions (purified by PEG/dextran two-phase partitioning) from roots of *Atnar2.1-35S:NAR2.1-myc4* line. **a.** ER marker detected by anti-Bip polyclonal antibody; **b.** tonoplast marker detected by anti-V-PPase polyclonal antibody; **c.** AtNRT2.1 detected by anti-AtNRT2.1 antibody and **d.** AtNAR2.1-myc detected by anti-myc antibody. In each blot: **Lane 1**: microsomal fraction; **Lane 2**: purified plasma membrane.

Identification of the intact AtNRT2.1/AtNAR2.1 complex

The *Atnar2.1-35S:NAR2.1-myc4* line, *Atnar2.1-2*, *Atnrt2.1*, *Atnrt2.1-nrt2.2* mutants and WT plants were grown under standard conditions (see above) and roots of these plants were used for the isolation of microsomal membranes and PEG/dextran generated PM fractions. These were solubilized in 1.5 % dodecyl maltoside and subjected to BN-PAGE in the first dimension. Resulting Western blots were probed with anti-NRT2.1 antibody. Figures 2-6a and 2-6b reveal that the anti-NRT2.1 antibody gave a positive reaction with a protein complex of molecular mass ~150 kDa that was present in both microsomes and purified PM fractions. The MW estimation of this complex was determined according to methods described previously (Yamaoka *et al.*, 1993; Yamaoka, 1998). To ensure that the ~150 kDa complex was not an artefact resulting from the presence of the 35S promoter in the 35S:NAR2.1-myc the above procedures were repeated using WT-derived membranes. Figure 2-6c shows that this complex was also present in membranes isolated from WT roots. No free NRT2.1 was detected in any of the BN-PAGE preparations shown in Figure 2-6. By contrast this complex was absent from samples prepared using roots of the *Atnar2.1-2* knockout mutant reported by Okamoto *et al.* (2005) and from the *Atnrt2.1* and *Atnrt2.1-nrt2.2* mutant lines (Li *et al.*, 2007) as shown in Figure 2-6d. When probed with anti-myc antibody, neither the WT nor the rescued line ~150 kDa complex gave any reaction to anti-myc antibody.

The entire lane from the BN-PAGE of microsomes from the *Atnar2.1-35S:NAR2.1-myc4* mutant was cut out and transferred horizontally to an SDS-polyacrylamide gel for a second dimension electrophoresis. After SDS-PAGE the gel was used for Western blotting and probed first with anti-myc antibody. This antibody reacted with a polypeptide of molecular mass ~ 26 kDa (Fig. 2-7a) that was derived from a region of the BN-PAGE gel corresponding to a molecular mass of ~ 150 kDa. After stripping, the PVDF membrane was probed with anti-AtNRT2.1 antibody to detect AtNRT2.1, at a M.W. of ~ 48 kDa. Figure 2-7b shows that AtNRT2.1 was also derived from the ~150 kDa region of the BN-PAGE lane. Overlapping the two immunoblots (Fig. 2-7c) clearly demonstrates that both AtNRT2.1 and AtNAR2.1 are derived from the same ~150 kDa region of the BN-PAGE lane. The above procedures were repeated using PEG/dextran-purified PM preparations with identical results

to those shown in Figure 2-7. Therefore, the intact oligomeric molecular complex of AtNRT2.1 and AtNAR2.1 was isolated for the first time in plants.

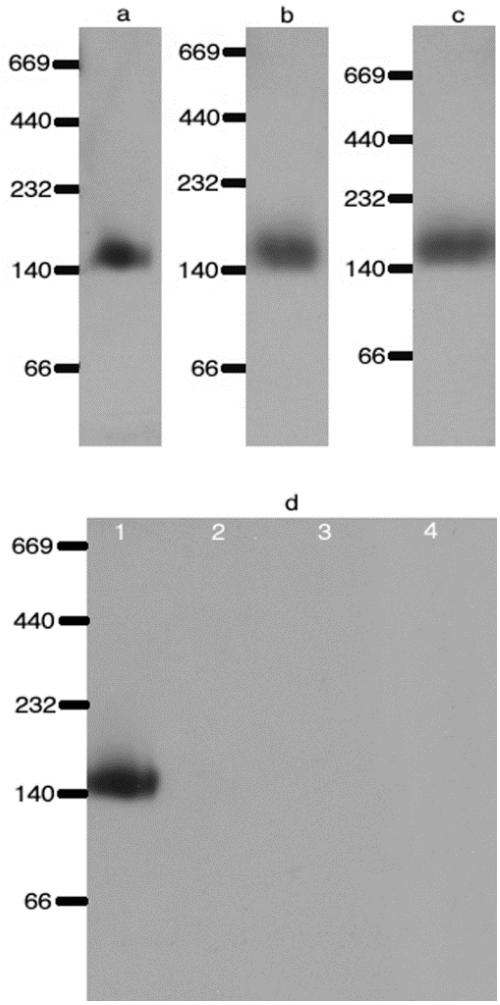

Figure 2-6. Western blots after Blue Native-PAGE and probing with anti-NRT2.1 antibody. **a**. Microsomal fraction from roots of the *Atnar2.1-35S:NAR2.1-myc4* line, **b.** PEG/dextran purified plasma membrane fraction from roots of the *Atnar2.1-35S:NAR2.1-myc4* line, **c.** microsomal fraction from roots of WT plants, **d.** Comparison of microsomal fraction from roots of WT-Col (lane 1), *Atnar2.1-2* (lane 2), *Atnrt2.1* (lane 3) and *Atnrt2.1-nrt2.2* (lane 4) mutant.

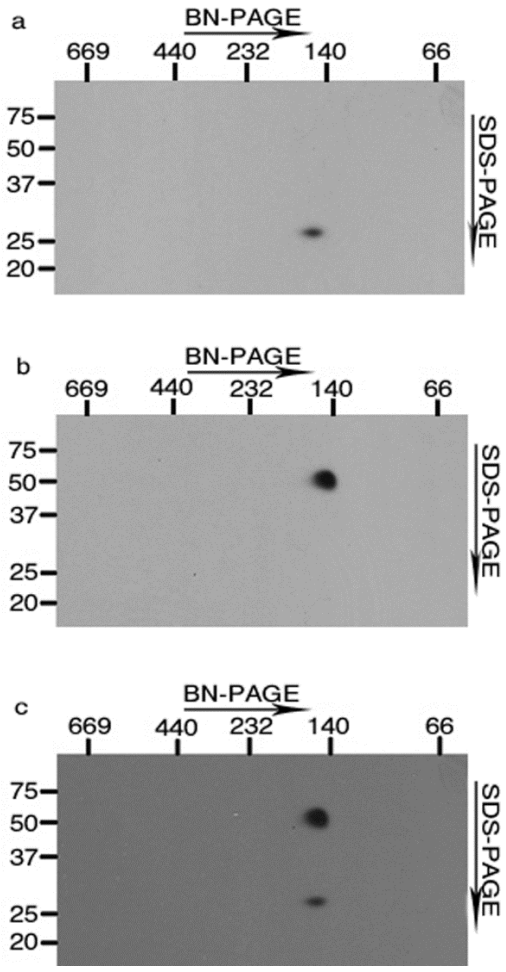

Figure 2-7. Separation of the native 150 kDa complex using SDS-PAGE in the second dimension. **a.** Western blot after SDS-PAGE of the blue native gel lane and probing with anti-myc antibody. **b.** After stripping the membrane, the same Western blot was probed with anti-NRT2.1 antibody; **c.** Overlap of image **a.** and **b.** demonstrates that the two polypeptides are derived from the same ~150 kDa region of the blue native gel.

The PM localization of the complex was also investigated by transient in vivo expression of split YFP-labelled AtNRT2.1 and AtNAR2.1 in WT Arabidopsis leaf protoplasts. Figure 6 shows bright field and fluorescence images of protoplasts transformed with both AtNRT2.1-cEYFP and AtNAR2.1-nEYFP (Fig. 2-8a), and of protoplasts transformed with either AtNRT2.1-cEYFP and nEYFP, or AtNAR2.1-nEYFP and cEYFP as controls (Fig. 2-8b and 2-8c, respectively). Only when both AtNRT2.1 and AtNAR2.1 were present was fluorescence, localized to PM, detected.

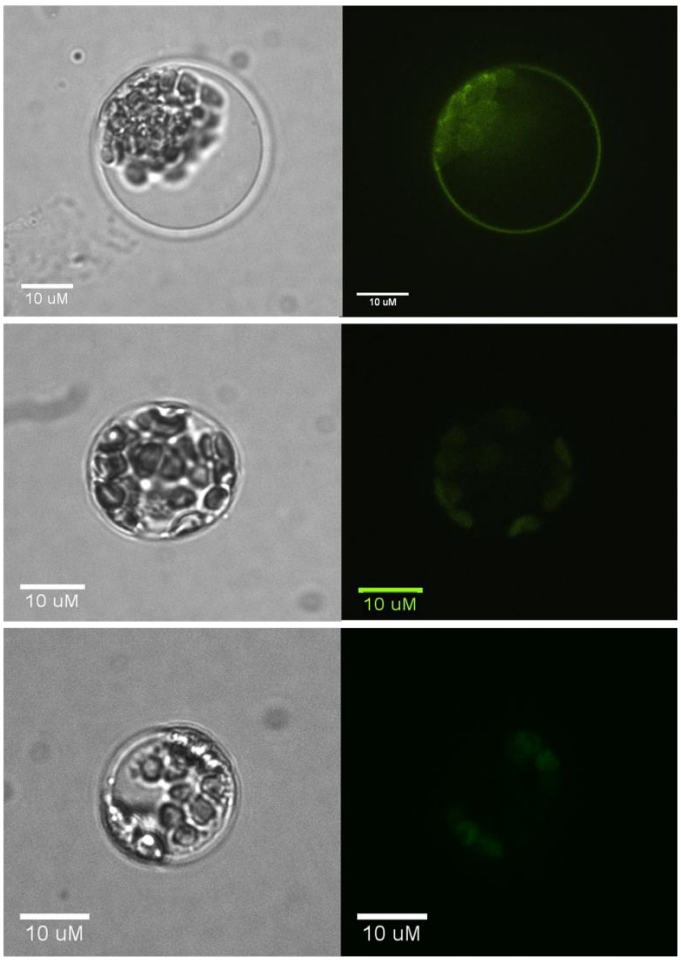

Figure 2-8. Interaction of AtNRT2.1 and AtNAR2.1 *in vivo.* Transient expression of split YFP constructs in *Arabidopsis* leaf protoplasts. Bright field (left) and fluorescence (right) images. Protoplasts were transfected with: **a.** *AtNRT2.1-cEYFP* and *AtNAR2.1-nEYFP*; **b.** *AtNAR2.1-nEYFP* and *cEYFP*; **c.** *AtNRT2.1-cEYFP* and *nEYFP*.

Half-life of the 150 kDa complex

Nitrate addition to nitrogen-starved plants profoundly induces genes coding for iHATS transporters, and as a result increases nitrate influx several fold after 3 to 12 hours (described in Introduction). In order to examine the effect of induction by nitrate on expression of the molecular complex of AtNRT2.1 and AtNAR2.1, I isolated microsomes from roots of WT plants that were subjected to different induction treatments and separated protein complexes on BN-PAGE. Figure 2-9b shows Western blot after probing with anti-NRT2.1 antibody. Surprisingly, the 150 kDa molecular complex was present even in uninduced plants that were

starved of nitrogen for 1 week (lane 2). Expression of the complex was increased by nitrate induction over time reaching the highest expression after 24 h (lanes 3-6), while mRNA expression of *AtNRT2.1* peaked at 6 h induction and then reduced at 12 and 24 h by approximately 60% (Fig. 2-9a). $^{13}NO_3^-$ influx also peaked at 6 h induction, and slowly decreased towards 12 and 24 h after induction with nitrate (Fig. 2-9c).

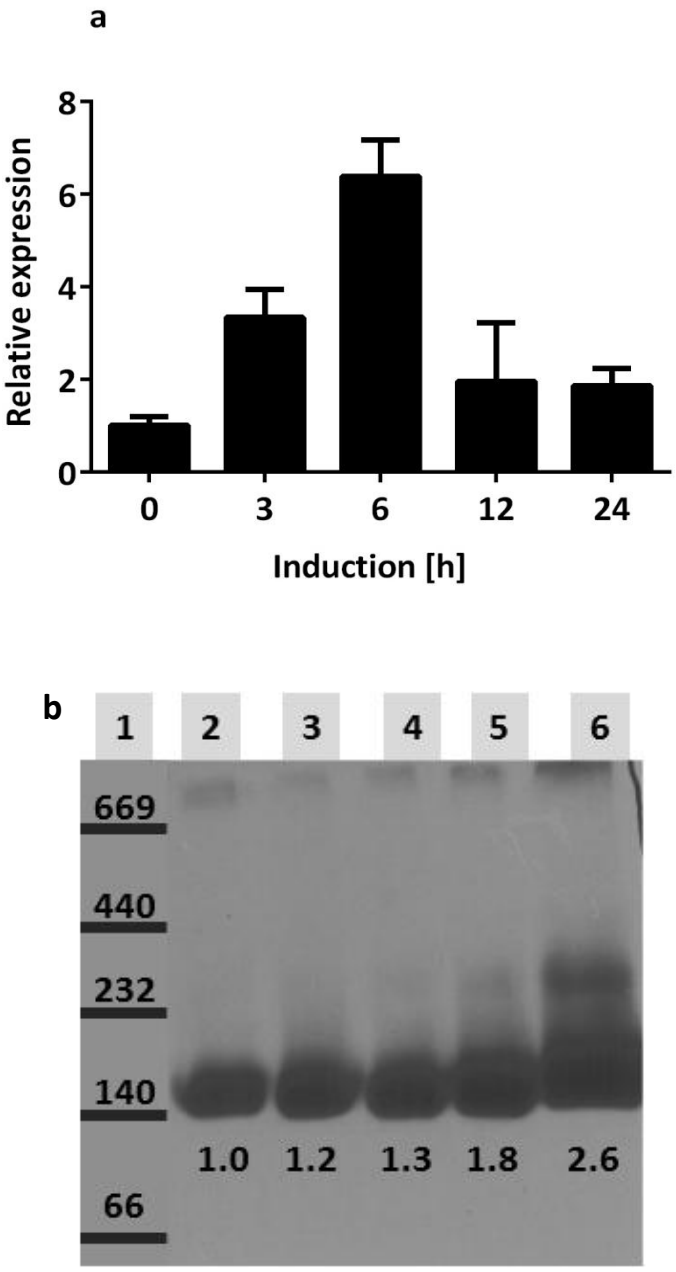

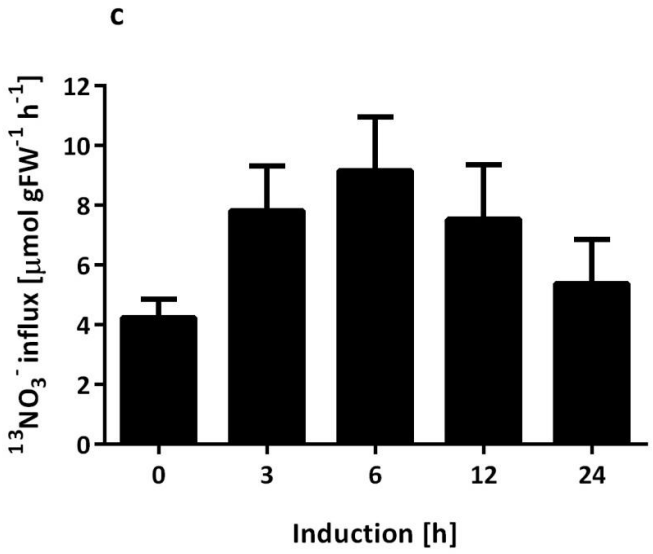

Figure 2-9. Effect of nitrate induction on NRT2.1 mRNA and the protein complex expression in roots of WT *Arabidopsis thaliana* plants. The 4-week old plants were starved of N for a week (**uninduced**), then induced with 1 mM KNO_3 for 3 to 24 h. **a**. Relative *AtNRT2.1* mRNA expression at different times of induction, calculated using *ACT2* expression as a reference (mean ± SE, n=4) **b**. Western blot of microsomal proteins isolated separated on a BN-PAGE and probed with anti-NRT2.1 antibody. Lanes: **1**. Molecular weight marker (kDa); **2.** uninduced; **3**. induction for 3 h; **4.** induction for 6 h; **5**. induction for 12 h; **6**. induction for 24 h. **c**. $^{13}NO_3^-$ influx into roots of WT plants after induction with 1 mM KNO_3 for 0 to 24 h. Influx was measured using 0.1 mM KNO_3 to characterize iHATS. Values shown are means ± SD of 5 replicates. Numbers below each band represent estimated relative amount of protein compared to lane 1, based on analysis of the Western blot membrane by ImageJ programme.

It is known that the addition of ammonium reduces the expression of NRT2 mRNA and, within minutes of ammonium addition, nitrate uptake in plants is reduced (discussed in the Introduction). In order to examine the complex stability and estimate half-life, I have isolated microsomes from roots of WT plants that were exposed to different durations of ammonium treatment and protein complexes were separated on BN-PAGE. Induced plants had the highest level of *AtNRT2.1* and *AtNAR2.1* expression, and *AtNRT2.1* exhibited much higher expression in induced plants compared to *AtNAR2.1*. Comparison of the expression of the two genes was done after confirming that the efficiencies of PCR reactions were comparable (Table 2-4). Exposure to ammonium diminished expression of both genes after only 1 h, by 50 % for *AtNAR2.1* and 80 % for *AtNRT2.1* (Fig. 2-10a). The effect of ammonium on

expression of the molecular complex, however, was markedly different. The 150 kDa complex showed strong stability, exhibiting significant disappearance from the membranes only after 24 h of ammonium treatment, with estimated half-life of 35.5 h, based on equation from a linear regression between time and relative protein amount
y = -1.6604x + 108.68 (R^2 = 0.9745), y=time, x=relative protein amount (Fig. 2-10b).

Table 2-4. Efficiency of primers used for DNA amplification in real-time PCR experiment. Values shown for each of the primer pairs are average threshold cycle number of 3 replicates. Slope is of a fitted linear regression line with threshold cycle on Y-axes and cDNA concentration on X-axes. Efficiency is calculated as $E=10^{(-1/slope)}$.

cDNA [ng]	***Actin***	***AtNAR2.1***	***AtNRT2.1***
0.013	26.17	26.82	26.68
0.064	23.72	24.46	23.99
0.32	21.48	21.92	21.83
1.6	19.05	19.78	19.72
Slope	**-3.55**	**-3.497**	**-3.369**
Efficiency	**1.9128207**	**1.9317513**	**1.9803224**

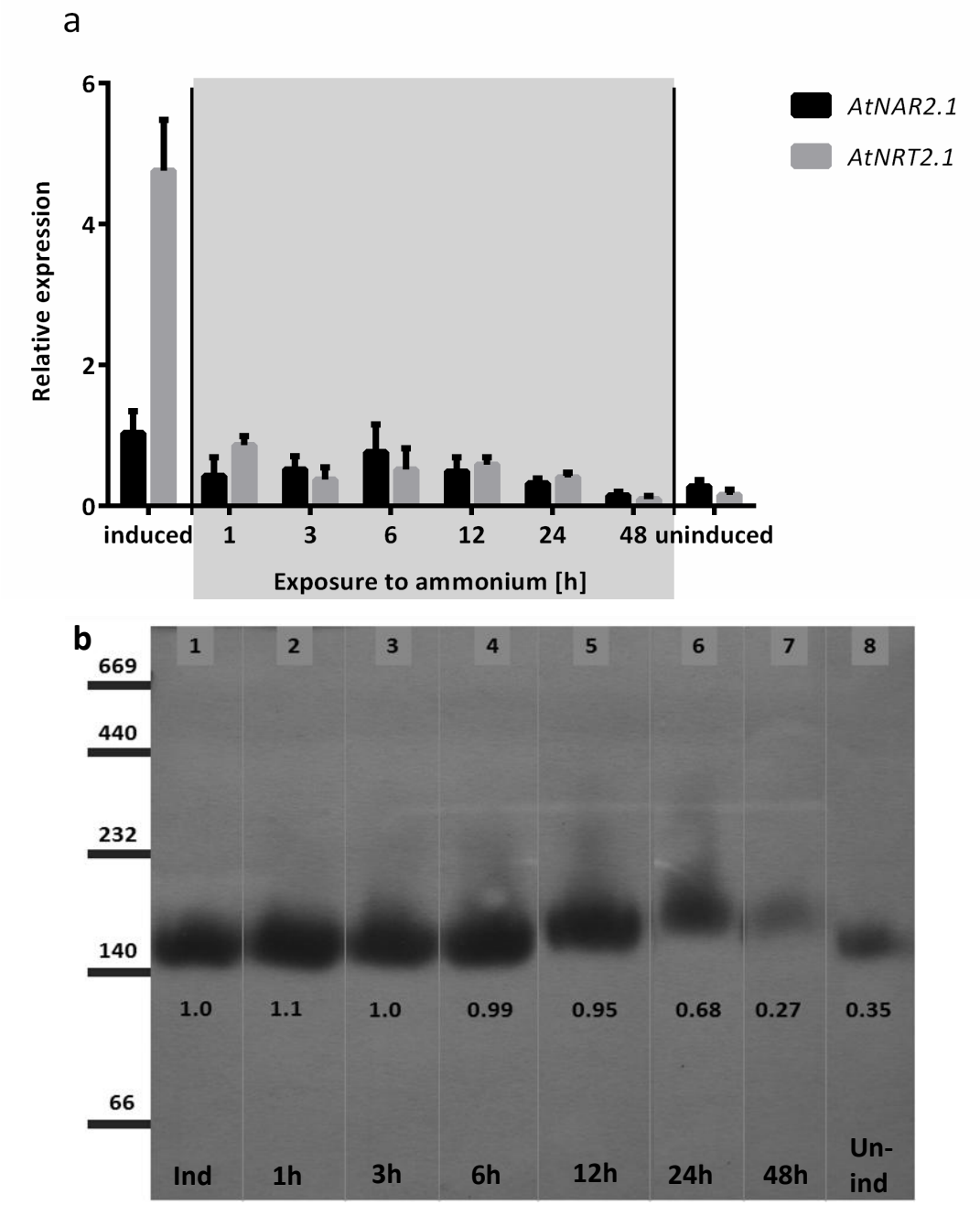

Figure 2-10. Effect of ammonium treatment on mRNA and protein expression of *AtNRT2.1* and *AtNAR2.1* in roots of WT plants. The 4-week old plants were starved of N for a week (**uninduced**), then supplied with 1 mM KNO_3 for 6 h (**induced**), and thereafter exposed to 1 mM ammonium for 1 to 48 h. **a**. Relative mRNA of expression, calculated using *ACT2* expression as a reference (mean ± SE, n=4). **b**. Western blot of microsomal proteins separated on a BN-PAGE and probed with anti-NRT2.1 antibody. Lanes: **1.** Induced; **2**. 1h ammonium; **3.** 3h ammonium; **4**. 6h ammonium; **5**. 12h ammonium; **6**. 24h ammonium; **7**. 48h ammonium; **8**. Uninduced. Numbers below each band represent estimated relative amount of protein compared to lane 1, based on analysis of the image by ImageJ programme.

Discussion

Inducible high-affinity nitrate influx depends upon coincident expression of two genes, namely *NRT2.1* and *NAR2.1* in several species, including *C. reinhardtii* (Quesada *et al.*, 1994), *A. thaliana* (Filleur *et al.*, 2001; Okamoto *et al.*, 2006; Orsel *et al.*, 2006; Li *et al.*, 2007), *H. vulgare* (Tong *et al.*, 2005) and in rice, wheat and the moss *Physcomitrella patens* (reviewed in Glass, 2009). Disruption of *AtNAR2.1* by a T-DNA insertion in *A. thaliana* reduced iHATS $^{13}NO_3^-$ influx to approximately 5% of WT values (Okamoto *et al.*, 2006, Orsel *et al.*, 2006). Nevertheless transcript abundance of *AtNRT2.1* was still relatively high, and it was subsequently demonstrated that the AtNRT2.1 polypeptide was absent in PM preparations from this mutant (Wirth *et al.*, 2007). The authors concluded that AtNAR2.1 is essential for proper targeting of AtNRT2.1 to the PM, and also suggested that AtNAR2.1 might be necessary to stabilize AtNRT2.1.

The data in this study demonstrates that the iHATS nitrate transporter is stable and functional only in the oligomeric form. Our anti-NRT2.1 antibody recognized the presence of AtNRT2.1 in microsomal membranes and in purified PM-enriched preparations from roots of WT plants and from roots of the *Atnar2.1-35S:NAR2.1-myc* line (Fig. 2-3 and 2-5). The absence of a reaction to membranes from the *Atnrt2.1* mutant (Fig. 2-3), demonstrates that the antibody is specific for AtNRT2.1, failing to recognize AtNRT2.2. Likewise, the antibody failed to recognize any of the other five NRT polypeptides in membranes from roots of *Atnrt2.1* or from *Atnrt2.1-nrt2.2* mutants. The absence of any reaction to membranes from *Atnar2.1* mutant (Fig. 2-3) confirms that AtNRT2.1 is absent from the PM in *Atnar2.1* mutant (Wirth *et al.*, 2007). Figure 2-3 confirms earlier observations that disruption of AtNAR2.1 in T-DNA mutants renders the mutant essentially incapable of growth on low concentrations of nitrate (Okamoto *et al.*, 2006; Orsel *et al.*, 2006) and our $^{13}NO_3^-$ assay demonstrated that HATS activity was reduced to ~ 6 % of WT values. The restoration of near WT plant growth and HATS activity establishes that *Atnar2.1-35S:NAR2.1-myc4* line is expressing a functional AtNAR2.1 (Fig. 2-1 and 2-2, Tables 1 and 2).

Data shown in Figures 2-4, 2-5 and 2-6 establish that AtNAR2.1 is localized in the PM, using PM-enriched fractions derived from sucrose-gradient centrifugation and in highly purified PEG/dextran purified preparations. The identity of the latter preparations was verified by the

extent of vanadate-inhibitable ATPase activity (Table 3) and their purity was established by the absence of ER or tonoplast membranes (Fig. 2-5). Thus both members of the two-component high-affinity nitrate transporter are localized in the PM of *A. thaliana* as they have been localized in barley root PM (Ishikawa *et al.*, 2009). Wirth *et al.* (2007) had earlier demonstrated that AtNRT2.1 was localized in the PM; we now establish that AtNAR2.1 is also localized in this membrane.

Microsome and PEG/dextran purified PM preparations from the *Atnar2.1-35S:NAR2.1-myc* line subjected to BN-PAGE and probed with anti-AtNRT2.1 antibody revealed a positive reaction with an entity of molecular mass ~150 kDa that was resolved into two polypeptides of molecular masses equal to ~48 and ~26 kDa when the entire BN-PAGE lane was subjected to a second dimension in SDS-PAGE. These polypeptides correspond to AtNRT2.1 and AtNAR2.1, respectively, based upon their reaction with the corresponding antibodies (Fig. 2-6 and 2-7). The co-migration of these two polypeptides from the ~150 kDa region of the BN-PAGE lane establishes that these PM polypeptides originated from a single ~150 kDa complex. This same 150 kDa complex was also present in roots of WT plants (Fig. 2-6c). The separation of these two polypeptides by SDS-PAGE demonstrates that the two polypeptides are held by non-covalent linkages, possibly between the C-terminus of AtNRT2.1 and the central portion of AtNAR2.1 as suggested in a study of the barley system (Ishikawa *et al.*, 2009). Interestingly, the absence of any free AtNRT2.1 in the BN-PAGE immunoblots (Fig. 2-6) and the localization of NAR2.1 in the PM strongly suggest that AtNRT2.1 is present only as a complex with AtNAR2.1. These observations argue against the suggestion (Wirth *et al.* 2007) that the role of NAR2.1 is in the processing of NRT2.1 rather than in a permanent PM association with NRT2.1.

In contrast to the study by Wirth *et al.*, (2007), we failed to detect anti-AtNRT2.1 reactive polypeptides at ~75 and ~120 kDa. Nor were polypeptides of this MW observed in the barley study (Ishikawa *et al.*, 2009). More importantly, Wirth *et al.* (2007) concluded that NAR2.1 was not a part of their 120 kDa polypeptide because the latter was still abundant in *Atnar2.1* mutant. Also if this polypeptide had contained AtNAR2.1 and AtNRT2.1, the latter should have been separated by the denaturing SDS treatment, as they were in our study (Fig. 2-7). The absence of our 150 kDa complex from membranes isolated from roots of the *Atnrt2.1*,

Atnrt2.1-nrt2.2 or the *Atnar2.1-2* mutants (Fig. 2-6d) is consistent with the involvement of both AtNRT2.1 and AtNAR2.1 in the complex. The combined molecular mass of a single sub-unit each of AtNRT2.1 and AtNAR2.1 is ~74 kDa. Therefore, given the estimated molecular mass of ~150 kDa for the native complex, I suggest that the functional inducible high-affinity nitrate transporter may be a tetramer consisting of two sub-units each of AtNRT2.1 and AtNAR2.1. The failure of the anti-myc antibody to recognize the AtNAR2.1 polypeptide in the ~ 150 kDa complex that so clearly contains both AtNRT2.1 and AtNAR2.1 polypeptides suggests that the proposed two sub-units of AtNRT2.1 may enclose the AtNAR2.1 sub-units making the myc peptide inaccessible to the antibody.

The results showing reconstituted fluorescence (Fig. 2-8) only when both AtNRT2.1 and AtNAR2.1 are transiently expressed in the leaf protoplasts confirms the intimate *in vivo* association between these polypeptides, while the sub-cellular pattern of fluorescence confirms the findings of the immunological methods (discussed above) with respect to the PM localization of the complex.

It was reported before that nitrate influx was down-regulated within 3 minutes of ammonium treatment, and returned to normal as quickly after removal of ammonium from external media (Lee and Drew, 1989). Behl *et al.* (1988) found that the treatment of nitrate-induced barley plants with an inhibitor of protein synthesis did not have a strong effect on net nitrate uptake, indicating a slow turnover of proteins involved in nitrate transport into roots. Also, a previous study of AtNRT2.1 expression in root membranes provided strong evidence that the protein is quite stable over time and its expression does not correlate well with mRNA expression or HATS nitrate uptake (Wirth *et al.*, 2007). However, in yeast *H. polymorpha* nitrate transporter YNT1 disappeared from the cells within 1.5 h after the addition of ammonium due to protein ubiquitinylation and proteolysis in vacuoles (Navarro *et al.*, 2006).

My findings suggest that the molecular complex of AtNRT2.1 and AtNAR2.1, that is a functional nitrate transporter, has a long half-life (estimated 35 h) in plasma membranes, and that expression of the complex does not correlate with gene expression or high-affinity nitrate influx in Arabidopsis (Fig. 2-9 and 2-10). This discrepancy between expression of the protein complex and nitrate influx could only be explained by posttranslational modifications that enable rapid control of nitrate influx. In agreement with this hypothesis are findings of

Lee and Drew (1989) who reported that nitrate uptake was down-regulated within 3 minutes of ammonium treatment, and returned to normal as fast after removal of ammonium. Garnett *et al.* (2013) found that reduction in nitrate supply led to a dramatic increase in the nitrate uptake capacity of maize, a response that was faster than changes in transcript levels of NRTs indicating possible short-term post-transcriptional regulation. Y. Wang *et al.* (2007) found that an *A. nidulans* nitrate reductase mutant had high levels of NRTA nitrate transporter expressed, but had 30 times lower nitrate uptake rates than WT strain, again providing evidence for posttranslational regulation. A recent work by Laugier *et al.* (2012) showed that Arabidopsis plants expressing *NRT2.1* constitutively continued to maintain down-regulation of nitrate uptake in response to ammonium and light conditions. Furthermore, the authors found that NRT2.1 protein abundance was not always well correlated with nitrate uptake, suggesting post-transcriptional and post-translational regulation (Laugier *et al.*, 2012). It still remains to be discovered which amino acids are crucial for posttranslational regulation of the molecular complex function involved in iHATS nitrate transport in plants.

Chapter 3. Nitrate transport capacity of the *Arabidopsis thaliana* NRT2 family members and their interactions with AtNAR2.1

Background

Nitrate uptake by plant roots from soil solution is mediated by members of three gene families, namely NRT1, NRT2 and NAR2 (see reviews by Miller *et al.*, 2009; Dechorgnat *et al.*, 2011; Wang *et al.*, 2012). Full activity of the inducible high-affinity nitrate transport system (iHATS) in roots of *Arabidopsis thaliana* requires expression of two transporters, NRT2.1 and NRT2.2, both of which are members of the Major Facilitator Superfamily (MFS). Evidence for this assertion is based upon the high degree of correlation between physiological activity of the iHATS and transcript abundance of *AtNRT2.1* and *AtNRT2.2* in WT lines and the reduction of iHATS in mutants disrupted in *AtNRT2.1* and or *AtNRT2.2* (Zhuo *et al.*, 1999; Filleur *et al.*, 2001; Okamoto *et al.*, 2003; Li *et al.*, 2007). Nevertheless, it was first shown in *Chlamydomonas reinhardtii* that the *NRT2.1* and *NRT2.2* genes require simultaneous expression of another gene called *NAR2* in order to express high-affinity nitrate transport (Quesada *et al.*, 1994). In *A. thaliana* also, disruption of NAR2.1 (formerly NRT3.1), in the T-DNA insertional mutant, *Atnar2.1*, caused an almost complete loss of inducible high-affinity nitrate influx (Okamoto *et al.*, 2006; Orsel *et al.*, 2006). Membrane interactions between *AtNRT2.1* and *AtNAR2.1* were clearly indicated earlier by heterologous expression in the yeast two-hybrid and *Xenopus* oocytes systems. Only when oocytes were injected with both *AtNRT2.1* and *AtNAR2.1* mRNA was nitrate uptake into oocytes detected (Orsel *et al.* 2006). In addition to Arabidopsis, the two-component nitrate uptake system of NRT2 and NAR2 has been demonstrated to be present in other plant species such as barley and rice (Glass, 2009; Ishikawa *et al.*, 2009; Ming *et al.*, 2011). Yeast two hybridization showed that OsNAR2.1 not only interacted with OsNRT2.1/OsNRT2.2, but also with OsNRT2.3a (Ming *et al.*, 2011). In a study of NRT2/ NAR2 interactions in barley, it was suggested that the C-terminus of HvNRT2.1 is possibly involved in binding to the HvNAR2.3 central region and that the Ser463 present in the HvNRT2.1 C-terminus plays a role in the binding ability (Ishikawa *et al.*, 2009).

In addition to *AtNRT2.1* and *AtNRT2.2*, there are five other members of the *NRT2* gene family in *A. thaliana*, *NRT2.3* to *NRT2.7* (Orsel *et al*., 2002; Okamoto *et al*., 2003). Quantitatively, *AtNRT2.1* and *AtNRT2.2* are responsible for approximately 80% of IHATS in *A. thaliana* (Li *et al*., 2007). The remaining 20% is probably due to expression of a constitutive high-affinity transport system (cHATS) and *AtNRT1.1*. A role for *AtNRT2.7* in seed nitrate accumulation has been proposed by Chopin *et al.* (2007a), while Dechornat *et al*. (2012) showed correlation between *AtNRT2.6* expression and reactive oxygen species accumulation in response to infection by *Erwinia amylovora*. Expression patterns of all *NRT2* genes have been documented (Orsel *et al*., 2002; Okamoto *et al*., 2003), but their nitrate transport capacity and possible interactions with AtNAR2.1, with the exception of NRT2.1 and NRT2.2, are unknown.

Objective

In the present study, I have used heterologous expression in the yeast two-hybrid system and transient expression in Arabidopsis leaf protoplasts to examine possible interactions between *AtNAR2.1* and the other *NRT2* genes (*AtNRT2.2* to *AtNRT2.7*) and to localize the demonstrated interactions *in vivo.* To explore the physiological functions of the NRT2 polypeptides I have used transient expression of *AtNRT2.1* to *AtNRT2.7* (plus or minus *AtNAR2.1*) and $^{15}NO_3^-$ uptake into *Xenopus* oocytes.

Materials and methods

Membrane Yeast-Two-Hybrid screening for interaction of *AtNRT2* gene family with *AtNAR2* as bait

Membrane Yeast-Two-Hybrid (Y-2-H) screening for interactions of *AtNRT2* gene family members with *AtNAR2* was evaluated using the DUAL membrane kit from Dualsystems Biotech AG (Switzerland). cDNA of *AtNAR2.1* was cloned into Y-2-H bait vector pTMBV4 using XbaI and StuI restriction sites in frame with C-Ubiquitin. Correct expression of the *AtNAR2.1* bait construct was confirmed by co-expression with control plasmid Alg5-NubI (positive control) and Alg5-NubG (negative control). By transforming the bait strain with an empty prey vector pDL2Nx, it was determined that addition of 5mM of 3-amino-1, 2, 4-

triazole (3-AT) to minimal media was sufficient to decrease the sensitivity of *HIS3* reporter gene. cDNAs of all *AtNRT2* genes except for *AtNRT2.2* and *AtNRT2.7* were cloned into pDL2Nx prey vector using BamHI and EcoRI restriction sites, in frame with N-Ubiqutin. *AtNRT2.2* and *AtNRT2.7* were cloned into pDL2xN prey vector using BamHI/ EcoRI and BamHI/ ClaI restriction sites, respectively. Sequences of oligonucleotide primers used to clone all 7 members of the *NRT2* family and *AtNAR2.1* are shown in Appendix A (Table 3A). PEG-mediated transformation of yeast strain DSY-1 with bait and prey constructs was done according to Dualsystems Biotech manual. Transformation efficiency was checked on SD plates (0.2% w/v Difco™ yeast nitrogen base without amino acids (BD Biosciences, USA) and ammonium sulfate, 0.5% w/v ammonium sulfate, 0.1% w/v dropout mix, 2% w/v dextrose, 2% w/v agar) without leucine and tryptophan amino acids in the dropout mix. Screening for interaction of NRT2 proteins with AtNAR2.1 was achieved on SD plates without leucine, tryptophan and histidine, and by assay of β –galactosidase activity as per manufacturer's manual. Bait dependency tests were performed to exclude false positives by co-transforming NRT2 clones with control bait pMBV-Alg5 provided with the DUALmembrane kit.

Arabidopsis leaf protoplast isolation, transfection and confocal fluorescence imaging

Interaction of NRT2 proteins with AtNAR2.1 was investigated *in vivo* using the split-YFP method and transient expression in Arabidopsis protoplasts (Citovsky *et al.*, 2006). cDNA of *AtNAR2.1* was fused in frame to the N-terminal half of YFP in pSAT1A-nEYFP-N1 (XhoI/BamHI restriction sites). cDNAs of all *NRT2* genes were fused in frame with the C-terminal half of YFP using pSAT4A-cEYFP-N1 vector. PCR-amplified cDNAs of AtNRT2.1, 2.2, 2.3, 2.5 and 2.7 were inserted into pSAT4A-cEYFP-N1 using XhoI and BamHI restriction sites, while for AtNRT2.4 and 2.6 cloning EcoRI and KpnI restriction sites were used. All primer sequences are provided in Appendix A (Table 5A). Negative controls were plasma membrane ABC transporters ABCG11 and ABCG12 fused to C-YFP and N-YFP halves, respectively, provided by McFarlane *et al.* (2010). In addition, co-transfection with complementary empty vector was used as control. Arabidopsis leaf protoplasts were isolated and transfected with purified plasmid DNA according to the protocol by Tiwari *et al.* (2006). Detailed protocol is described in Chapter 2 of this thesis. The transfected protoplasts were visualized using the Spinning Disk PerkinElmer UltraView VoX Microscope (equipped

with Leica DMI6000 inverted microscope and Hamamatsu 9100-02 CCD camera) and Volocity software (PerkinElmer, USA).

AtNAR2.1 and *AtNRT2* gene family cloning and cRNA synthesis for *Xenopus* oocytes injections

cDNAs of all *AtNRT2* genes (*NRT2.1, NRT2.2, NRT2.3, NRT2.4, NRT2.5, NRT2.6, NRT2.7*) and *AtNAR2.1* were amplified using High Fidelity Phusion polymerase (Finnzymes, Finland). Primer sequences included Gateway® Technology recombination sites (Appendix A, Table 4A). Amplified cDNAs were combined with donor vector pDONR221 (Invitrogen, USA) using BP Clonase II (Invitrogen, USA) in BP recombination reaction to obtain entry clones. The entry clones were sequenced using M13 forward and reverse primers. Destination clones were prepared by LR recombination reaction utilizing pDONR221 clones, pGEMHE destination vector and LR Clonase II enzyme mix (Invitrogen, USA). pGEMHE vector contains 5' and 3' untranslated sequences of β-globin gene from *Xenopus laevis* to increase translation efficiency of heterologous RNA (Liman *et al.*, 1992). pGEMHE clones were digested with NheI enzyme, and 1 µg of digested purified DNA was used to synthesize cRNA with AmpliCap™ T7 High Yield Message Maker Kit (Epicentre, USA). Integrity of cRNA was determined on formamide denaturing TAE agarose gel (Masek *et al.*, 2005). Concentrations of cRNA were measured using RiboGreen® RNA kit (Molecular Probes, Invitrogen, USA), and adjusted to 500 ng μl^{-1}.

Xenopus oocytes harvesting and injections

Xenopus oocytes were harvested according to the protocol by Hill *et al.* (2005). Ovaries were surgically removed from a *Xenpous laevis* frog, and oocytes defoliculated in a 50 ml Falcon tube in Ca-free Ringers solution (96 mM NaCl, 2 mM KCl, 1 mM $MgCl_2$, 5 mM MES, pH 7.5) with 1.7 % (w/v) collagenase and 0.05 % (w/v) trypsin inhibitor, for 90 min with rotation. After digestion, oocytes were washed 3 times in hypotonic buffer (100mM K_2HPO_4, 0.1 % (w/v) BSA, pH 6.5), and then incubated for 10 min in fresh hypotonic buffer. Oocytes were then washed 2 times in Ca-free Ringers solution, and once in Ca-Ringers solution. Thereafter, oocytes were stored in Ca-Ringers solution supplied with 50 µg/ml tetracycline, 100 units/ml penicillin, 100 µg/ml streptomycin, and 5% (w/v) heat-inactivated Horse Serum (Sigma Aldrich, USA). Healthy-looking oocytes (stage V-VI) were selected for micro

injection of cRNA. Glass microcapillaries (Drummond Scientific, USA) were pulled using a Narishige puller on heat settings of 11.83 and 9. Capillary tips for injection were ground at a 45°-angle on Microgrinder EG-400 (Narishige, Japan). Selected oocytes were injected with 50 µl of RNAse-free water or cRNA using Nanoject II Auto-nanoliter injector (Drummond Scientific, USA). 25 ng was used for single gene cRNA injection, and 50 ng of cRNA was used for injection of *NRT2* cRNA together with *AtNAR2.1* (cRNA mixed 1:1 ratio).

Uptake of $K^{15}NO_3$ in *Xenopus* oocytes

Oocytes were incubated for 1 day after injection in Ca-Ringers solution (96 mM NaCl, 2 mM KCl, 0.6 mM $CaCl_2$, 1 mM $MgCl_2$, 5 mM MES, pH 7.5) supplied with 50 µg/ml tetracycline, 100 units/ml penicillin, 100 µg/ml streptomycin, and heat-inactivated Horse Serum (Sigma Aldrich, USA) to promote protein expression before the uptake experiments. During the second day of incubation Ca-Ringers was supplied with antibiotics only. Twenty oocytes were selected per treatment and washed once in N-free MBS uptake solution (96mM NaCl, 2mM KCl, 2mM $CaCl_2$, 1mM $MgCl_2$, 5mM MES; pH 6.5) for 5 min before the experiment. After washing solution was removed, 5 ml of MBS uptake solution with 500 µM $K^{15}NO_3$ (>98 atom % ^{15}N, Sigma Aldrich, USA) was added and healthy oocytes were incubated for 12 h at 18°C. Thereafter, oocytes were briefly washed 3 times in 5 ml of ice-cold N-free MBS, and single oocytes transferred into tin capsules (8x5mm, SerCon, UK), dried at 50°C for 2 days, pressed in the tin capsules, and isotope ratio was measured using SerCon Isotope Ratio Mass Spectrometer IRMS 20-22. Values obtained represent ^{15}N enrichment compared to standard atmospheric $^{15}N/^{14}N$ ratio (delta ^{15}N air).

Results

Membrane yeast two hybrid interactions

Yeast-two-hybrid heterologous expression was used to assess possible interaction between AtNAR2.1 and all members of the Arabidopsis NRT2 family. AtNAR2.1 was fused to the C-terminal half of ubiquitin using a bait vector, and each of the NRT2 genes was fused to the N-terminal half of ubiquitin in a prey vector. Yeast was transformed with AtNAR2.1 as bait and each of the NRT2 genes as prey individually. In addition, negative control bait vector (pMBV-Alg5) transformation was used for each of the NRT2 constructs. High transformation efficiency was confirmed on minimal nutrient media without leucine (for bait

vector) and tryptophan (for prey vector), as shown in Figure 3-1a and 3-1b. Screening for putative interaction was achieved using minimal nutrient media without leucine, tryptophan and histidine. Fig. 3-1a shows that NRT2 constructs did not interact with the negative control bait plasmid, while AtNRT2.1, 2.2, 2.3, 2.4, 2.5 and 2.6 showed significant growth when co-transformed with AtNAR2.1 as bait on minus His media (Fig. 3-1b). These results in the yeast system were confirmed by positive β-galactosidase assays (Fig. 3-1c). By contrast, AtNRT2.7, co-transformed with AtNAR2.1 as bait, failed to grow on media without histidine or give a positive β-galactosidase assay (Fig. 3-1b and 3-1c).

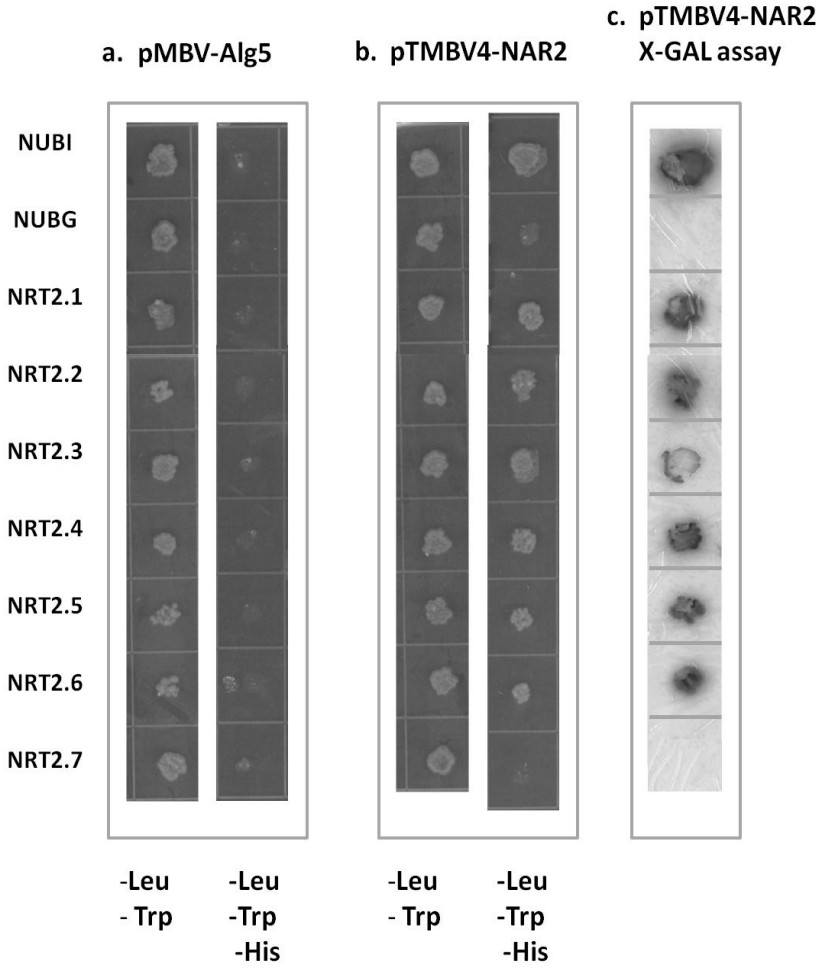

Figure 3-1. Heterologous expression and screening for interactions with AtNAR2.1 in the yeast two hybrid system. **a**. Expression of *NRT2* genes with negative control bait pALG5, growth of yeast on selective media without leu and trp (left panel), and without leu, trp and his (right panel). **b**. Expression of *NRT2* genes with *AtNAR2.1* bait, growth of yeast on selective media without leu and trp (left panel), and without leu, trp and his (right panel). **c**. X-gal assay on yeast colonies expressing *AtNAR2.1* and *NRT2* genes.

Transient *in planta* interactions between *AtNAR2.1* and *AtNRT2* genes in Arabidopsis protoplasts

The interactions of genes from the AtNRT2 family with AtNAR2.1 and possible localization of the interaction was investigated by transient *in vivo* expression of split YFP-labeled AtNAR2.1 and NRT2 genes in Arabidopsis leaf protoplasts. Fig. 3-3 shows bright field and fluorescence images of protoplasts transformed with one of *AtNRT2.2-cEYFP*, *AtNRT2.3-cEYFP*, *AtNRT2.4-cEYFP*, *AtNRT2.5-cEYFP*, *AtNRT2.6-cEYFP* and *AtNRT2.7-cEYFP* together with *ABCG12-nEYFP* vector as negative control. Only a very small amount of fluorescence was detected in the control protoplasts, mainly due to intrinsic fluorescence of the chloroplast (Fig. 3-3). On the other hand, protoplasts transformed with *AtNRT2.2-cEYFP* to *AtNRT2.6-cEYFP* and *AtNAR2.1-nEYFP* exhibited strong fluorescence localized mainly in the PM (Fig. 3-2). Protoplasts transfected with *AtNRT2.7-cEYFP* and *AtNAR2.1-nEYFP* failed to show strong fluorescence (Figure 3-2), indicating poor interaction of AtNRT2.7 with AtNAR2.1. It should be noted that in a previous Chapter 2 (Fig. 2-8) we demonstrated strong interactions between AtNRT2.1 and AtNAR2.1 in this protoplast system.

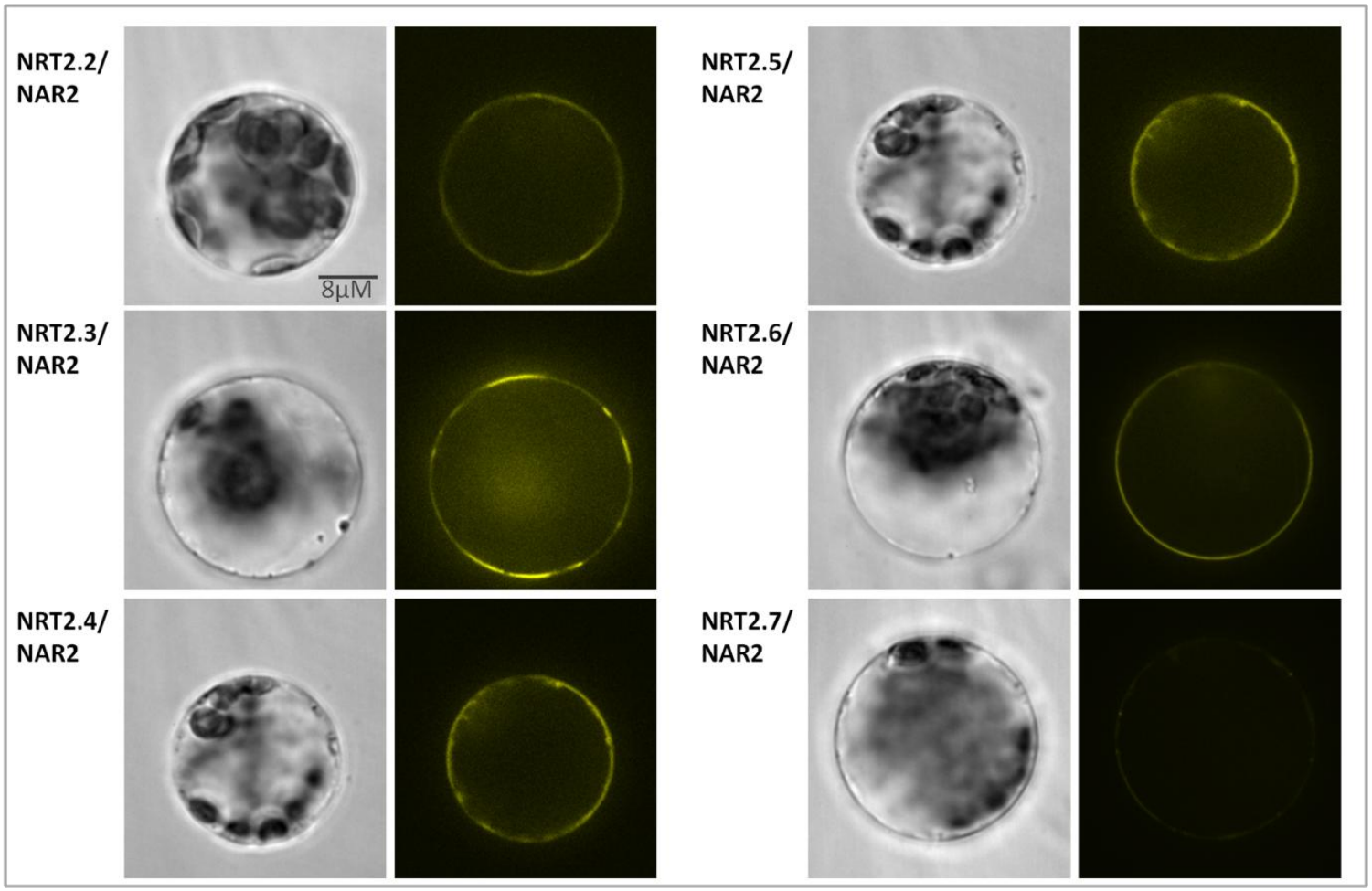

Figure 3-2. Bright field (left) and confocal fluorescence images (right) of protoplasts transfected with *NRT2.2-2.7* genes fused to cEYFP and *NAR2.1-nEYFP*.

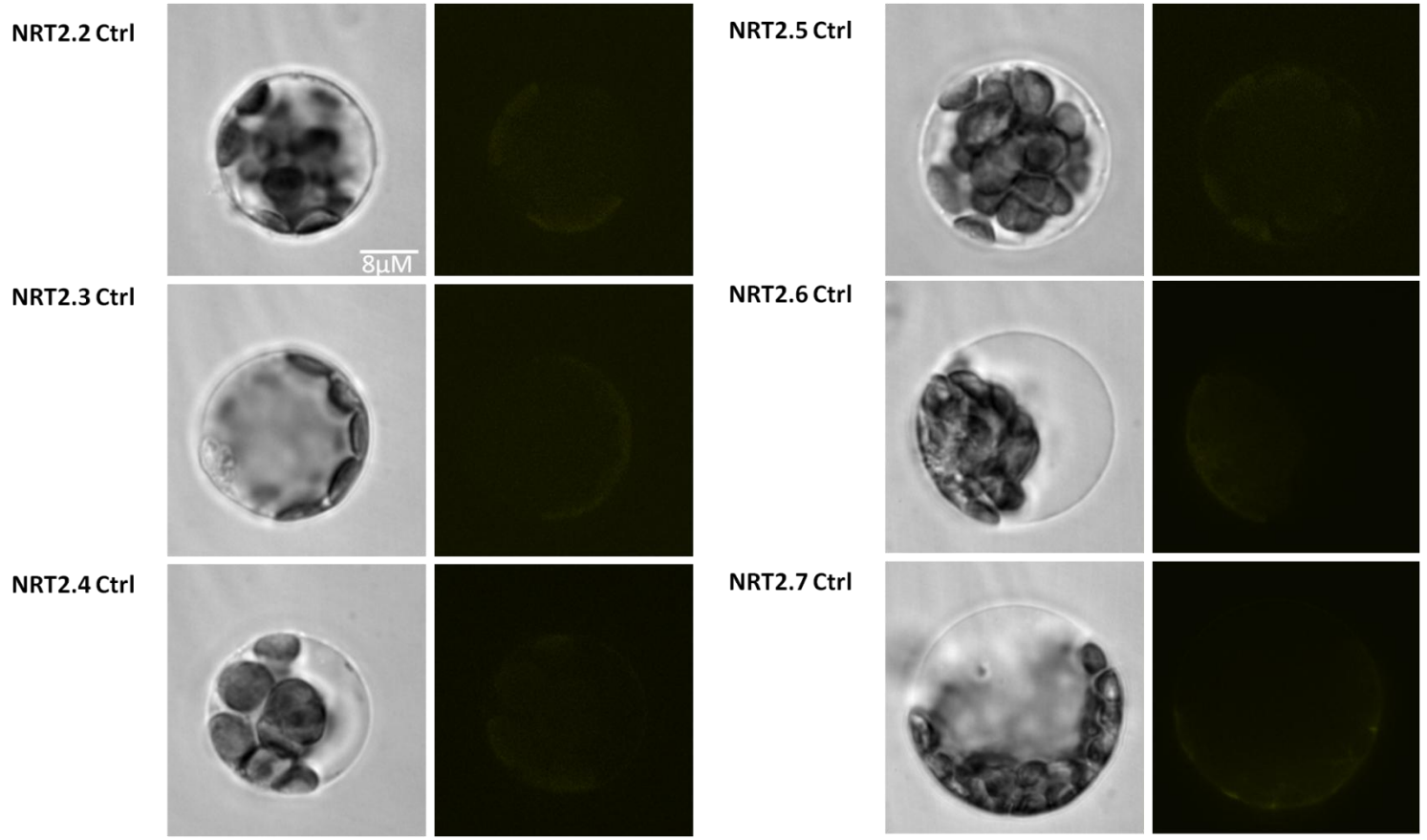

Figure 3-3. Bright field (left) and confocal fluorescence images (right) of protoplasts transfected with *NRT2.2-2.7* genes fused to cEYFP and ABCG12fused to nEYFP used as negative control.

Uptake of $K^{15}NO_3$ into *Xenopus laevis* oocytes

Controls for the putative interactions were provided by injecting healthy oocytes with either water, or with 25 ng of cRNA encoding each of AtNAR2.1, AtNRT2.1, AtNRT2.2, AtNRT2.3, AtNRT2.4, AtNRT2.5, AtNRT2.6 and AtNRT2.7. To test for functional interactions between AtNAR2.1 and AtNRT2 proteins, oocytes were also injected with mixtures of AtNAR2.1 cRNA and cRNA of each of the *NRT2* genes. After 2 days of cRNA expression, injected oocytes were incubated in 0.5 mM $K^{15}NO_3$ for 12 h. Uptake of $K^{15}NO_3$ was evaluated through measurement of ^{15}N enrichment of oocytes by Isotope Ratio Mass Spectrometry, and expressed compared to standard atmospheric $^{15}N/^{14}N$ ratios (delta ^{15}N air). Oocytes expressing NRT2s co-injected with AtNAR2.1 showed significant ($p<0.05$) increase in $^{15}NO_3$ uptake when compared to oocytes injected with NRT2s alone (Fig. 3-4). AtNRT2.5 showed the most prominent increase in $^{15}NO_3^-$ uptake, while AtNRT2.4 and AtNRT2.7 gave the lowest increment. Values presented are from a single experiment, with at least 8 oocytes per cRNA injection. Experiments were repeated 3 times and showed similar values.

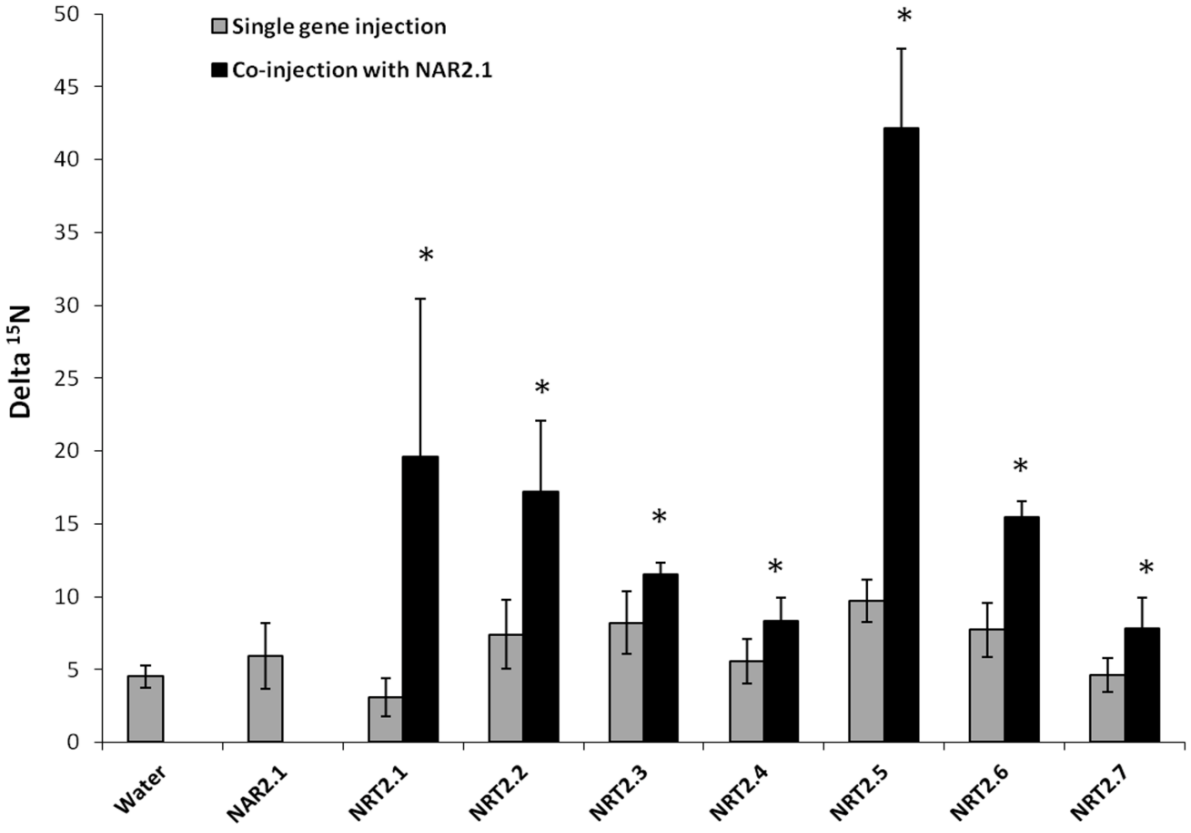

Figure 3-4. $K^{15}NO_3$ uptake into *Xenopus* oocytes. Grey bars: oocytes injected with water, cRNA of NAR2.1 alone, and single NRT2 genes; Black bars: oocytes injected with mixture

of NAR2.1 and individual NRT2 genes cRNA. ^{15}N enrichment per oocyte is expressed as delta ^{15}N compared to standard atmospheric $^{15}N/^{14}N$ ratio. Values are average of n=8 ± SD. ANOVA followed by *t* tests for single and co-injection with NAR2.1; * significant at $P<0.05$.

Discussion

Functional iHATS nitrate transport in Arabidopsis by AtNRT2.1 requires co-expression of AtNAR2.1. The results of the earlier studies using the yeast two-hybrid system had established that AtNAR2.1 interacts with AtNRT2.1 (Orsel *et al.*, 2006). The results of the present yeast two-hybrid study establish that AtNAR2.1 also interacts with AtNRT2.2, AtNRT2.3, AtNRT2.4, AtNRT2.5, and AtNRT2.6 based upon growth on minus histidine media and the β-galactosidase test (Fig. 3-1). The fact that AtNRT2.7 failed to interact with AtNAR2.1 represents an exception to the apparent generality that all of the Arabidopsis NRT2s interact with AtNAR2.1. The *in vivo* assays of the association between AtNAR2.1 and AtNRT2.2-2.7, by means of the split YFP-labeled AtNAR2.1 and NRT2 genes in Arabidopsis leaf protoplasts confirmed the results of the yeast two-hybrid assays. Thus in this expression system using Arabidopsis protoplasts, fluorescence of the split YFP was recovered after co-transfection of all NRT2s with AtNAR2, except that AtNRT2.7 gave only a very weak fluorescence signal (Fig. 3-2). Based upon these observations, AtNRT2.7 may be unique among AtNRT2 transporters. Further support for this hypothesis is provided by the following reports:

1. AtNRT2.7 was shown to be a tonoplast transporter (Chopin *et al.*, 2007a).
2. Of all AtNRT2s, AtNRT2.7 shows the lowest amino acid sequence similarity with AtNRT2.1 (Orsel *et al.*, 2002).
3. A recent phylogenetic study of NRT genes, demonstrated that the AtNRT2.7 is the most divergent of all NRT2s and that there are no NRT2.7-like genes in genomes of sequenced grasses or in poplar (Plett *et al.*, 2010).

The results of the *Xenopus* study establish that AtNRT2.1, AtNRT2.2, AtNRT2.5 and AtNRT2.6 all strongly promote nitrate influx when co-injected with AtNAR2.1. AtNRT2.3, AtNRT2.4 and AtNRT2.7 all produced much smaller, yet statistically significant, increases of nitrate influx (Fig. 3-4). Interestingly, Chopin *et al.* (2007a) concluded that in the *Xenopus*

assay AtNRT2.7 alone (in the absence of AtNAR2.1) was able to increase $^{15}NO_3^-$ uptake over and above water-injected oocytes. However, the authors did not assay the effect of co-injecting AtNAR2.1.

Chapter 4. Diverse mechanisms for nitrate transporter function in *A. thaliana* and *A. nidulans*

Background

Although HATS in Arabidopsis depends upon expression of both AtNRT2.1 and AtNAR2.1, in the fungus *Aspergillus nidulans* no equivalent to the AtNAR2.1 gene is present (Unkles, personal communication) and in the *Xenopus* oocyte system nitrate fluxes were generated when AnNRTA (the Aspergillus NRT2 homolog) alone was expressed (Zhou *et al.*, 2000b). In addition to NRTA, a second closely-related HATS (NRTB) participates in nitrate uptake in *A. nidulans* (Unkles *et al*., 2001). There appears to be no other nitrate transporter, because *nrtA-nrtB* null mutants fail to grow on nitrate and show no $^{13}NO_3^-$ influx (Fig. 4-1).

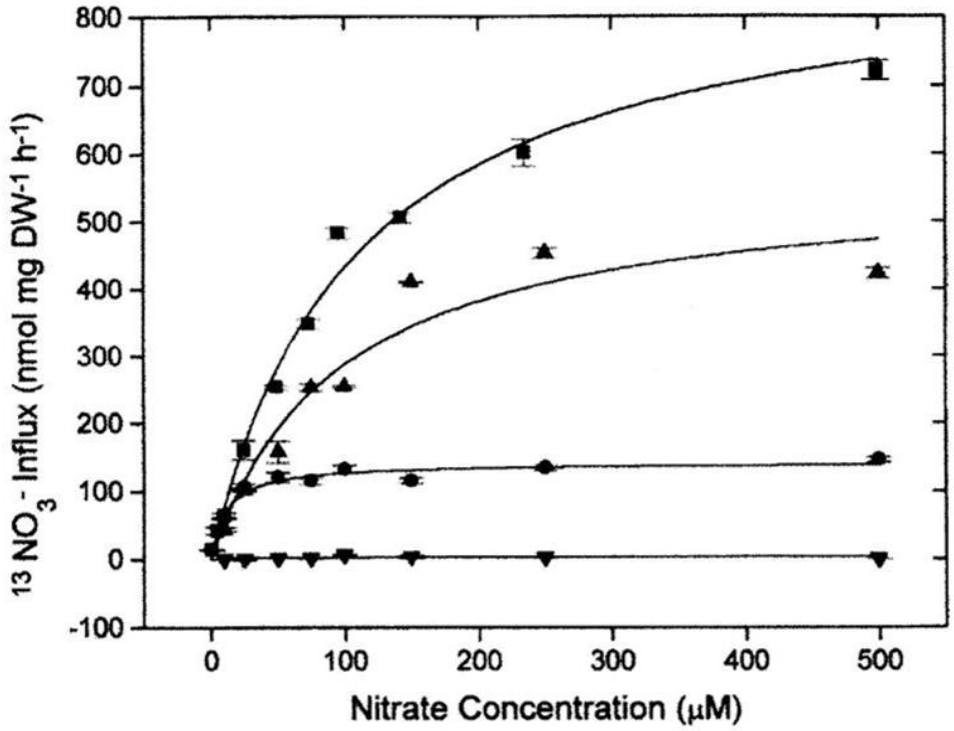

Figure 4-1. $^{13}NO_3^-$ influx values for *Aspergillus nidulans* wild type (squares), mutant *nrtA747*, expressing only NRTB protein (circles), mutant *nrtB110*, expressing only NRTA protein (upright triangles), and the double mutant *nrtB110 nrtA747*, expressing neither protein (inverted triangles), measured at various nitrate concentrations. Adapted by permission from Macmillan Publishers Ltd: The EMBO Journal (Unkles *et al.*, 2001), copyright (2001).

By contrast, and consistent with other lines of evidence, in *C. reinhardtii* only when both CrNRT2.1 and CrNAR2 were co-injected into *Xenopus* oocytes was nitrate influx obtained.

This was also the case for the barley homologs HvNRT2.1 and HvNRT2.3 (Tong *et al.*, 2005). This difference between the fungal and plant systems may be related to the central cytoplasmic loop between transmembrane regions 6 and 7 and/or to the long plant C-terminus. In plants (including *Chlamydomonas*) the cytoplasmic loop is considerably smaller than that of *A. nidulans* and *H. polymorpha*. For example, the *A. thaliana* NRT2.1 loop consists of 21 amino acids compared to 91 amino acids in the *A. nidulans* NRTA.

Objective

In order to characterize iHATS nitrate transport by the AtNRT2.1/AtNAR2.1 complex in the absence of possible confounding effects of other plant nitrate transporters, and to further explore the interactions between AtNRT2.1 and AtNAR2.1, expression of AtNRT2.1 and AtNAR2.1 was examined in the fungus *Aspergillus nidulans*. In addition, AtNRT2.1 was modified whereby a chimeric protein was designed by substituting the AtNRT2.1 central loop (between 6^{th} and 7^{th} membrane spanning region) with the *A. nidulans* central loop. Functional properties of the chimeric protein NRT2.1-AnLoop were tested in *A. nidulans*, *Xenopus* oocytes and Arabidopsis.

Material and methods

Fungal Strains

A. nidulans strains used in this study, wild type biA1 and the double deletion mutant T110, nrtA747 nrtB110 (disrupted in both *NRTA* and *NRTB* genes), were described earlier by Unkles *et al.* (2001).

A. nidulans transformation

Details of the selection strategy and transformation procedure for *A. nidulans* were described previously (Riach and Kinghorn, 1996). For direct selection on minimal medium containing nitrate as sole nitrogen source, strain JK900 (*nrtA747 nrtB110*) was used as recipient, and for indirect selection on the basis of arginine prototrophy, strain JK1060 (*nrtA747 nrtB110 argB2*) was the recipient. Conidia of the fungal strains (two 90 mm plates) were inoculated into 2 flasks with 400 ml of minimal media (Appendix B) with 5 mM urea added as a N source and 400 µl 1000x Vitamins stock (Appendix B). The flasks were stored in a freezer for 4 h, and then grown overnight at 25°C, on a shaker platform at 250 rpm. The young mycelia were harvested through Calbiochem® Miracloth and washed with chilled 0.6 M

$MgSO_4$. The cells were resuspended in 5 ml of OSMO (Appendix B), and 1 ml of Glucanex® (Novozymes, Denmark) solution (100 mg enzyme in 1 ml OSMO) was added, plus 1 extra ml of OSMO used to wash the enzyme tube, and 0.25 ml of BSA solution (12 mg/ml OSMO). The cells were shaken at 30°C, 60-80 rpm for 3.5 h to release protoplasts. The protoplasts were separated from the cell debris by adding an equal volume of trapping buffer (Appendix B) to the suspension and centrifuging at 5000 rpm at 4°C for 20 min. Protoplasts accumulate at the interface of trapping buffer and cell suspension, and were harvested using a Pasteur pipette and washed in 15 ml cold sorbitol-tris-calcium buffer (STC) (Appendix B). After being recovered by centrifugation (5 min at 7000 rpm), the protoplasts were resuspended in an appropriate volume of STC (90 µl needed for one transformation). 90 µl of protoplasts were added to a sterile 10 ml tube containing DNA and STC to 10 µl (0.5 µg DNA and 0.5-0.7 µg pHELP plasmid (Gems and Clutterbuck, 1993). 25 µl of 60% PEG 6000 was added to each tube, and incubated at room temperature for 20 min. Thereafter 1 ml of the PEG was added to the tube and incubated for 20 min at room temperature. 5 ml of STC was added to the tube and spun at 3500 rpm for 5 min. The pellets were resuspended in 100 µl of STC and spread on 2 minimal media selection plates with 1.2 M sorbitol as osmoticum and 10 or 100 mM sodium nitrate for direct selection, or 5 mM ammonium tartrate for indirect selection. Plates were incubated at 37°C for 4-5 days.

Generation of fungal expression constructs

A plasmid for nitrate inducible expression of *AtNRT2.1* was generated by amplification of the coding region from Arabidopsis root cDNA to create a fragment with *Eco*RI ends, which was cloned into vector pMUT (Unkles *et al*., 2005) such that the coding region was under the control of the *A. nidulans nrtA* promoter and terminator, yielding plasmid pMUT2186. Plasmids for nitrate-inducible co-expression of the *AtNRT2.1* and *AtNAR2.1* were generated in the twin reporter vector pTRAN3-1 (Punt *et al*., 1991) such that the *AtNRT2.1* coding region was under the control of the *niiA* promoter and the *AtNAR2.1* under the control of the *niaD* promoter in plasmid pATP. Plasmid pATP2 contained the genes in exchanged order with respect to the promoters. Plasmids pMUT and pTRAN3-1 also contain the *argB** gene for indirect selection targeting to the *argB* locus allowing for both direct and indirect selection strategies with these vectors. For expression of the chimeric protein, the coding region of AtNRT2.1 with *Eco*RI ends was cloned into pUC8. *Eco*RV and *Xho*I sites were

introduced by PCR overlap extension (Warrens *et al*., 1997) in the regions encoding the N-terminal and C-terminal ends, respectively, of the predicted loop 6/7 between transmembrane domains 6 and 7. The DNA encoding *A. nidulans* loop 6/7 was amplified by PCR with *Eco*RV and *Xho*I ends and cloned in replacement of the AtNRT2.1 loop 6/7 region. The EcoRI fragment was cloned into pMUT such that the recombinant coding region was under the control of the *A. nidulans nrtA* promoter and terminator to give plasmid pNRT2.1loop. Expression of the resulting protein would result in a chimera composed of AtNRT2.1 N-terminal region up to and including residue D248 and the C-terminal region from F268 (inclusive), encompassing 91 residues of the predicted NRTA loop 6/7 from residues P223 to S313 inclusive. In addition, the final cloning introduced a sequence encoding a V5 epitope tag fusion to the C-terminus of the protein. PCR amplified regions of all plasmids were verified by DNA sequencing of the amplified region and covering the cloning sites.

Crude membrane preparation from *A. nidulans*

Conidia from one 90-mm plate were inoculated into 200 ml minimal media (Appendix B) including 10 mM proline and 200 µl vitamins (1000x stock), and grown at 37°C, 250 rpm for 4 h 20 min. 2 ml of 1M KNO_3 were added and incubated for additional 100 min until conidia had just germinated. Cells were harvested through Miracloth, washed with cold water, and frozen in liquid nitrogen. Approximately 300 mg of cells were ground in liquid N_2 using mortar/ pestle, and further macerated in 10 ml cold extraction buffer (50 mM sodium phosphate, 300 mM NaCl, 10% glycerol, pH 7). The solution was centrifuged at 5000 g for 10 min, 4°C, to remove cell debris. Supernatant was transferred to a fresh tube, and centrifuged at 80000g for 30 min at 4°C. The pellet was resuspended in 70 µl of extraction buffer, and diluted 4 times with SDS sample buffer (50 mM Tris-HCl pH6.8, 25% glycerol, 2% (w/v) SDS, 0.01% (w/v) bromophenol blue) prior to separation on SDS-PAGE, and Western blotting.

$^{13}NO_3^-$ influx in *A. nidulans*

Growth of strains and assay of ^{13}N-nitrate influx at the standard concentration range for high-affinity transport (10 to 250 µM) were as detailed in Unkles *et al.* (2004). One 90 mm plate of conidia was inoculated in 200 ml minimal media with vitamins and 5 mM urea (Appendix B), and grown for a total of 6.5 h at 37°C. 100 min prior to harvesting 1 ml of 1 M potassium nitrate was added to induce the nitrate assimilation genes. Following harvesting by filtration

through Miracloth and washing in N-free minimal media to remove excess nitrate, mycelia were resuspended in 60 ml of fresh N-free minimal media in 250 ml Erlenmeyer flasks. The flasks were shaken in a water bath at 37°C, and prior to the start of influx measurement, supplied with appropriate concentration of potassium nitrate and an aliquot of $^{13}NO_3^-$ stock. After 5 min nitrate uptake, 10 ml aliquots of cells were filtered individually through 25 mm glass fiber filters (type GF/C, Whatman, Maidstone, UK) and washed twice with 200 ml of 200 µM nitrite to remove unabsorbed tracer. Each filter was placed into a plastic scintillation vial and the radioactivity measured by counting in a gamma counter (MINAXI Auto-Gamma 5000 series, Packard Instruments, USA). Three 30 ml samples of cell suspension used in the experiment were filtered and air-dried to estimated dry weights needed to calculate influx.

Plant growth conditions and transformation

Atnar2.1-2 mutant was used as a recipient of the chimeric protein AtNRT2.1-AnLoop described above. The *AtNRT2.1-AnLoop* was amplified from *A. nidulans* DNA template by high fidelity enzyme (Phusion®, Finnzymes) and ligated into pGreenII0179 vector (Hellens *et al.*, 2000a; Hellens *et al.*, 2000b) using XmaI and XbaI restriction sites, downstream of CaMV 35S promoter. Plant transformation and selection of transformants are described in Chapter 2 of this thesis. Arabidopsis plants WT (Wassilewskija), *Atnar2.1-2* and *Atnar2.1-35S:NRT2.1-AnLoop* lines were grown on solid low and high nitrate MS salts media as described in Chapter 2 of this thesis.

mRNA expression in *A. thaliana*

Total RNA was isolated from young Arabidopsis plants (WT and *Atnar2.1-35S:NRT2.1-AnLoop*) using TRIzol® (Invitrogen, USA), then RT-PCR reaction performed to synthesize cDNA as described in Chapter 2. In order to confirm expression of the gene coding for the chimeric protein with the modified 6/7 loop, PCR was done on the cDNA template using primers specific to the *A. nidulans* loop sequence (F 5'GATATCACCCCGACTGGAAA3' and R 5'CTCGAGGCTGAATATAACATTAAAAG3'). Isolated RNA was used as a negative control template to check for possible DNA contamination.

Membrane yeast-two-hybrid protein interaction

Details of membrane yeast-two-hybrid experimental design are given in Chapter 3. Primers used to amplify and clone *AtNRT2.1-AnLoop* were the same as those used for *AtNRT2.1*.

Once the gene was cloned into appropriate vectors, sequences were verified by DNA sequencing.

Expression of AtNRT2.1-AnLoop in *Xenopus* oocytes

Details of experimental methods involved in expression of AtNRT2.1-AnLoop in *Xenopus* oocytes are given in Chapter 3. Primers used to amplify and clone *AtNRT2.1-AnLoop* were the same as those used for *AtNRT2.1*. Once the gene was cloned into appropriate vectors, sequences were verified by DNA sequencing.

Results

Expression of AtNT2.1 and AtNAR2.1, and AtNRT2.1-AnLOOP in *Aspergillus nidulans*

In order to attempt to express AtNRT2.1, either alone or together with AtNAR2.1 in *Aspergillus nidulans*, we made use of the double deletion mutant *nrtA747 nrtB110* (disrupted in both *nrtA* and *nrtB* genes) that is incapable of growth on nitrate as sole source of N (Unkles *et al.*, 2001). None of our transformants were capable of growth on nitrate as a sole N source, indicating that AtNRT2.1/AtNAR2.1 complex is either not expressed or non-functional in *A. nidulans*. Next, the *AtNRT2.1* central cytoplasmic loop (between transmembrane regions 6 and 7) was replaced by the much larger *A. nidulans* loop to generate *AtNRT2.1-AnLoop* (Fig. 4-2a and 4-2b). The AnLoop shares between 17 and 24 % amino acid sequence identity with NAR2.1-like proteins from different plant species (Table 4-1). Resulting *A. nidulans* recombinants were found to grow successfully on nitrate as sole N source, and Western blot analysis using anti-V5 antibody confirmed that the chimeric protein AtNRT2.1-AnLoop was expressed in membranes of *A. nidulans* (Fig. 4-3). Unkles *et al.* (2001) examined nitrate influx in WT and mutants of *Aspergillus* nitrate transporters NRTA and NRTB (Fig. 4-1). The authors clearly demonstrated inability of the double *nrta nrtb* mutant to take up nitrate. The *AtNRT2.1-AnLoop* was able to complement the double mutant phenotype, where $^{13}NO_3^-$ influx measurements of *Aspergillus* double mutant strain expressing AtNRT2.1-AnLoop gave values that were close to those of WT. Figure 4-4 shows data from one such experiment that gave Km and Vmax values of 14.4 ± 4 µM and 789.4 ± 47 nmol mg^{-1}DW h^{-1}, respectively. A direct fit of this data to a hyperbolic Michaelis-Menten curve gave an r^2 value of 0.86.

a

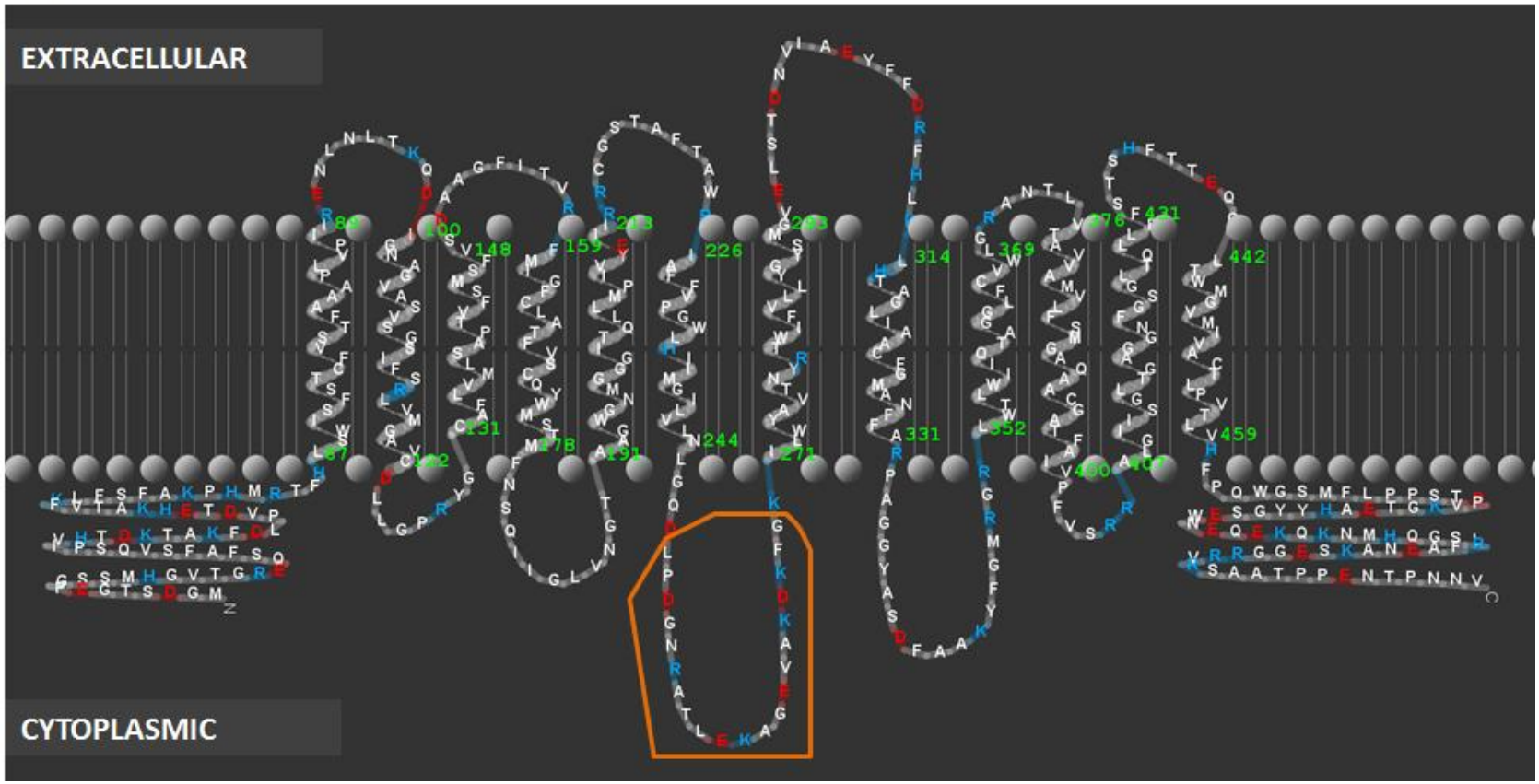

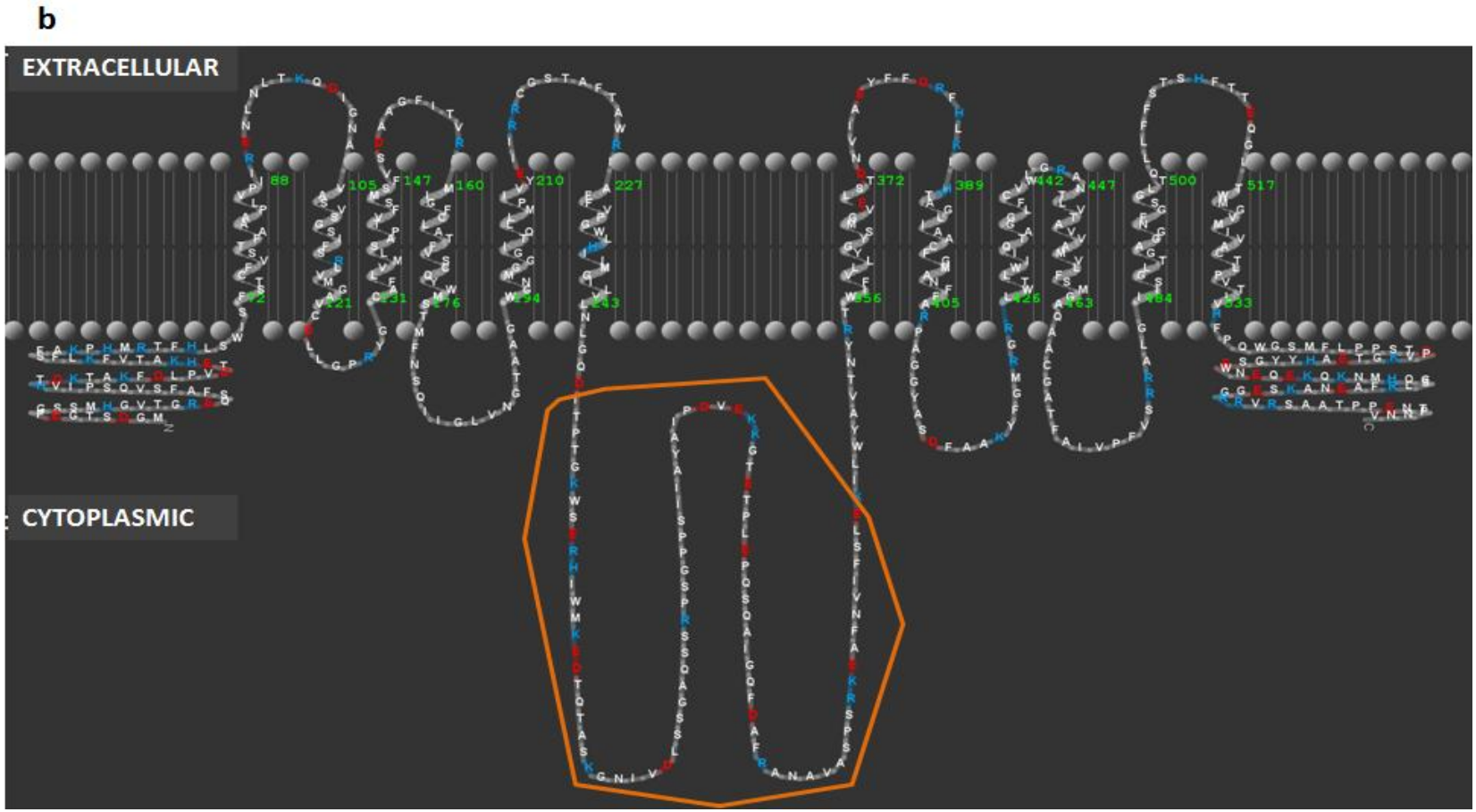

Figure 4-2. a. Two-dimensional model of Arabidopsis AtNRT2.1 polypeptide. **b**. Two-dimensional model of Arabidopsis AtNRT2.1 polypeptide with central cytosolic loop from *Aspergillus nidulans* NRTA; positively charged residues are in blue and negatively charged residues in red. The central cytoplasmic loops are framed in orange. Models made by TMRPres2D (Spyropoulos *et al.*, 2004) based on topology prediction by HMMTOP 2.0 server (Tusnády and Simon, 1998; Tusnády and Simon, 2001).

Table 4-1. Percent of amino acid sequence identity between *Aspergillus nidulans* loop (between transmembrane regions 6 and 7) and NAR2.1 homologs from different plant species. Identity calculated by Muscle alignment software (Edgar, 2004)

Protein Sequence	% Identity
AnLoop	**100.00**
gi|37955231| [Hordeum vulgare subsp. Vulgare]	**24.14**
gi|482549803| hypothetical protein [Capsella rubella]	**23.91**
gi|356563139| high-affinity nitrate transporter NAR2.1-like [Glycine max]	**22.83**
AtNAR2.1	**21.74**
gi|223550420| conserved hypothetical protein [Ricinus communis]	**21.74**
gi|297733682| unnamed protein product [Vitis vinifera]	**21.74**
gi|470126346| high-affinity nitrate transporter NAR2.1-like [Fragaria vesca]	**19.57**
gi|283132357| component of high affinity nitrate transporter [Lotus japonicus]	**19.57**
gi|222834907| predicted protein [Populus trichocarpa]	**17.39**

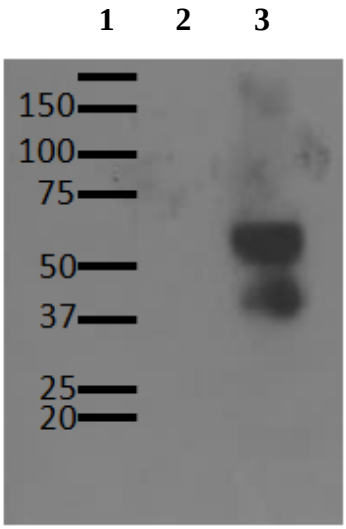

Figure 4-3. Western blot of membrane protein isolated from young mycelia cells of *Aspergillus nidulans* after SDS-PAGE, probed with anti-V5 antibody. Lane 1: Precision Plus^{TM} protein standard. Lane 2: wild type cells; Lane 3: AtNRT2.1-AnLoop cells.

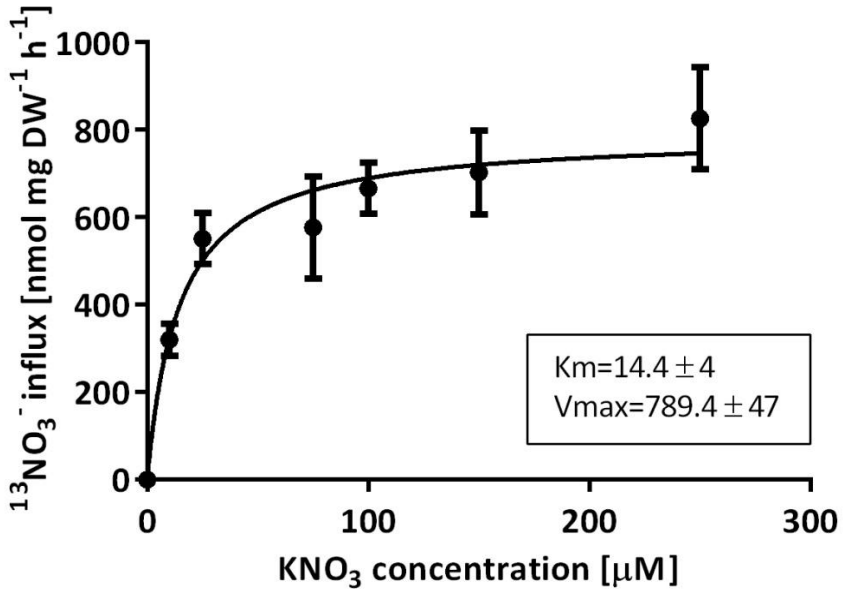

Figure 4-4. $^{13}NO_3^-$ influx in *Aspergillus nidulans* double mutant *nrtB110 nrtA747* expressing *AtNRT2.1-AnLoop*. Values are average of n=5 ± SD. The fitted line is a direct Michaelis-Menten fit, with estimated vales for Km [μM] and Vmax [nmol mg DW^{-1} h^{-1}].

Heterologous expression of AtNRT2.1-AnLOOP with and without AtNAR2.1

In order to check the effect of the central loop modification on interaction of AtNRT2.1 with AtNAR2.1, I co-expressed both polypeptides in the Y2H system. Co-expression of AtNRT2.1-AnLoop with AtNAR2.1 as bait in the yeast-two-hybrid system failed to provide any evidence of interaction between the two proteins, while positive control NUBI and AtNRT2.1 showed strong interaction with ATNAR2.1 (Fig. 4-5b). The interaction was confirmed by β-galactosidase assay where blue-colored product of X-gal hydrolysis appeared quickly in yeast cells expressing both AtNRT2.1 and AtNAR2.1, but not in cells with AtNRT2.1-AnLoop and AtNAR2.1 (Fig. 4-5c).

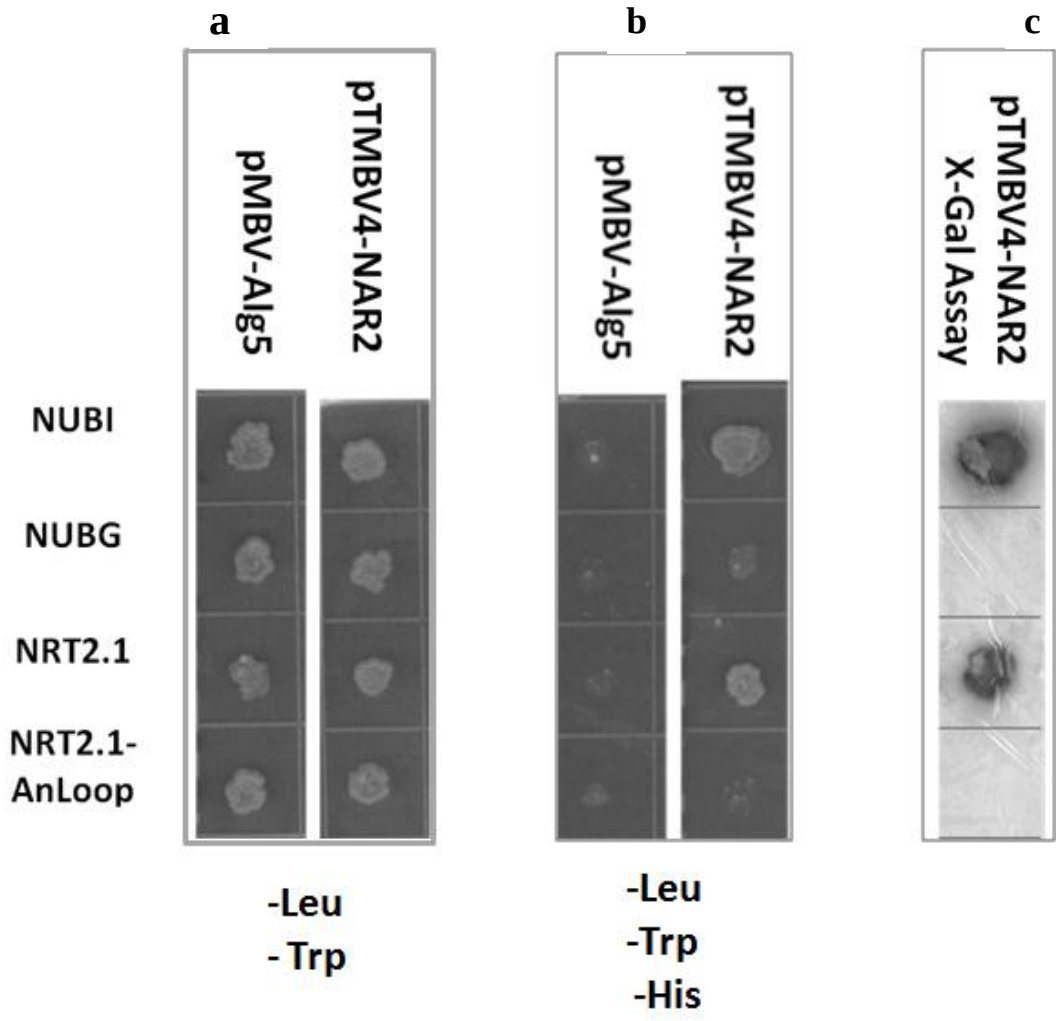

Figure 4-5. Heterologous expression and screening for interactions with AtNAR2.1 in the yeast two hybrid system. **a**. Expression of *NRT2.1* and *NRT2.1-AnLoop* with negative control bait pALG5 and *AtNAR2.1*, growth of yeast on selective media without leu and trp. **b.** Expression of *NRT2.1* and *NRT2.1-AnLoop* with negative control bait pALG5 and *AtNAR2.1*, growth of yeast on selective media without leu, trp and his. **c.** X-gal assay on yeast colonies expressing *AtNAR2.1* and *NRT2.1* and *NRT2.1-AnLoop*.

Interaction between AtNRT2.1-AnLOOP and AtNAR2.1, and the capacity of AtNRT2.1-AnLOOP to transport nitrate were also examined in *Xenopus* oocytes. Controls for the putative interactions were provided by injecting healthy oocytes with either water, or with 25 ng of cRNA encoding each of AtNRT2.1 and AtNRT2.1-AnLoop. To test for functional interactions between AtNAR2.1 and the two proteins, oocytes were also injected with mixtures of AtNAR2.1 cRNA and cRNA of each of the two genes. After 2 days of cRNA expression, injected oocytes were incubated in 0.5 mM $K^{15}NO_3$ for 12 h. Uptake of $K^{15}NO_3$

was evaluated through measurement of ^{15}N enrichment of oocytes by Isotope Ratio Mass Spectrometry, and expressed compared to standard atmospheric $^{15}N/^{14}N$ ratios (delta ^{15}N air). Oocytes expressing AtNRT2.1 co-injected with AtNAR2.1 showed significant increase in $^{15}NO_3$ uptake when compared to oocytes injected with NRT2s alone (Fig. 4-6). On the other hand, AtNRT2.1-AnLoop showed no significant ^{15}N enrichment compared to water-injected oocytes, either expressed alone or co-expressed with AtNAR2.1 (Fig. 4-6).

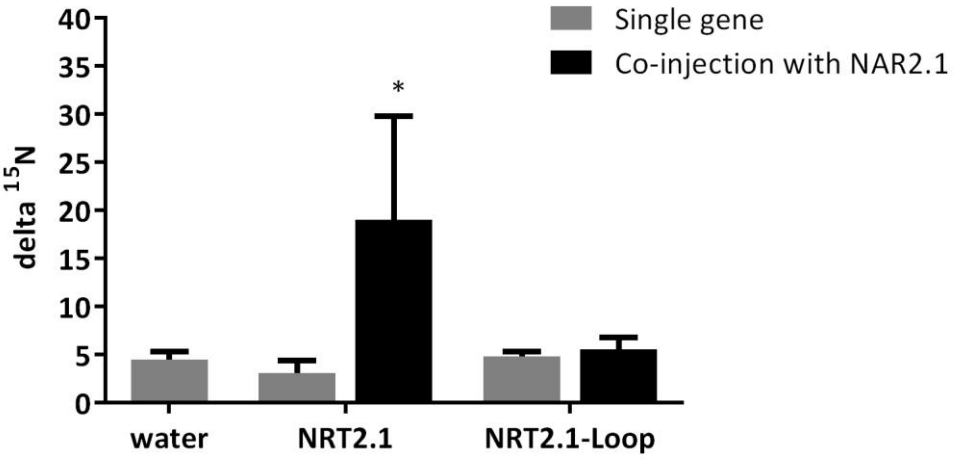

Figure 4-6. $K^{15}NO_3$ uptake into *Xenopus* oocytes. Grey bars: oocytes injected with water, cRNA of single *AtNRT2.1* and *AtNRT2.1-AnLoop* genes; Black bars: oocytes injected with mixture of *AtNAR2.1* and individual *AtNRT2.1* and *AtNRT2.1-AnLoop* cRNA. ^{15}N enrichment per oocyte is expressed as delta ^{15}N compared to standard atmospheric $^{15}N/^{14}N$ ratio. Values are average of n=10 ± SD; * indicates significance as in Fig. 3-4.

Expression of AtNRT2.1-AnLoop in Arabidopsis

When *AtNRT2.1-AnLoop* was expressed in Arabidopsis mutants *Atnar2.1-1* (defective in HATS) under strong 35S CaMV promoter, plants exhibited phenotype similar to that of the *Atnar2.1-1* mutant plants, even though mRNA expression analysis confirmed that the modified loop was expressed in transgenic lines (Fig. 4-7). Figure 4-8a shows poor growth of *Atnar2.1-1* and transformed *Atnar2.1-1-35S:NRT2.1-AnLoop* compared to WT on low nitrate nutrient media (250 µM KNO_3). All three genotypes show similar growth on 10 mM KNO_3 media (Fig. 4-8b).

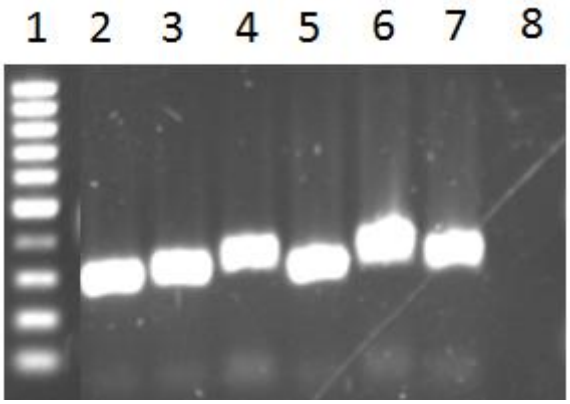

Figure 4-7. Expression of *AtNRT2.1-AnLoop* mRNA in seedlings of different lines of *Atnar2.1-2- 35S: AtNRT2.1-AnLoop*. Lanes: **1**. 100bp DNA marker (GeneRuler, Fermentas, USA); **2**. Transformant line 1; **3**. Transformant line 2; **4**. Transformant line 3; **5**. Transformant line 4; **6**. Transformant line 5; **7**. Transformant line 6; **8**. *Atnar2.1-2* mutant

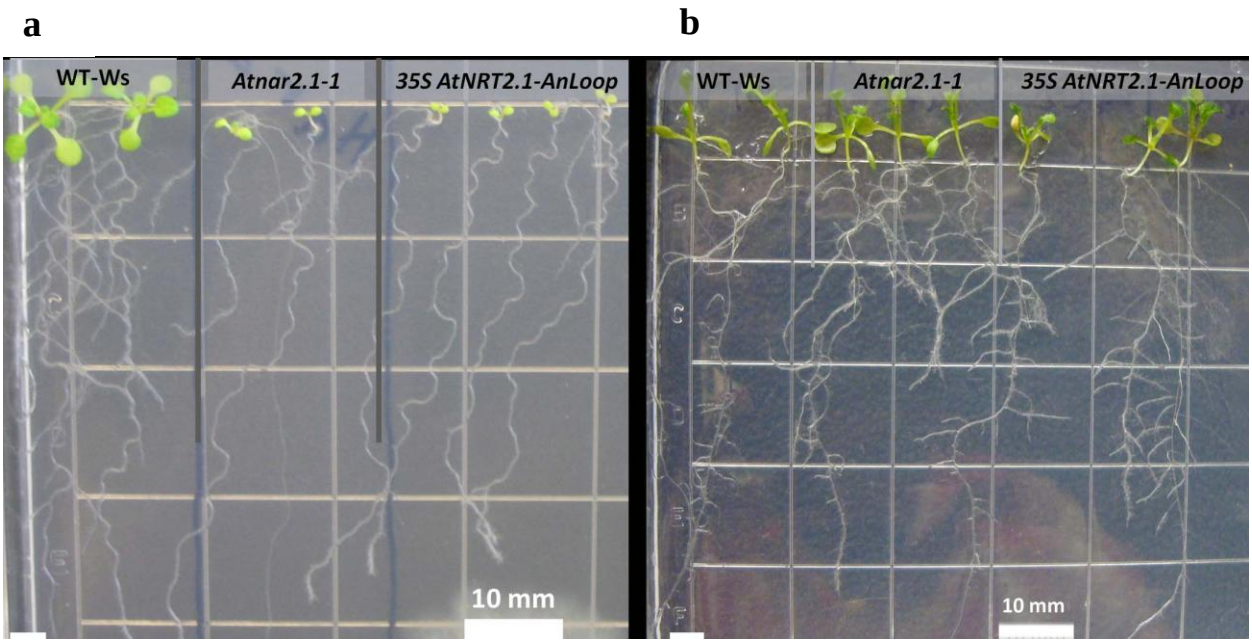

Figure 4-8. Growth of various *Arabidopsis thaliana* lines (WT-Ws, *Atnar2.1* mutant, and *Atnar2.1-35S:AtNRT2.1-AnLoop*) on ½ strength MS salts agar media containing: **a**. 0.25 mM KNO_3 and **b**. 5 mM KNO_3.

Discussion

The plant NRT2 family of Nitrate-Nitrite Porters (NNPs) belongs to the Major Facilitator Superfamily of transporters. They all have 12 predicted transmembrane regions (TMR's)

connected by short hydrophilic loops, except between TMR 6 and 7 where the cytoplasmic loop is larger. Nevertheless, the cytoplasmic loop length differs greatly among different species. Good examples are Arabidopsis with a relatively small loop of 21 amino acids and *Aspergillus nidulans* with a substantially longer loop of 91 amino acids (Forde, 2000; Fig. 4-1). Both polypeptide ends of NNPs are located at the cytosolic side of the PM (reviewed in Forde, 2000; Law *et al.*, 2008; Saier *et al.*, 1999; Fig. 4-1).

Evidence presented in Chapter 2 of the 150 kDa AtNAR2.1/AtNRT2.1 complex localized in PM preparations from roots of *A. thaliana* suggests that this complex is the functional unit responsible for high-affinity nitrate influx. It appears therefore that this two-component high-affinity nitrate transport system for nitrate uptake from soils is universal among plants. Nevertheless, this is not the case in *A. nidulans*, in which NRTA, the NRT2.1 homolog, was able to generate nitrate currents in the Xenopus system in the absence of NAR2 (Zhou *et al.*, 2000b). The reason for this difference is unclear since the predicted polypeptide sequence for the *A. nidulans* high-affinity transporter, NRTA, is sufficiently similar to the Arabidopsis and barley high-affinity transporters that degenerate primers based upon the *A. nidulans* sequence were used to identify the plant homologs (Trueman *et al.*, 1996; Zhuo *et al.*, 1999). All attempts to complement the double mutant phenotype in *A. nidulans* by expressing the plant homolog AtNRT2.1, either alone or together with AtNAR2.1 were unsuccessful. Only when the plant central loop was replaced by the *A. nidulans* loop was nitrate uptake achieved (Fig. 4-2 and 4-4). This, it should be stressed, was in the absence of AtNAR2.1. This observation suggests that both the *A. nidulans* and the Arabidopsis NRT transporters contain all required structural/functional properties to function independently as high-affinity transporters. Yet, in addition, AtNRT2.1 also requires expression of AtNAR2.1 in order to retain AtNRT2.1 within the PM and to bring about high-affinity nitrate transport (Wirth *et al.*, 2007; Chapter 2). What, then, is the basis for NAR2.1's role, with respect to AtNRT2.1, in planta? A prominent difference between the fungal and plant NRT2 polypeptides is the much larger central loop of *A. nidulans* compared to that of A. thaliana (Forde, 2000). Since replacing the short plant central loop with the longer fungal loop appears to render AtNAR2.1 redundant in *A. nidulans*, we conclude that a possible function of NAR2 in plants is to accommodate or stabilize the appropriate conformation of the NRT2 proteins within plant plasma membranes.

The results of earlier studies using the yeast two-hybrid system had established that AtNAR2.1 interacts with AtNRT2.1 (Orsel *et al.*, 2006). The results presented in Chapter 3 established that AtNAR2 also interacts with AtNRT2.2, AtNRT2.3, AtNRT2.4, AtNRT2.5, and AtNRT2.6 based upon growth on minus histidine media and the β-galactosidase test. The modified AtNRT2.1 (NRT2.1-AnLoop) failed to provide evidence of interaction with AtNAR2.1 (Fig. 4-5). That NRT2.1-AnLoop gave no evidence of interaction with NAR2.1 is consistent with the apparent redundancy of AtNAR2.1 seen in the *A. nidulans* transformants, expressing AtNRT2.1-AnLoop in a double deletion mutant (JK900, nrtA747 nrtB110) background (Fig. 4-4).

The results of the *Xenopus* study established that AtNRT2.1, AtNRT2.2, AtNRT2.5 and AtNRT2.6 all strongly promote nitrate influx when co-injected with AtNAR2.1 (Chapter 3, Fig. 3-4). The failure of NRT2.1-AnLoop to promote significant nitrate transport (Fig. 4-6) in *Xenopus* is consistent with the yeast two-hybrid assays, but different from functional *A. nidulans* nitrate uptake. Likewise, the failure of AtNRT2.1-AnLoop to provide functional nitrate uptake in the absence of AtNAR2.1 in *A. thaliana* (Fig. 4-7 and 4-8) is in agreement with the *Xenopus* oocytes uptake (Fig. 4-6). The results of nitrate uptake in *Xenopus* oocytes and *A. thaliana* (Fig. 4-6 and 4-8) are not consistent with the data from influx experiments in *A. nidulans* (Fig. 4-2). This inconsistency could be explained by differences between NRTA and AtNRT2.1-AnLoop, and distinct membrane properties of the three organisms (*A. nidulans*, *A. thaliana* and *X. laevis* oocytes).

Taken together, the present findings suggest the importance of the short central cytoplasmic loop (between TMRs 6 and 7) of AtNRT2.1 for interaction with AtNAR2.1. One hypothesis of NAR2's role is that through the interaction of NAR2.1 and NRT2.1 to form the 150 kDa complex referred to in Chapter 2, AtNRT2.1 is folded, stabilized and retained in the PM to realize high-affinity nitrate transport. In the case of the *A. nidulans* NRTA transporter, this same function may be provided by the large central loop that is shown (table 4.1) to have, on average, 21.4 % sequence homology with NAR2.1. However, this percentage sequence homology, while suggestive, is inconclusive and requires further analysis.

Chapter 5. Arabidopsis *NRT2.5* encodes a constitutive high affinity nitrate transporter in roots

Background

More than 100 million tonnes of nitrogen (N) fertilizers are applied annually worldwide to foster crop yields (Fig. 1). Nitrogen fertilizers are applied excessively and with low N-use efficiency, because a significant portion of the fertilizers is lost from the soil (Glass, 2003) due to leaching and denitrification (reviewed in Cameron *et al.*, 2013). Nitrate availability fluctuates greatly in soil, in part because of the above sources of loss and because of various seasonal edaphic factors (Wolt, 1994). Plants have developed different transport systems that allow them to adapt to changes of N availability in the environment. Uptake of nitrate at high external concentrations is accomplished mainly by Low Affinity Transport Systems (LATS). LATS are encoded by NRT1 genes, and in *Arabidopsis thaliana* NRT1.1 and NRT1.2 are the major contributors to inducible LATS and constitutive LATS, respectively (Tsay *et al*., 1993; Huang *et al*. 1999). At concentrations below 0.5 mM nitrate uptake is achieved through High Affinity Transport Systems (HATS). It is accepted that the HATS system also has two components: inducible and constitutive, iHATS and cHATS, respectively (reviewed in Glass and Siddiqi, 1995; Crawford and Glass, 1998; Wang *et al*., 2012). iHATS transport in Arabidopsis is achieved through the activity of *AtNRT2.1* and *AtNRT2.2* (Filleur *et al*., 2001; Li *et al*., 2007). In addition to these MFS transporters, expression of a non-related, small protein AtNAR2.1 is required for functional iHATS nitrate uptake (Okamoto *et al*., 2006; Orsel *et al*., 2006). In Chapter 2, I have shown that the functional nitrate transporter is a molecular complex of AtNRT2.1 and AtNAR2.1, localized in the plasma membranes of Arabidopsis roots.

Despite the importance of the cHATS system of nitrate uptake as a prerequisite for the induction of iHATS, as well as enzymes such as nitrate reductase, and ample physiological evidence for the existence of constitutive nitrate HATS (cHATS) in plants, no gene encoding this system has been identified. This transport system is present in plants even before they have been exposed to external nitrate. cHATS in barley was measured using a sensitive $^{13}NO_3^-$ technique in N-starved plants by Siddiqi *et al*. (1990) as well as by net nitrate uptake

(Behl *et al*., 1988; Aslam *et al.*, 1992) . Siddiqi *et al*. (1990) found that the nitrate fluxes due to cHATS were saturable at 0.2 mM KNO_3, exhibiting 27 fold lower Vmax and 4 fold lower Km than fluxes associated with iHATS in plants induced with nitrate. Wang and Crawford isolated an EMS-mutagenized Arabidopsis line that was resistant to 0.1 mM chlorate, a toxic nitrate analogue (Wang and Crawford, 1996) in which constitutive nitrate net uptake was impaired in the mutant (named *nrt2*), and inducible HATS was delayed. Electrophysiological studies showed that there was very little response to 0.25 mM nitrate in the *nrt2* mutant, compared to strong initial membrane depolarization in WT plants. However, Wang and Crawford did not identify the gene responsible for cHATS. cHATS is also reduced by 90% in *Atnar2.1-2* mutants compared to WT (Okamoto *et al.*, 2006), suggesting that *AtNAR2.1* gene may be necessary for the function of the cHATS transporter, as was demonstrated for iHATS (Okamoto *et al.*, 2006; Orsel *et al.*, 2006, Chapter 2). In summary, genes encoding the major high-affinity nitrate transport system (iHATS), namely AtNRT2.1, AtNRT2.2 and AtNAR2.1, and those responsible for inducible and constitutive low-affinity nitrate transport (iLATS and cLATS) have been identified and characterized in Arabidopsis. What remains to be identified is the gene or genes responsible for cHATS.

In addition to NRT2.1 and NRT2.2, the Arabidopsis NRT2 family has 5 other members. Chopin *et al*. (2007a) found that *AtNRT2.7* is strongly expressed in maturing seed, with subcellular localization in the tonoplast. Based on the fact that T-DNA mutants of the gene exhibit lower nitrate content in seed than WT, the authors proposed a role of AtNRT2.7 in seed nitrate loading. AtNRT2.4 is expressed in root and shoot phloem, is upregulated by N starvation and localized to the plasma membrane (Kiba *et al*., 2012). The authors also found that Arabidopsis *nrt2.4* mutants exhibit lower nitrate uptake than WT at external NO_3^- concentration below 100 µM, and have lower NO_3^- levels in leaf exudates. *AtNRT2.6* is more expressed in vegetative than generative organs and its expression is induced by high nitrate levels (Dechorgant *et al*., 2012). The authors found that *AtNRT2.6* expression was increased after inoculation of plants with the pathogenic bacterium *Erwinia amylovora* and that *nrt2.6* mutants exhibit higher susceptibility to the pathogen. Kechid *et al.* (2013) showed that *AtNRT2.5* and *AtNRT2.6* play an important role in plant growth regulation in response to growth-promoting rhizobacterium *Phylliobacterium brassicacearum* strain STM196. A role for the *AtNRT2.3* gene remains unknown.

Objective

I have demonstrated that all AtNRT2 family members are capable of nitrate uptake in *Xenopus* oocytes when co-expressed with AtNAR2.1 (Chapter 3). The most prominent ^{15}N enrichment in oocytes was observed for NRT2.5/NAR2.1 co-expression, indicating the possible importance of this gene in nitrate transport in plants. To investigate this hypothesis, I have functionally characterized *AtNRT2.5* gene by measuring nitrate fluxes in Arabidopsis WT plants and T-DNA mutants of the NRT2.5 gene.

Material and methods

Plant material and growth conditions

T3 generation seed of T-DNA insertion mutants GABI-Kat 213H10 (*Atnrt2.5-1*), provided by NASC (Scholl et al., 2000) and GABI-Kat 046H04 (*Atnrt2.5-2*), provided by GABI-Kat (Kleinboelting et al., 2012) was used to select homozygous plants by segregation analysis on sulfadiazine (7.5 mg ml^{-1}) MS plates. The insertions were confirmed using PCR with the following primers: T-DNA left border 5'-ATAATAACGCTGCGGACATCTACATTTT-3', gene specific:

Atnrt2.5-1

5'-GATGAGCTCCATGTTCTCTGG-3' and 5'-ATCAACTGTGTTAAGACCGCG-3';

Atnrt2.5-2

5'-ATGGAGGTCGAAGGCAAAG-3' and 5'-TCAAGTTTGGGGATGAGTCG-3'.

The position of the T-DNA insertion was confirmed by sequencing using T-DNA-specific primer 5'-ATATTGACCATCATACTCATTGC-3' and gene-specific primer *Atnrt2.5*-1 5'-CAATCAAGCAACTCAATACCAAAA-3'and *Atnrt2.5-2* 5'-CTCAAAACCGGATTAGTTGAAAAA-3'. Seeds were sterilized in 1% commercial bleach (plus 0.01% Tween 20) for 15 min, and left for 3 days in sterile water at 4°C prior to sowing on MS plates. WT-Col and *Atnrt2.5* mutants were grown hydroponically in 1/10 strength Johnson's solution under non-sterile conditions as described in Chapters 1 and 2. The hydroponic solution was aerated continuously and replaced once weekly with freshly-prepared solution. Plants were grown for 4 weeks, and then deprived of nitrogen for the fifth week. Growth conditions in the growth room were 8h of light (100 µmol m^{-2} s^{-1} at plant level) and 16h of dark, at corresponding temperatures of 24°C and 20°C, respectively, and a relative humidity ~70%.

RT-PCR and real time RT-PCR

Total RNA was isolated from tissue of hydroponically grown plants by PureLink® RNA Mini kit (Invitrogen, USA) according to the manufacturer's protocol. Protocols for RT-PCR and real-time PCR are described in Chapter 2. Sequences of oligonucleotide primers used in the real-time PCR DNA amplification are given in Appendix A (Table 6A).

Tissue-nitrate concentration measurement

Nitrate concentration was measured according to the method by Cataldo *et al.* (1975). Plants were grown hydroponically for 4 weeks, and then starved of nitrogen for one week. Half of the N-starved plants were supplied with 1 mM KNO_3 for 6 hours, and all plants were washed in N-free nutrient solution before harvesting for 5 min. Shoots and roots were separated and weighed before instant freezing in liquid N_2. To determine tissue nitrate concentration, distilled water was added to each sample at a ratio of 10 ml water per 1 g fresh material. Samples were immediately boiled for 20 min. After cooling to room temperature, liquid contents were decanted to fresh tubes and extracts were used for colorimetric assays. 50 µl of the extract was mixed with 200 µl of 5 % (w/v) salicylic acid in concentrated H_2SO_4. After 20 min incubation at room temperature, 4.75 ml of 2M NaOH was added to the mixture and vortexed briefly. Samples were cooled to room temperature before absorbance at 410 nm was measured in a Shimadzu BioSpec 1601 spectrophotometer (Shimadzu Corporation, Japan). Calculation of nitrate concentration was based on a standard curve of samples ranging from 0 to 15 mM KNO_3.

$^{13}NO_3^-$ influx measurements

Nitrate influx, using $^{13}NO_3^-$, was measured as described in the Chapters 1 and 2. The basic components of the solution for pre-treatment, influx, and desorption were the same as those of the growth media, except that KNO_3 at designated concentrations replaced NH_4NO_3. Prior to measuring $^{13}NO_3^-$ influx, plants were pretreated for 5 min with solution containing appropriate KNO_3, and then transferred for 5 min into the influx solution, which was labelled with $^{13}NO_3^-$. After the influx period, roots were desorbed with non-labelled solution (identical to pre-treatment solution) for 2 min to desorb the radioactive isotope from the apoplast. Gamma emission was measured using a gamma-counter (MINAXI Auto-Gamma 5000 series, Packard Instruments, USA).

Statistical analysis

Statistical analysis of data, including ANOVA and testing slope differences, was done using GraphPad Prism 6 software (GraphPad Software Inc., USA).

Results

Characterization of *AtNRT2.5* T-DNA insertion lines

The *AtNRT2.5* gene is located on the first half of Chromosome 1, close to two major HATS transporters *AtNRT2.1* and *AtNRT2.2,* and LATS *AtNRT1.1* (Fig. 5-1a). The physiological importance of the gene was evaluated by use of Arabidopsis T-DNA –insertion mutants. Homozygous plants were selected from GABI-kat T-DNA insertion lines GK-213H10 (*Atnrt2.5-1*) and GK-046H04 (*Atnrt2.5-2*) by segregation analysis on sulfadiazine MS plates and positions of the insertions were verified by sequencing. Insertions in both lines are located in the exons; in the 2nd exon 1042 bp after ATG in *Atnrt2.5-1,* and in the 1st exon 415 bp after the start codon (ATG) in *Atnrt2.5-2* (Fig. 5-1b).

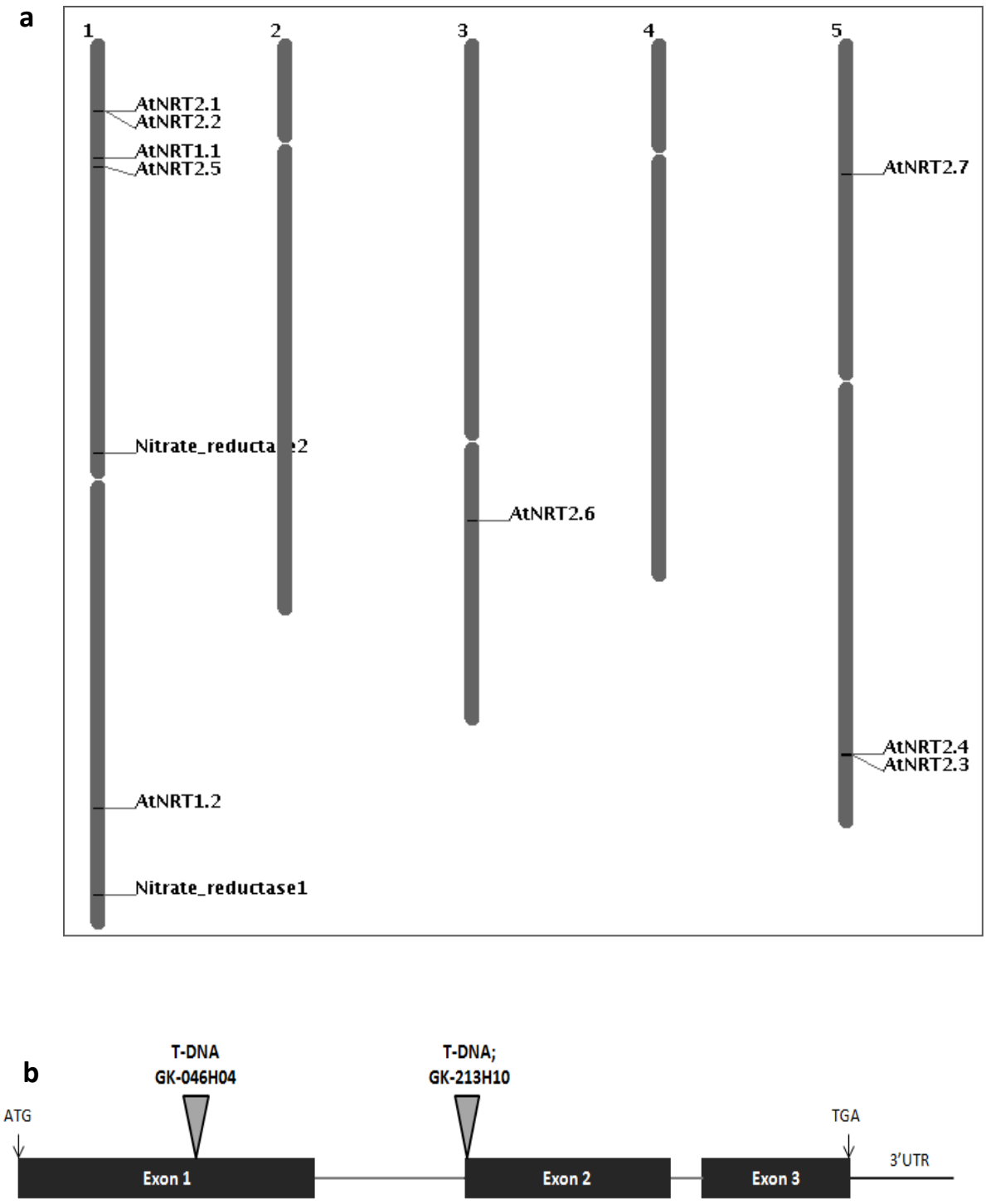

Figure 5-1. a. Schematic representation of the chromosome position of *AtNRT2.1* (AT1G08090), *AtNRT2.2* (AT1G08100), *AtNRT2.3* (AT5G60780), *AtNRT2.4* (AT5G60770), *AtNRT2.5* (AT1G12940), *AtNRT2.6* (AT3G45060), AtNRT2.7 (AT5G14570), *AtNRT1.1* (AT1G12110), *AtNRT1.2* (AT1G69850), *AtNR1*- Nitrate_reductase1 (AT1G77760) and *AtNR2*-Nitrate_reductase2 (AT1G37130), drawn by TAIR Chromosome Map Tool (http://www.arabidopsis.org/jsp/ChromosomeMap/tool.jsp); **b**. Diagram of *AtNRT2.5* gene

showing positions of T-DNA insertions in GK-213H10 (*Atnrt2.5-1*) and GK-046H04 (*Atnrt2.5-2*), in the 2nd and 1st exons, respectively.

PCR after reverse transcription from total RNA of WT and mutants established the absence of *AtNRT2.5* expression in the mutants (Fig. 5-2), classifying the *Atnrt2.5-1* and *Atnrt2.5-2* as *AtNRT2.5* knock-out lines.

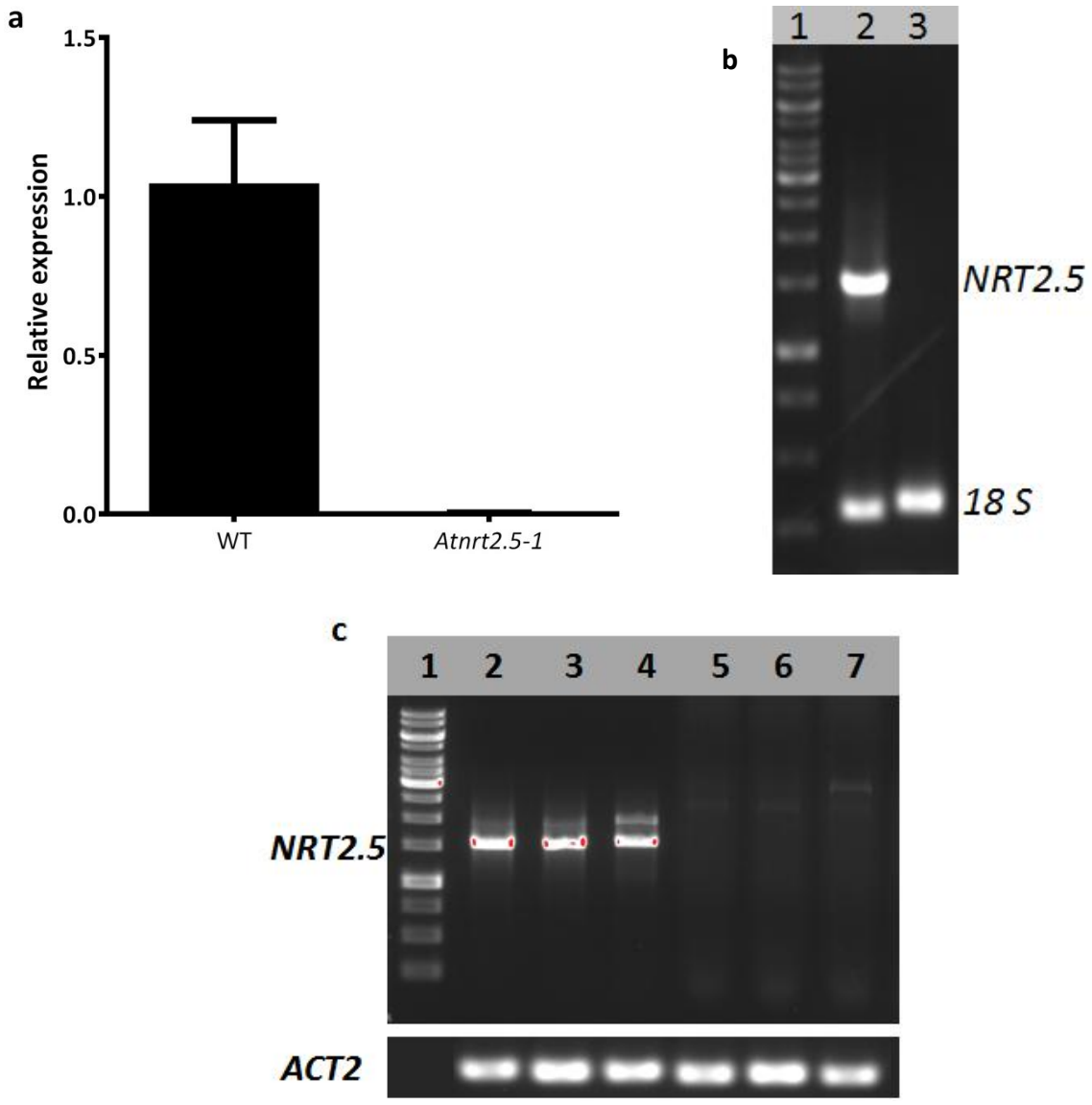

Figure 5-2. *AtNRT2.5* expression in *Arabidopsis thaliana* WT and T-DNA-insertion mutants. **a**. relative expression of *AtNRT2.5* normalized to *ACT2* gene expression (mean ± SE of n=3); **b**. DNA gel (SYBR Gold stain) of PCR products (cDNA after RT-PCR template) using *AtNRT2.5* and *18S* primers, lane1: 1kb DNA ladder (GeneRuler™, Fermentas), lane 2: WT, lane 3: *Atnrt2.5-1*; **c**. DNA gel of PCR products (cDNA after RT-PCR template) using *AtNRT2.5* and *ACT2* primers, lane1: 1kb DNA ladder, lanes 2-4: WT, lanes 5-7: *Atnrt2.5-2*.

$^{13}NO_3^-$ influx is reduced in *Atnrt2.5* mutants

Nitrate influx into WT and mutant Arabidopsis plants was measured using the sensitive ^{13}N methodology. ^{13}N-Nitrate influx at low concentration (100 µM) in both induced and uninduced Arabidopsis plants was significantly reduced in *Atnart2.5.1* mutants compared to WT (Fig. 5-3). The flux at 100 µM was reduced by 45 % in induced and 60 % in uninduced *Atnart2.5.1* mutant plants compared to WT plants. Fluxes at higher concentration (500 µM) in uninduced plants were reduced by 50 % in *Atnrt2.5.1* mutants (Fig. 5-3b), while they were not significantly different in nitrate-induced plants (Fig. 5-3a).

Further characterization of the nitrate influx was done in uninduced plants, at a range of low concentrations (10-250 µM). *Atnrt2.5.1* mutants exhibited reduced nitrate influx compared to WT (Fig. 5-4a) at all concentrations examined, with an average reduction of 63 %. Influx in both WT and *Atnrt2.5* was fitted to rectangular hyperbolae, adhering to Michaelis-Menten kinetics (Fig. 5-4a). Nitrate influx that was due to AtNRT2.5 (the difference between WT and *Atnrt2.5* influx) also showed saturable kinetics, with estimated Km of 10.75 µM and Vmax of 2.3 µmol g FW^{-1} h^{-1} (Fig. 5-4b).

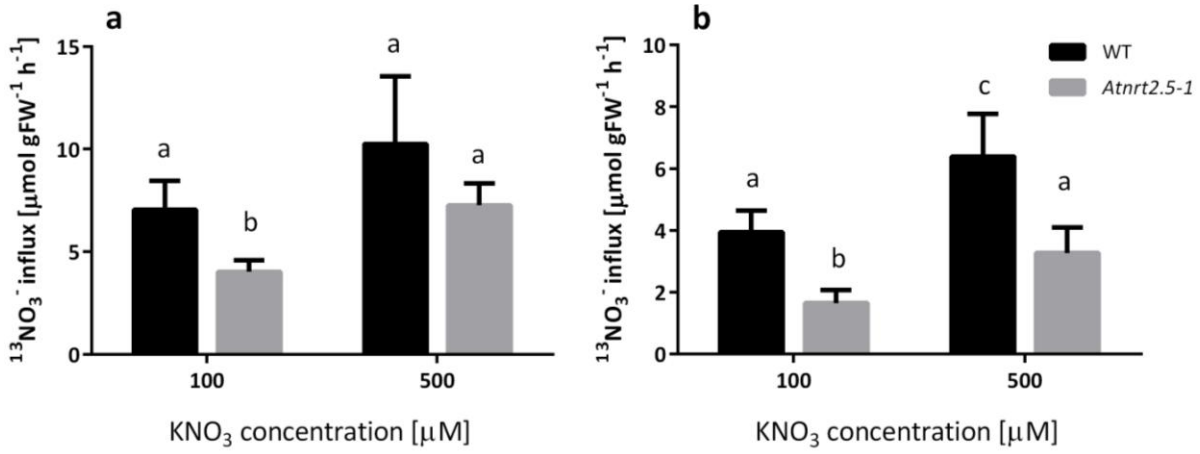

Figure 5-3. $^{13}NO_3^-$ influx into roots of *Arabidopsis thaliana* WT-Col (black bars) and *Atnrt2.5-1* (gray bars). Plants were hydroponically-grown for 4 weeks, then starved of N for 1 week. **a**. influx of induced plants (1 mM KNO_3 for 6 h); **b**. influx of uninduced plants (no nitrate pre-treatment). Bars are means ± SD of 6 replicates, analyzed by ANOVA; different letters indicate significant mean differences at $P \leq 0.05$.

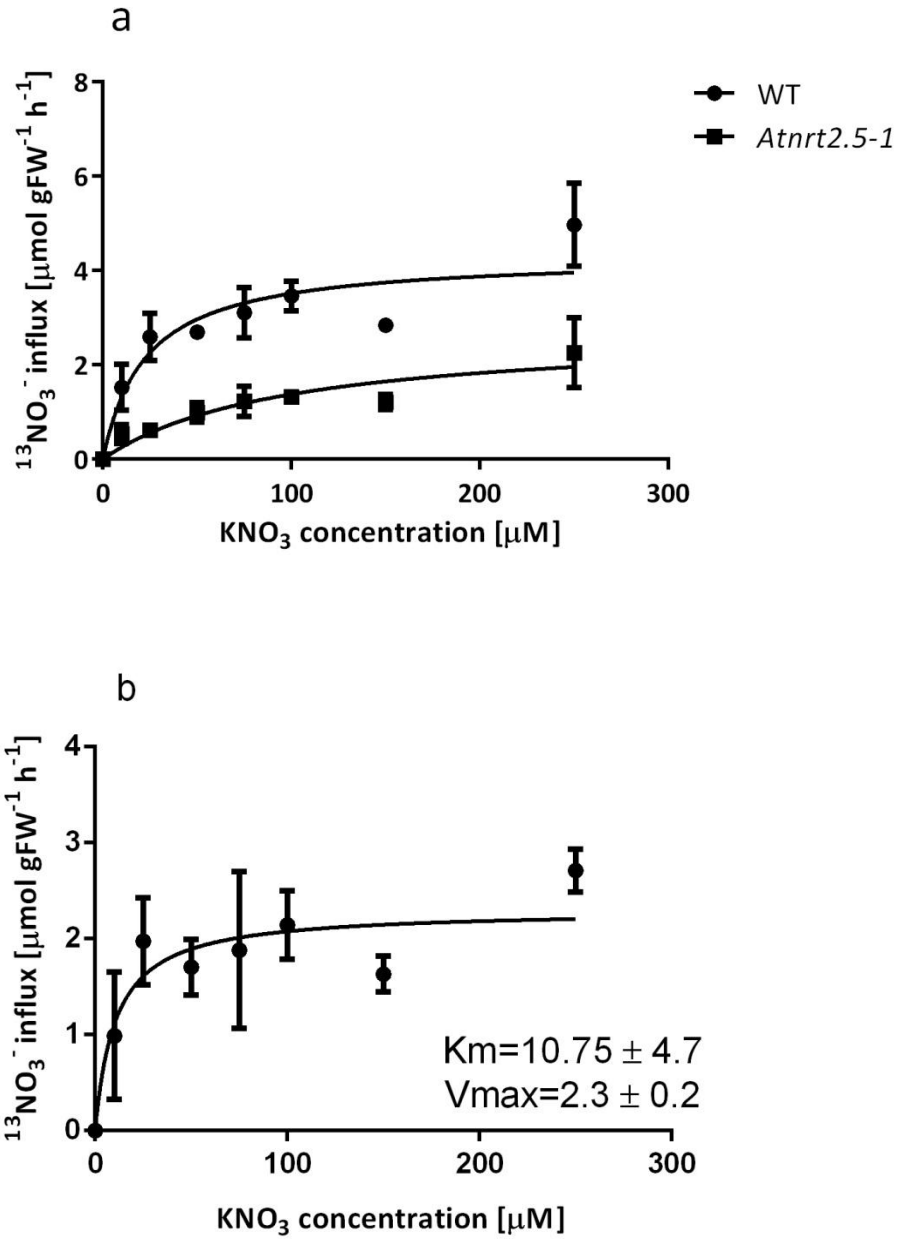

Figure 5-4. Concentration-dependant $^{13}NO_3^-$ influx in *Arabidopsis thaliana* grown under uninduced conditions. **a**. $^{13}NO_3^-$ influx in WT-Col (circles) and *Atnrt2.5-1* mutant (squares); **b**. $^{13}NO_3^-$ influx due to NRT2.5 (difference of influx between WT and *Atnrt2.5-1*). Values are average of n=4 ± SD. The fitted lines are direct Michaelis-Menten fit, with estimated vales for Km [µM] and Vmax [µmol g FW^{-1} h^{-1}].

In order to confirm the reduced nitrate influx mutant phenotype, the second insertion allele *Atnrt2.5-2* was analysed. *Atnrt2.5-2* also showed reduced nitrate influx compared to WT in uninduced (N-starved) plants (Fig. 5-5a). The level of reduction was similar to that observed for *Atnrt2.5-1* which was around 50 % in this experiment (Fig. 5-5a). Differences between nitrate influx of WT and *Atnrt2.5-2* in induced plants were not statistically significant as observed in the *Atnrt2.5-1* mutant. Measurements of the concentration-dependent $^{13}NO_3^-$ influx confirmed the reduction of influx in *Atnrt2.5-2.* At all examined high-affinity range concentrations (10-150 µM KNO_3), *Atnrt2.5-2* exhibited lower nitrate influx, reduced on average by more than 60% of WT values (Fig. 5-5b).

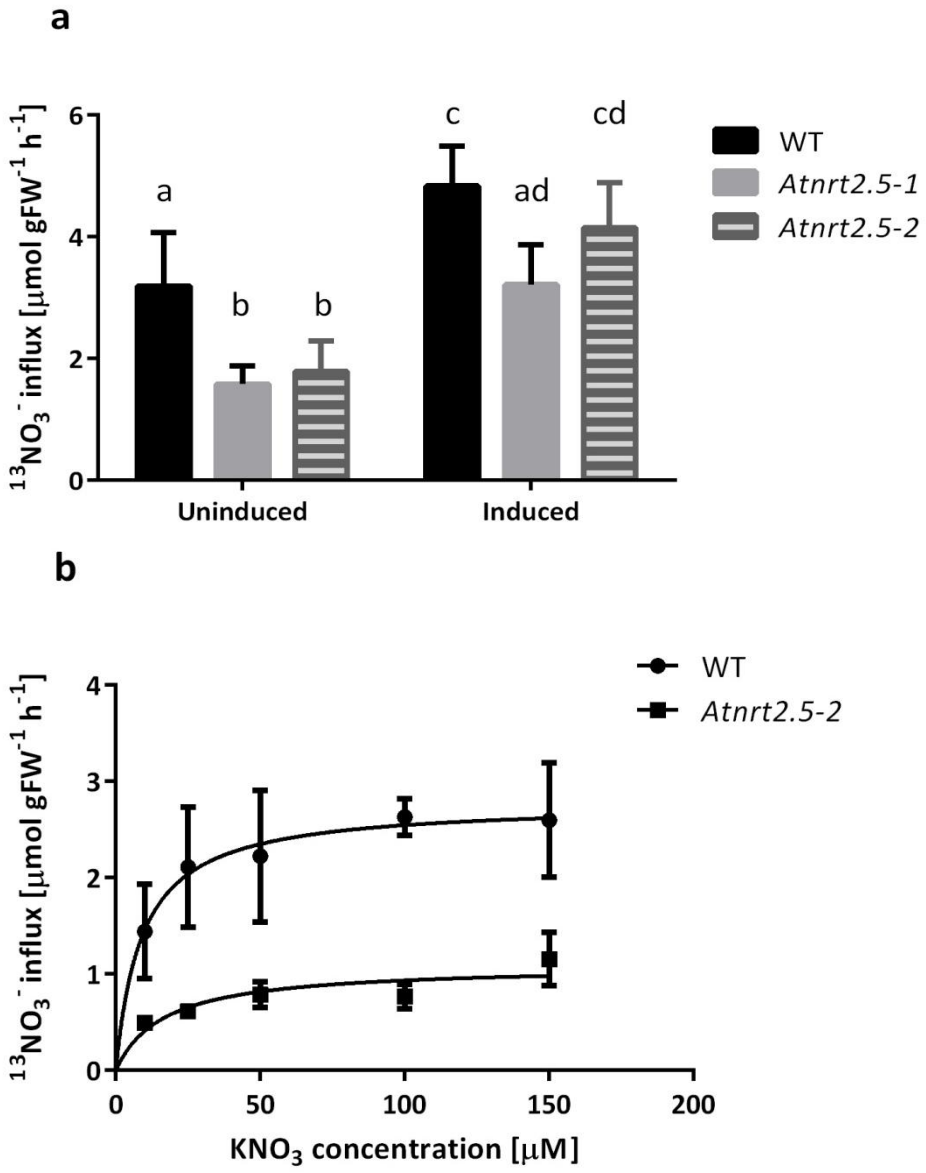

Figure 5-5. $^{13}NO_3^-$ influx into roots of *Arabidopsis thaliana* WT-Col and *Atnrt2.5*. Plants were hydroponically-grown for 4 weeks, then starved of N for 1 week. **a**. influx of induced (1 mM KNO_3 for 6 h) and uninduced plants, WT black bars, *Atnrt2.5-1* grey bars and *Atnrt2.5-2* striped bars; bars are means ± SD of 6 replicates, analyzed by ANOVA followed by *t* tests; different letters indicate significant mean differences at P≤0.05; **b**. concentration-dependant $^{13}NO_3^-$ influx in WT-Col (circles) and *Atnrt2.5-2* mutant (squares), values are average of n=4 ± SD. The fitted line is a direct Michaelis-Menten fit.

The use of the ^{13}N-labeled nitrate allowed me to determine retention of ^{13}N label in roots as distinct from subsequent transfer to shoots. The experimental set-up was the same as for previous influx experiments, except for the final radioactive signal counting, where instead of measuring the whole plant emissions (roots plus shoots counted together in single vials), roots and shoots were placed into separate vials for counting. Retention of label in roots was significantly lower in *Atnrt2.5-1* mutants compared to WT, reduced by 50 % and 35 % in uninduced and induced plants, respectively (Fig. 5-6a). No differences were observed between tracer flux to shoots of WT and the T-DNA insertion line (Fig. 5-6b).

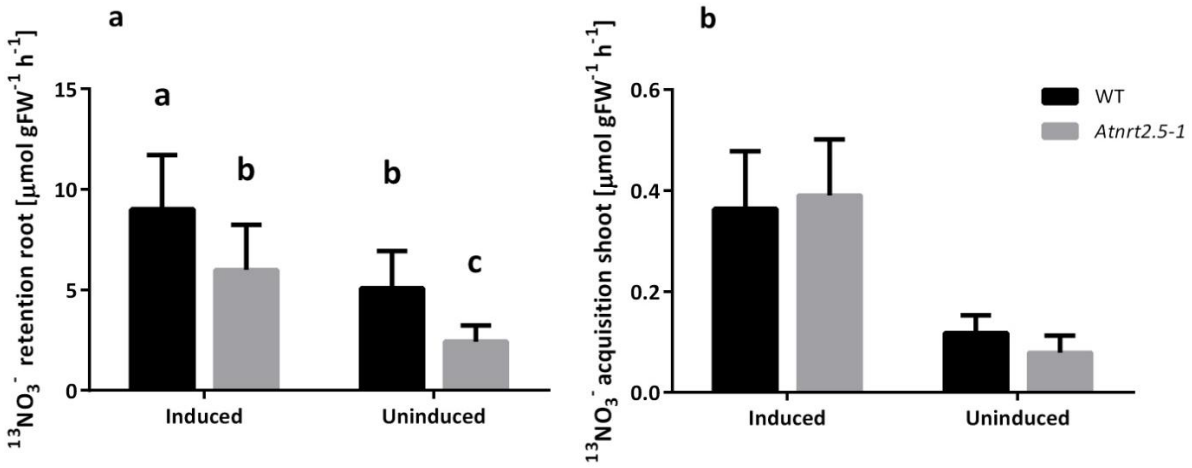

Figure 5-6. ^{13}N retention in roots and accumulation in shoots of *Arabidopsis thaliana* WT-Col (black bars) and *Atnrt2.5-1* (gray bars) at 100 µM KNO_3. Plants were hydroponically-grown for 4 weeks, then starved of N for 1 week. Induced plants were pretreated with 1 mM KNO_3 for 6 h. **a**. ^{13}N retention in roots of induced and uninduced plants; **b**. ^{13}N acquisition of shoots of induced and uninduced plants. Bars are means ± SD of 9 replicates. analyzed by ANOVA followed by *t* tests. Different letters indicate significant mean differences at P≤0.05.

Growth of WT and *Atnrt2.5-1* on high and low nitrate

Growth of WT and *Atnrt2.5-1* mutant under low and high nitrate conditions was evaluated by measuring plant weight and root length. Root fresh weights of hydroponically-grown plants at low and high nitrate (0.25 and 5 mM, respectively) were not significantly different between the two genotypes (Fig. 5-7a). Shoot fresh weights of *Atnrt2.5-1* plants grown at low nitrate supply were lower than those of WT, while they were not different when grown at 5 mM KNO_3 (Fig. 5-7b). In agreement with the fresh root weight data, the total root lengths of WT and *Atnrt2.5-1* mutants were not different in plants grown at low or high nitrate half-strength MS-agar substrate (Fig. 5-7c).

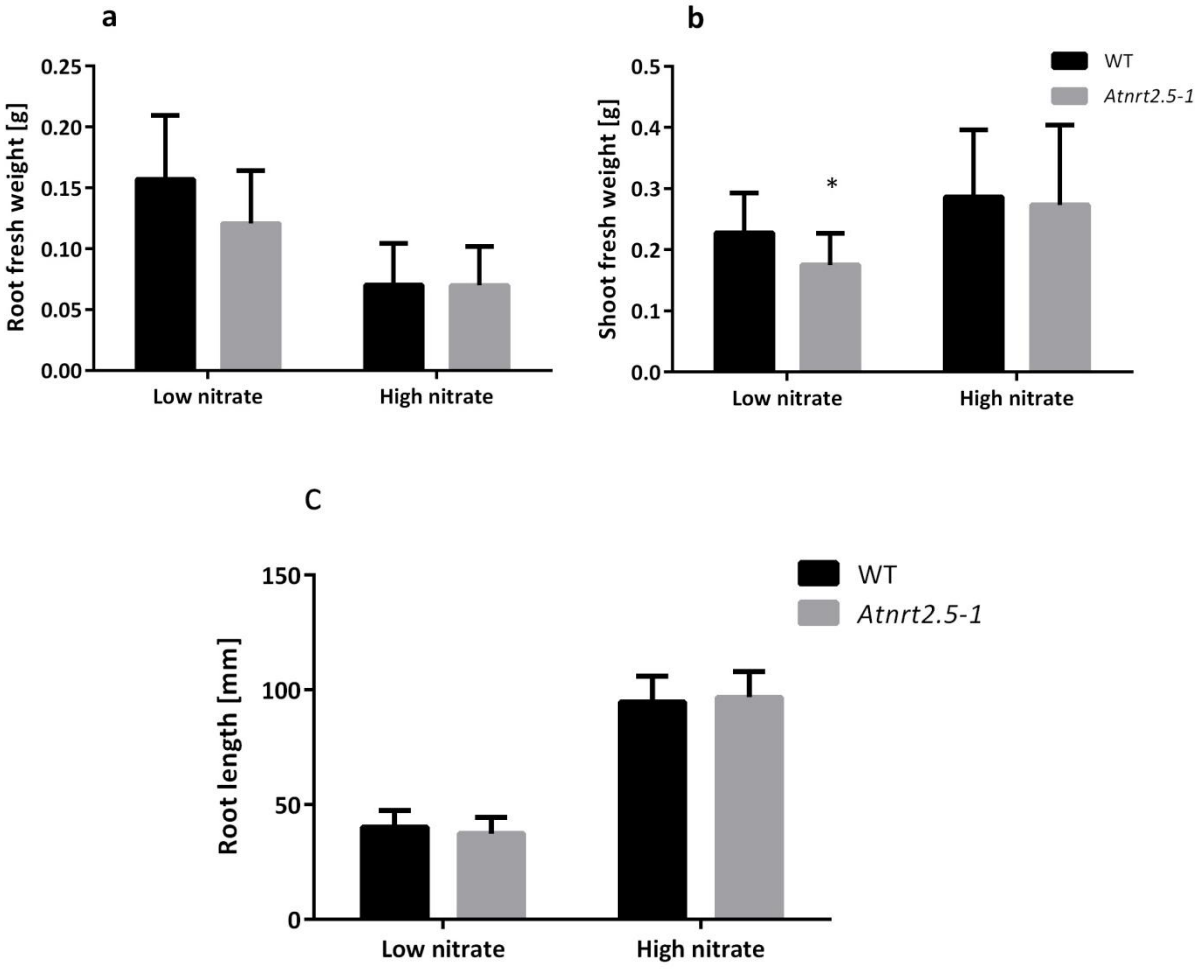

Figure 5-7. Growth of *Arabidopsis thaliana* WT (black bars) and *Atnrt2.5-1* (gray bars). **a**. root and **b**. shoot fresh weight of hydroponically-grown plants for 5 weeks at low nitrate (250 µM KNO_3) or high nitrate (5 mM KNO_3); **c**. total root length of 2-week old plants grown on low (250 µM KNO_3) or high nitrate (5 mM KNO_3) solid MS media. Bars are means ± SD of

15 replicates. Analyzed by ANOVA followed by *t* tests. Asterisk represents significant difference at P≤0.05.

Tissue nitrate concentration

Nitrate concentration from fresh tissue was determined colorimetrically according to the method by Cataldo *et al*. (1975). *Atnrt2.5-1* plants exhibited significantly lower nitrate concentration in roots and shoots of induced plants compared to WT (Fig. 5-8a and 5-8b, respectively). Nitrate concentration in roots and shoots of uninduced was lower than that of induced plants, but there were no differences between tissue nitrate concentration of uninduced WT and mutant plants (Fig. 5-8).

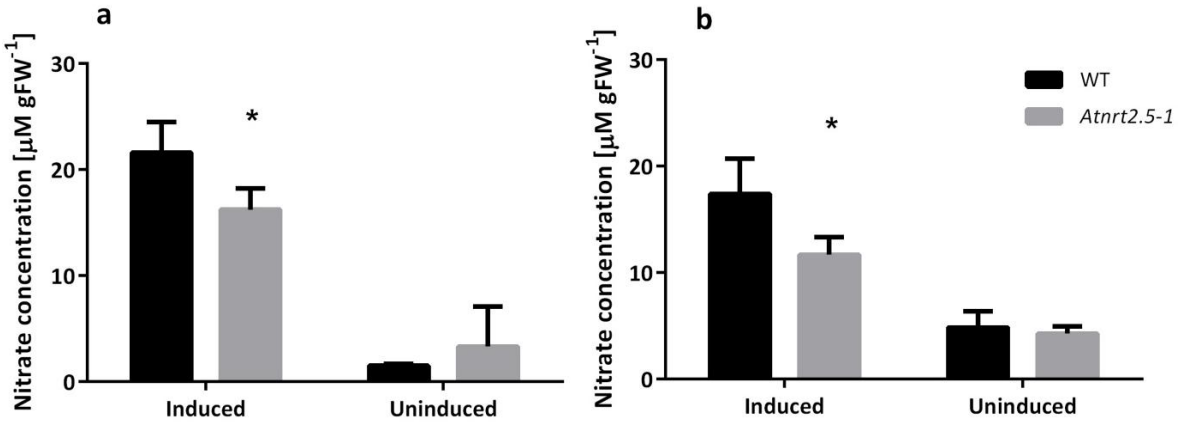

Figure 5-8. Tissue nitrate concentration of *Arabidopsis thaliana* WT (black bars) and *Atnrt2.5-1* (gray bars), hydroponically-grown plants for 4 weeks, then starved of N for 1 week. **a**. Nitrate concentration in roots of induced (1 mM KNO_3 for 6 h) and uninduced plants; **b**. Nitrate concentration in shoots of induced (1 mM KNO_3 for 6 h) and uninduced plants. Bars are means ± SD of 5 replicates. analyzed by ANOVA followed by *t* tests. Asterisk represents significant difference at P≤0.05.

Regulation of expression of *AtNRT2.5*

Real-time PCR using *AtNRT2.5* primers in WT plants demonstrated that *AtNRT2.5* expression was 13 times higher in root than in shoot tissue of plants after being starved of nitrogen for 1 week (Fig. 5-9a). Furthermore, expression of the *AtNRT2.5* is highest in plants starved of nitrogen (uninduced), and is down-regulated by nitrate and ammonium treatment after 3, 6 and 24 h (Fig. 5-9b). Nitrate treatment had a more pronounced effect on inhibition of *AtNRT2.5* expression than ammonium, reducing *AtNRT2.5* expression below the detection limits after 24 h (Fig. 5-9b). The double mutant *Atnrt2.1-nrt2.2* (lacking expression of the

two major iHATS transporters) has previously been described by Li *et al*. (2007). These plants exhibited a strong phenotype on low nitrate supply showing reduced lateral root and shoot growth (Li *et al*., 2007). Figure 5-9c reveals that the expression of *AtNRT2.5* was significantly higher in the double mutant than in WT plants, under both uninduced and induced conditions (6 h induction with KNO_3).

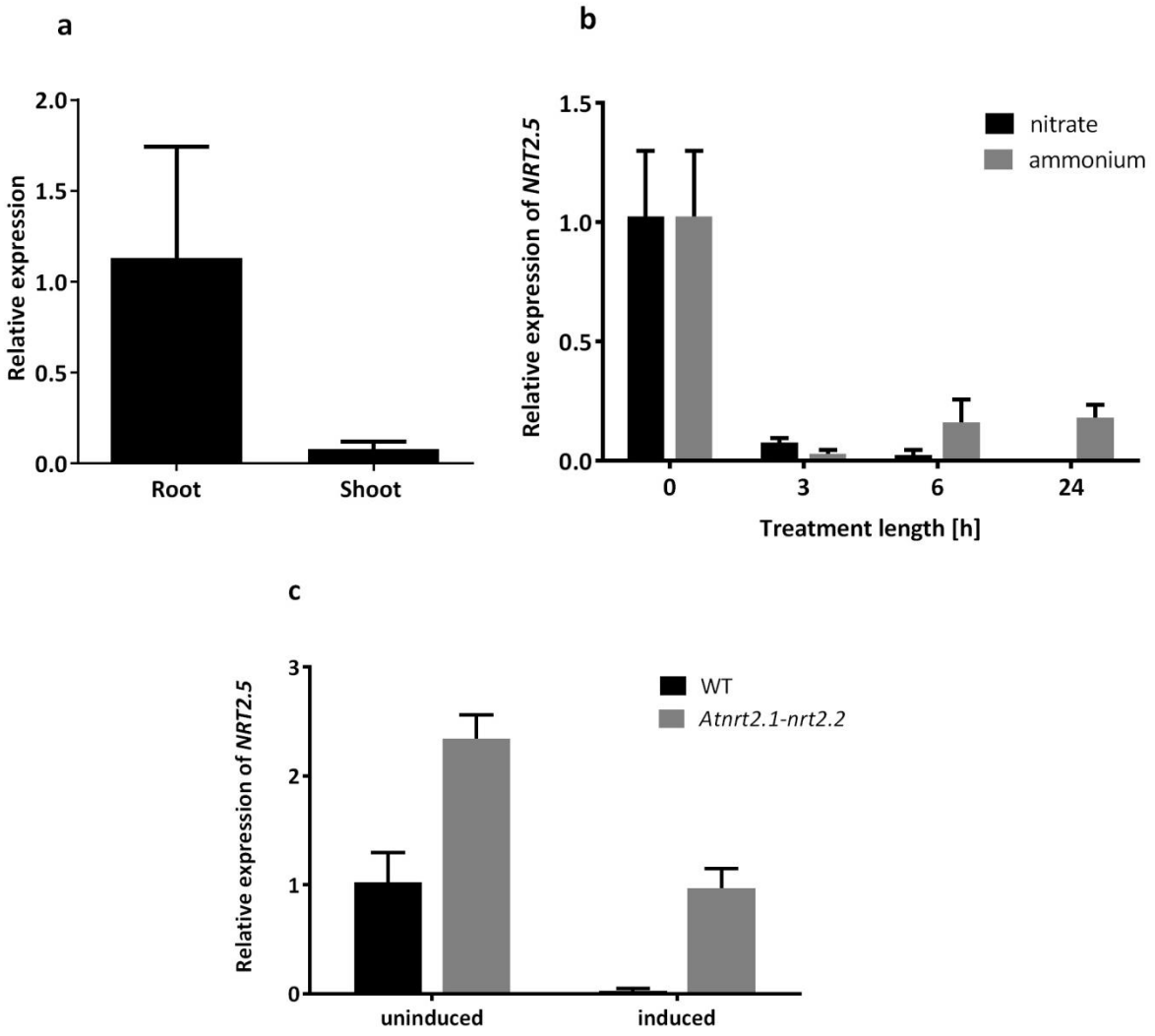

Figure 5-9. Relative expression of *AtNRT2.5* from total RNA of *Arabidopsis thaliana* hydroponically-grown plants for 4 weeks, then starved of N for 1 week. **a**. expression in roots and shoots of uninduced plants; **b**. effect of nitrate (1 mM KNO_3) or ammonium (1 mM $NH_4H_2PO_4$) treatment on expression of *AtNRT2.5* in roots of WT plants (0 h is equivalent to uninduced plants); **c**. expression of *AtNRT2.5* in roots of WT and double mutant *Atnrt2.1-nrt2.2* in uninduced and induced (1 mM KNO_3 for 6 h) plants. Expression calculated using *ACT2* expression as a reference. Bars represent mean ± SD, n=4.

Expression of other nitrate transporter genes in roots of *Atnrt2.5-1* mutant

In order to examine the possibility of up regulation of other nitrate transport genes in the *Atnrt2.5* mutant, their expression in roots of uninduced plants was quantified using real-time RT-PCR. Real-time PCR primers efficiency was determined from the slopes of dilution curves. The slopes were not significantly different and the efficiencies were between 2 and 3 (Table 5-1).

Table 5-1. Efficiency of primers used for DNA amplification in real-time PCR experiment. Slope is of a fitted linear regression line with threshold cycle (average of 3 replicates) on Y-axes and cDNA concentration on X-axes. Efficiency is calculated as $E=10^{(-1/slope)}$.

Gene	Slope	Efficiency
AtNRT2.1	-2.305	2.715
AtNRT2.2	-2.143	2.928
AtNRT2.3	-3.022	2.142
AtNRT2.4	-3.351	1.988
AtNRT2.5	-3.311	2.005
AtNRT2.6	-2.447	2.562
AtNRT2.7	-3.155	2.075
AtNRT1.1	-2.608	2.418
AtNRT1.2	-3.583	1.901

Relative expression was calculated based on expression of the reference gene *ACTIN2* according to Pfaffl (2001). Figure 5-10a exhibits the expression of *NRT2* and *NRT1* genes relative to the expression of *AtNRT2.1* (100%). *AtNRT2.1* had the highest level of expression of all examined genes, while *AtNRT2.3* and *AtNRT2.7* showed very low levels of expression in roots of both WT and mutant plants (Fig. 5-10a). *AtNRT2.1*, *AtNRT2.2*, *AtNRT2.4* and *AtNRT1.1* showed significantly lower expression in the *Atnrt2.5-1* mutants (Fig. 5-10a and 5-10b).

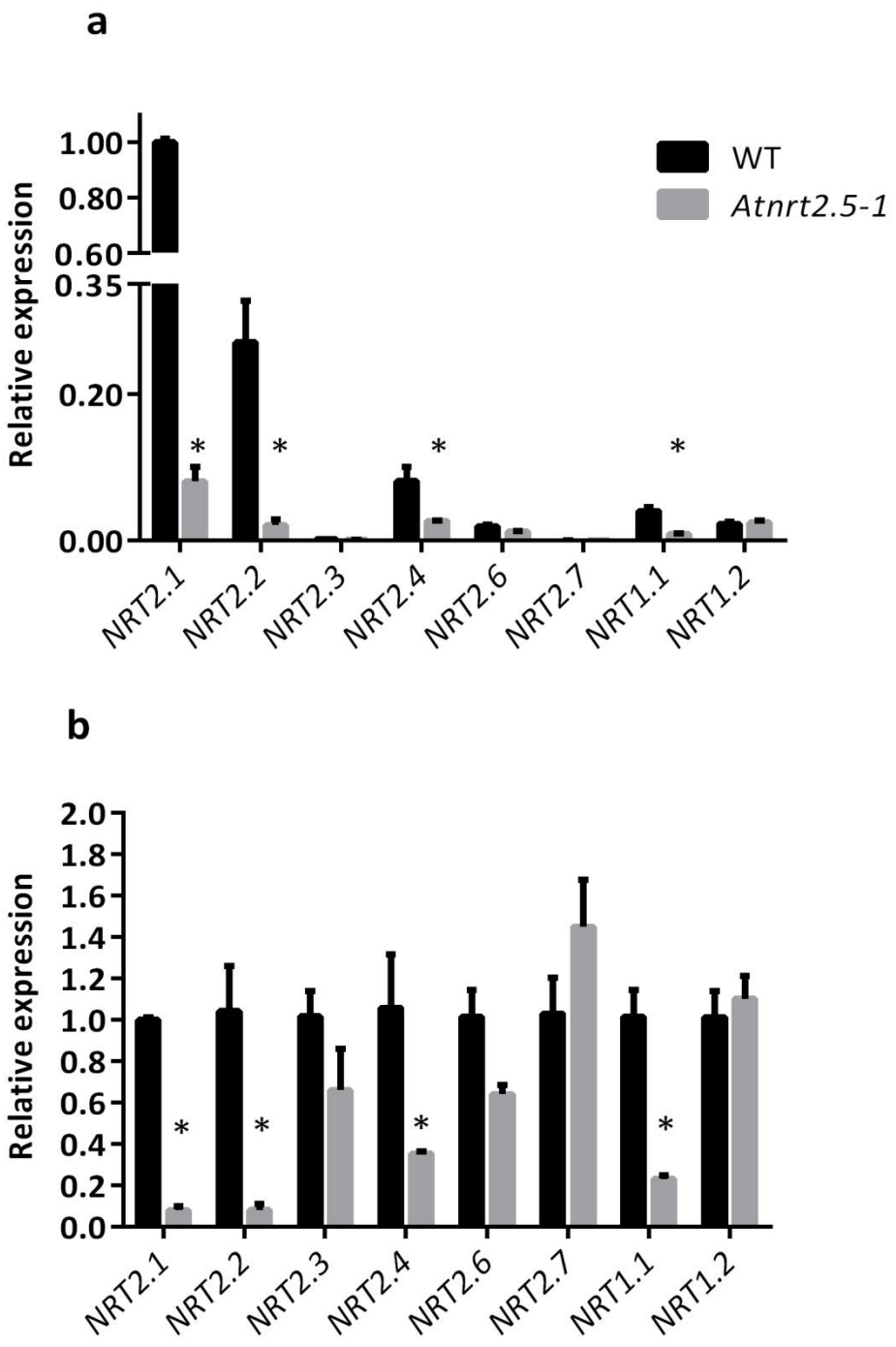

Figure 5-10. Relative expression of other nitrate transporter genes in *Arabidopsis thaliana* WT-Col and *Atnrt2.5-1* mutant, in uninduced plants. Expression calculated using *ACT2* expression as a reference gene. **a**. mRNA levels of expression of NRT2.1-2.7 and NRT1.1-2 relative to NRT2.1 expression; **b**. mRNA levels of expression of NRT2.1-2.7 and NRT1.1-2 (mean ± SE, n=3) relative to expression of each gene in WT, analyzed by ANOVA followed by *t* tests. Asterisks represent significant difference at $P \leq 0.05$.

AtNRT2.5 orthologs

Fifteen highly similar proteins were found in different plant species using BLAST search and AtNRT2.5 peptide sequence as a query in EnsemblPlants genome database (http://plants.ensembl.org/index.html). The predicted protein sequences are between 491 and 520 amino acids long, and have 12 putative transmembrane regions (predicted by HMMTOP 2; Tusnády and Simon, 1998; Tusnády and Simon, 2001). Alignment of the sequences revealed many highly conserved regions among species, without many gaps in the alignment (Fig. 5-11). Only N and C terminal portions of the polypeptides differ significantly among species (Fig. 5-11). Identity and similarity of the amino acid sequences were calculated using SIAS Server (Pedro Reche, http://imed.med.ucm.es/Tools/sias.html) and the Muscle alignment data from Figure 5-11. The identity/similarity matrix is shown in Table 5-2. The identity was in the 64 to 97 % range, while similarity varied from 80 to 99 %. *Arabidopsis thaliana* NRT2.5 showed the lowest identity of ~64 % with *Oryza sativa* (Os01g50820) sequence, and at the other end the highest amino acid identity of ~75 % with *Theobroma cacao* (1EG010451) sequence.

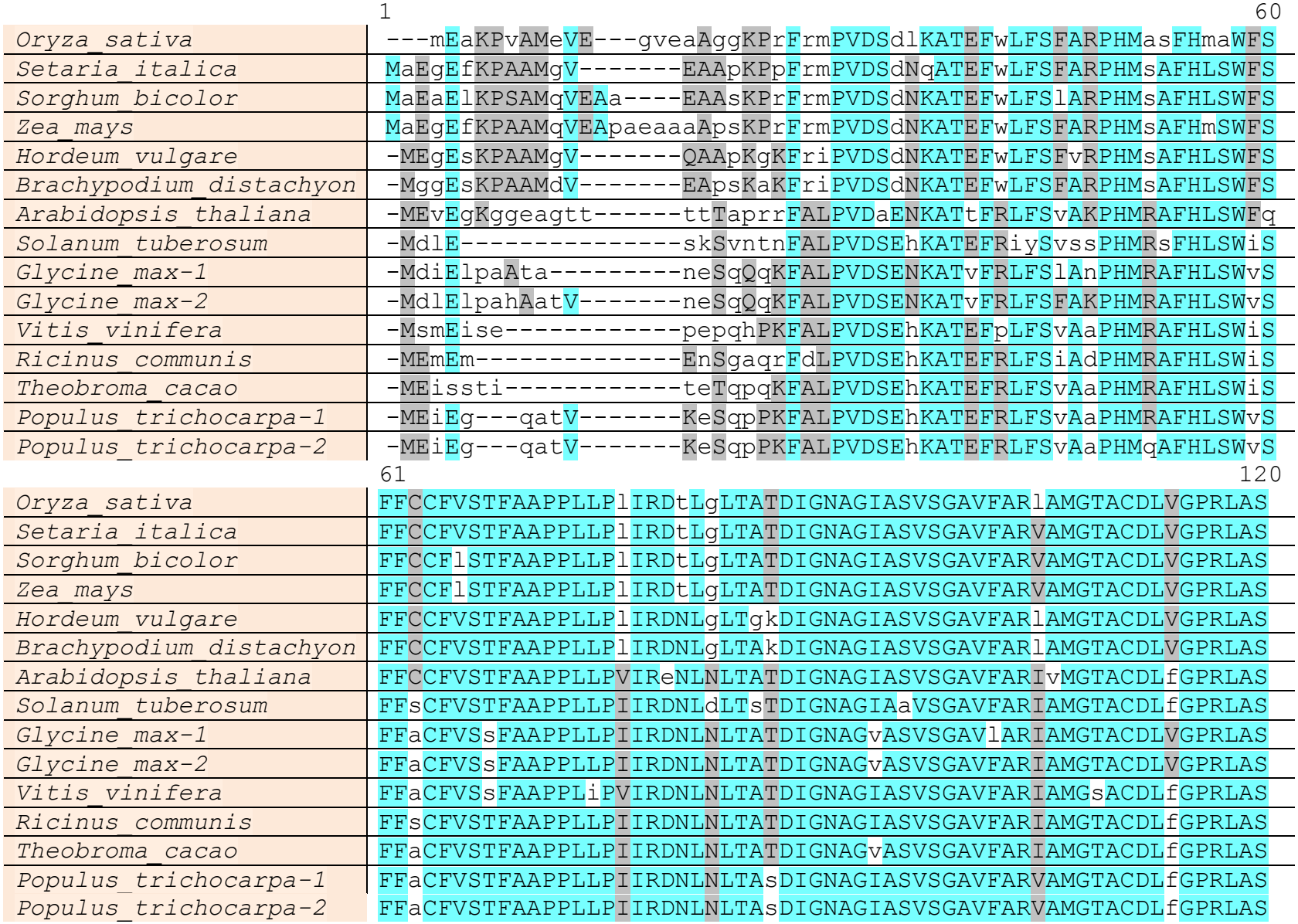
1
60
Oryza_sativa ---mEaKPvAMeVE---gveaAggKPrFrmPVDSdlKATEFwLFSFARPHMasFHmaWFS
Setaria_italica MaEgEfKPAAMgV-------EAApKPpFrmPVDSdNqATEFwLFSFARPHMsAFHLSWFS
Sorghum_bicolor MaEaElKPSAMqVEAa----EAAsKPrFrmPVDSdNKATEFwLFSlARPHMsAFHLSWFS
Zea_mays MaEgEfKPAAMqVEApaeaaaApsKPrFrmPVDSdNKATEFwLFSFARPHMsAFHmSWFS
Hordeum_vulgare -MEgEsKPAAMgV-------QAApKgKFriPVDSdNKATEFwLFSFvRPHMsAFHLSWFS
Brachypodium_distachyon -MggEsKPAAMdV-------EApsKaKFriPVDSdNKATEFwLFSFARPHMsAFHLSWFS
Arabidopsis_thaliana -MEvEgKggeagtt------ttTaprrFALPVDaENKATtFRLFSvAKPHMRAFHLSWFq
Solanum_tuberosum -MdlE---------------skSvntnFALPVDSEhKATEFRiySvssPHMRsFHLSWiS
Glycine_max-1 -MdiElpaAta---------neSqQqKFALPVDSENKATvFRLFSlAnPHMRAFHLSWvS
Glycine_max-2 -MdlElpahAatV-------neSqQqKFALPVDSENKATvFRLFSFAKPHMRAFHLSWvS
Vitis_vinifera -MsmEise------------pepqhPKFALPVDSEhKATEFpLFSvAaPHMRAFHLSWiS
Ricinus_communis -MEmEm--------------EnSgaqrFdLPVDSEhKATEFRLFSiAdPHMRAFHLSWiS
Theobroma_cacao -MEissti------------teTqpqKFALPVDSEhKATEFRLFSvAaPHMRAFHLSWiS
Populus_trichocarpa-1 -MEiEg---qatV-------KeSqpPKFALPVDSEhKATEFRLFSvAaPHMRAFHLSWvS
Populus_trichocarpa-2 -MEiEg---qatV-------KeSqpPKFALPVDSEhKATEFRLFSvAaPHMqAFHLSWvS
61
120
Oryza_sativa FFCCFVSTFAAPPLLPlIRDtLgLTATDIGNAGIASVSGAVFARlAMGTACDLVGPRLAS
Setaria_italica FFCCFVSTFAAPPLLPlIRDtLgLTATDIGNAGIASVSGAVFARVAMGTACDLVGPRLAS
Sorghum_bicolor FFCCFlSTFAAPPLLPlIRDtLgLTATDIGNAGIASVSGAVFARVAMGTACDLVGPRLAS
Zea_mays FFCCFlSTFAAPPLLPlIRDtLgLTATDIGNAGIASVSGAVFARVAMGTACDLVGPRLAS
Hordeum_vulgare FFCCFVSTFAAPPLLPlIRDNLgLTgkDIGNAGIASVSGAVFARlAMGTACDLVGPRLAS
Brachypodium_distachyon FFCCFVSTFAAPPLLPlIRDNLgLTAkDIGNAGIASVSGAVFARlAMGTACDLVGPRLAS
Arabidopsis_thaliana FFCCFVSTFAAPPLLPVIReNLNLTATDIGNAGIASVSGAVFARIvMGTACDLfGPRLAS
Solanum_tuberosum FFsCFVSTFAAPPLLPIIRDNLdLTsTDIGNAGIAaVSGAVFARIAMGTACDLfGPRLAS
Glycine_max-1 FFaCFVSsFAAPPLLPIIRDNLNLTATDIGNAGvASVSGAVlARIAMGTACDLVGPRLAS
Glycine_max-2 FFaCFVSsFAAPPLLPIIRDNLNLTATDIGNAGvASVSGAVFARIAMGTACDLVGPRLAS
Vitis_vinifera FFaCFVSsFAAPPLiPVIRDNLNLTATDIGNAGIASVSGAVFARIAMGsACDLfGPRLAS
Ricinus_communis FFsCFVSTFAAPPLLPIIRDNLNLTATDIGNAGIASVSGAVFARIAMGTACDLfGPRLAS
Theobroma_cacao FFaCFVSTFAAPPLLPIIRDNLNLTATDIGNAGvASVSGAVFARIAMGTACDLfGPRLAS
Populus_trichocarpa-1 FFaCFVSTFAAPPLLPIIRDNLNLTAsDIGNAGIASVSGAVFARVAMGTACDLfGPRLAS
Populus_trichocarpa-2 FFaCFVSTFAAPPLLPIIRDNLNLTAsDIGNAGIASVSGAVFARVAMGTACDLfGPRLAS

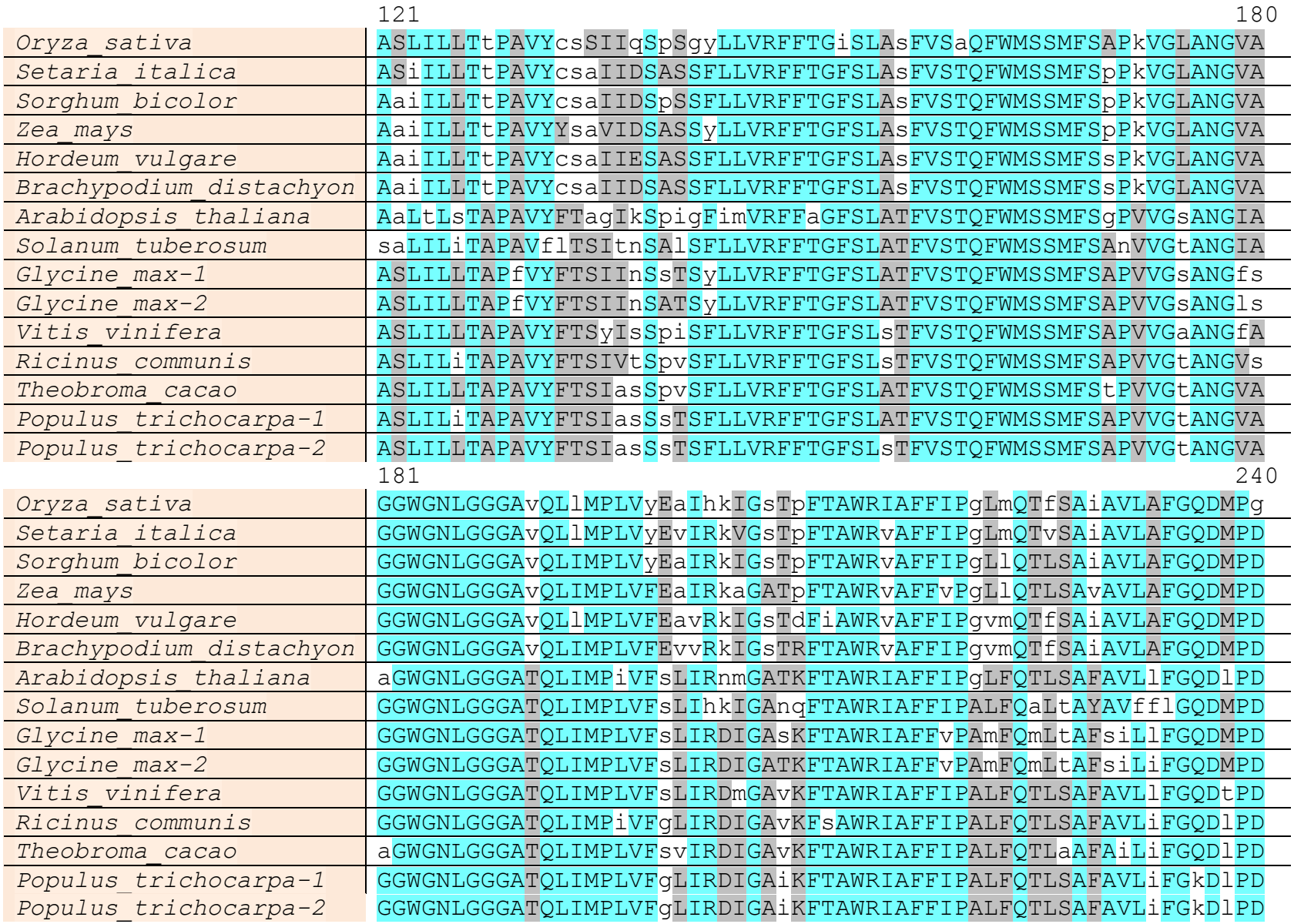
121
180
Oryza_sativa ASLILLTtPAVYcsSIIqSpSgyLLVRFFTGiSLAsFVSaQFWMSSMFSAPkVGLANGVA
Setaria_italica ASiILLTtPAVYcsaIIDSASSFLLVRFFTGFSLAsFVSTQFWMSSMFSpPkVGLANGVA
Sorghum_bicolor AaiILLTtPAVYcsaIIDSpSSFLLVRFFTGFSLAsFVSTQFWMSSMFSpPkVGLANGVA
Zea_mays AaiILLTtPAVYYsaVIDSASSyLLVRFFTGFSLAsFVSTQFWMSSMFSpPkVGLANGVA
Hordeum_vulgare AaiILLTtPAVYcsaIIESASSFLLVRFFTGFSLAsFVSTQFWMSSMFSsPkVGLANGVA
Brachypodium_distachyon AaiILLTtPAVYcsaIIDSASSFLLVRFFTGFSLAsFVSTQFWMSSMFSsPkVGLANGVA
Arabidopsis_thaliana AaLtLsTAPAVYFTagIkSpigFimVRFFaGFSLATFVSTQFWMSSMFSgPVVGsANGIA
Solanum_tuberosum saLILiTAPAVflTSItnSAlSFLLVRFFTGFSLATFVSTQFWMSSMFSAnVVGtANGIA
Glycine_max-1 ASLILLTAPfVYFTSIInSsTSyLLVRFFTGFSLATFVSTQFWMSSMFSAPVVGsANGfs
Glycine_max-2 ASLILLTAPfVYFTSIInSATSyLLVRFFTGFSLATFVSTQFWMSSMFSAPVVGsANGls
Vitis_vinifera ASLILLTAPAVYFTSyIsSpiSFLLVRFFTGFSLsTFVSTQFWMSSMFSAPVVGaANGfA
Ricinus_communis ASLILiTAPAVYFTSIVtSpvSFLLVRFFTGFSLsTFVSTQFWMSSMFSAPVVGtANGVs
Theobroma_cacao ASLILLTAPAVYFTSIasSpvSFLLVRFFTGFSLATFVSTQFWMSSMFStPVVGtANGVA
Populus_trichocarpa-1 ASLILiTAPAVYFTSIasSsTSFLLVRFFTGFSLATFVSTQFWMSSMFSAPVVGtANGVA
Populus_trichocarpa-2 ASLILLTAPAVYFTSIasSsTSFLLVRFFTGFSLsTFVSTQFWMSSMFSAPVVGtANGVA
181
240
Oryza_sativa GGWGNLGGGAvQLlMPLVyEaIhkIGsTpFTAWRIAFFIPgLmQTfSAiAVLAFGQDMPg
Setaria_italica GGWGNLGGGAvQLlMPLVyEvIRkVGsTpFTAWRvAFFIPgLmQTvSAiAVLAFGQDMPD
Sorghum_bicolor GGWGNLGGGAvQLIMPLVyEaIRkIGsTpFTAWRvAFFIPgLlQTLSAiAVLAFGQDMPD
Zea_mays GGWGNLGGGAvQLIMPLVFEaIRkaGATpFTAWRvAFFvPgLlQTLSAvAVLAFGQDMPD
Hordeum_vulgare GGWGNLGGGAvQLlMPLVFEavRkIGsTdFiAWRvAFFIPgvmQTfSAiAVLAFGQDMPD
Brachypodium_distachyon GGWGNLGGGAvQLIMPLVFEvvRkIGsTRFTAWRvAFFIPgvmQTfSAiAVLAFGQDMPD
Arabidopsis_thaliana aGWGNLGGGATQLIMPiVFsLIRnmGATKFTAWRIAFFIPgLFQTLSAFAVLlFGQDlPD
Solanum_tuberosum GGWGNLGGGATQLIMPLVFsLIhkIGAnqFTAWRIAFFIPALFQaLtAYAVfflGQDMPD
Glycine_max-1 GGWGNLGGGATQLIMPLVFsLIRDIGAsKFTAWRIAFFvPAmFQmLtAFsiLlFGQDMPD
Glycine_max-2 GGWGNLGGGATQLIMPLVFsLIRDIGATKFTAWRIAFFvPAmFQmLtAFsiLiFGQDMPD
Vitis_vinifera GGWGNLGGGATQLIMPLVFsLIRDmGAvKFTAWRIAFFIPALFQTLSAFAVLlFGQDtPD
Ricinus_communis GGWGNLGGGATQLIMPiVFgLIRDIGAvKFsAWRIAFFIPALFQTLSAFAVLiFGQDlPD
Theobroma_cacao aGWGNLGGGATQLIMPLVFsvIRDIGAvKFTAWRIAFFIPALFQTLaAFAiLiFGQDlPD
Populus_trichocarpa-1 GGWGNLGGGATQLIMPLVFgLIRDIGAiKFTAWRIAFFIPALFQTLSAFAVLiFGkDlPD
Populus_trichocarpa-2 GGWGNLGGGATQLIMPLVFgLIRDIGAiKFTAWRIAFFIPALFQTLSAFAVLiFGkDlPD

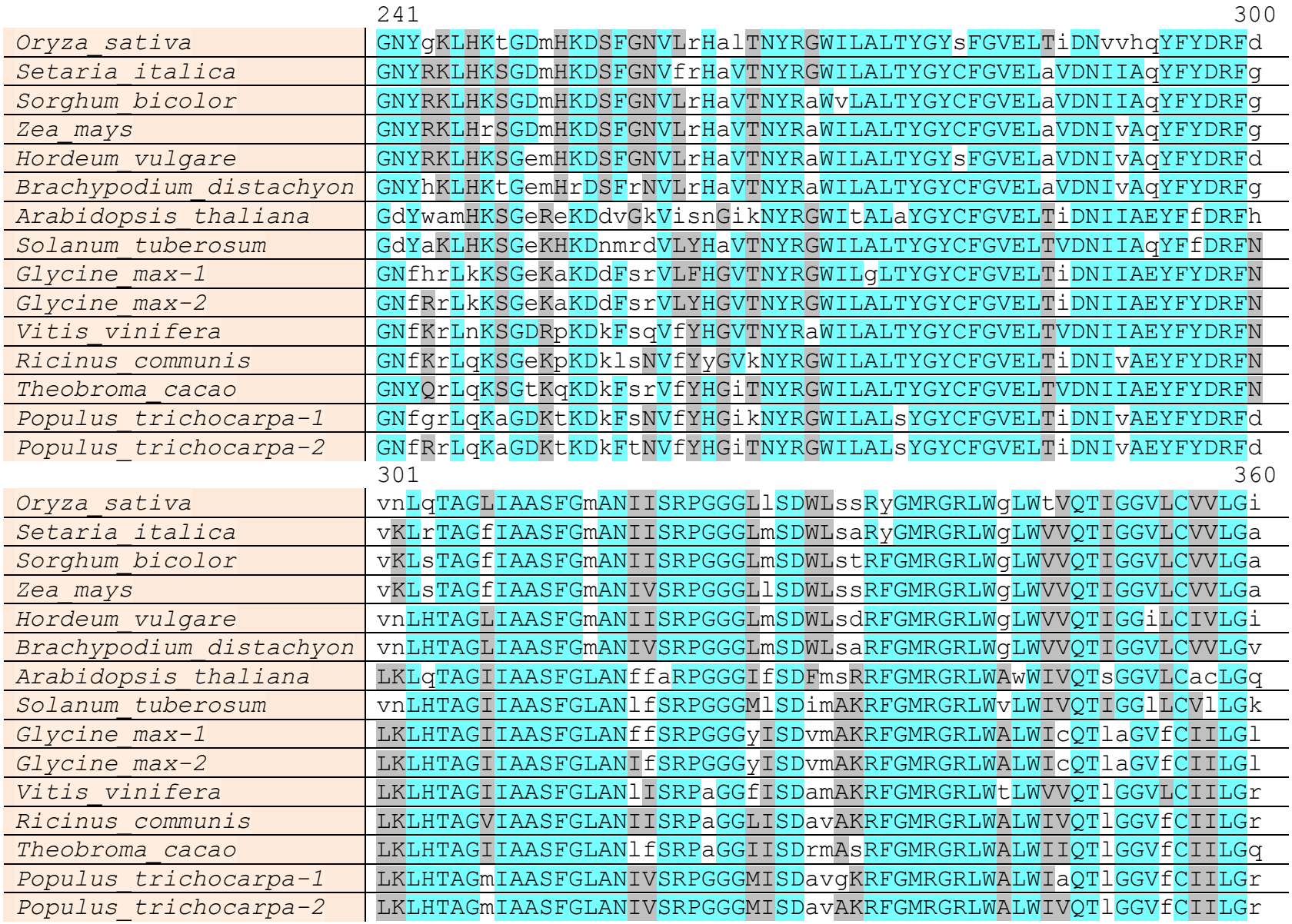
241
300
Oryza_sativa GNYgKLHKtGDmHKDSFGNVLrHalTNYRGWILALTYGYsFGVELTiDNvvhqYFYDRFd
Setaria_italica GNYRKLHKSGDmHKDSFGNVfrHaVTNYRGWILALTYGYCFGVELaVDNIIAqYFYDRFg
Sorghum_bicolor GNYRKLHKSGDmHKDSFGNVLrHaVTNYRaWvLALTYGYCFGVELaVDNIIAqYFYDRFg
Zea_mays GNYRKLHrSGDmHKDSFGNVLrHaVTNYRaWILALTYGYCFGVELaVDNIvAqYFYDRFg
Hordeum_vulgare GNYRKLHKSGemHKDSFGNVLrHaVTNYRaWILALTYGYsFGVELaVDNIvAqYFYDRFd
Brachypodium_distachyon GNYhKLHKtGemHrDSFrNVLrHaVTNYRaWILALTYGYCFGVELaVDNIvAqYFYDRFg
Arabidopsis_thaliana GdYwamHKSGeReKDdvGkVisnGikNYRGWItALaYGYCFGVELTiDNIIAEYFfDRFh
Solanum_tuberosum GdYaKLHKSGeKHKDnmrdVLYHaVTNYRGWILALTYGYCFGVELTVDNIIAqYFfDRFN
Glycine_max-1 GNfhrLkKSGeKaKDdFsrVLFHGVTNYRGWILgLTYGYCFGVELTiDNIIAEYFYDRFN
Glycine_max-2 GNfRrLkKSGeKaKDdFsrVLYHGVTNYRGWILALTYGYCFGVELTiDNIIAEYFYDRFN
Vitis_vinifera GNfKrLnKSGDRpKDkFsqVfYHGVTNYRaWILALTYGYCFGVELTVDNIIAEYFYDRFN
Ricinus_communis GNfKrLqKSGeKpKDklsNVfYyGVkNYRGWILALTYGYCFGVELTiDNIvAEYFYDRFN
Theobroma_cacao GNYQrLqKSGtKqKDkFsrVfYHGiTNYRGWILALTYGYCFGVELTVDNIIAEYFYDRFN
Populus_trichocarpa-1 GNfgrLqKaGDKtKDkFsNVfYHGikNYRGWILALsYGYCFGVELTiDNIvAEYFYDRFd
Populus_trichocarpa-2 GNfRrLqKaGDKtKDkFtNVfYHGiTNYRGWILALsYGYCFGVELTiDNIvAEYFYDRFd
301
360
Oryza_sativa vnLqTAGLIAASFGmANIISRPGGGLlSDWLssRyGMRGRLWgLWtVQTIGGVLCVVLGi
Setaria_italica vKLrTAGfIAASFGmANIISRPGGGLmSDWLsaRyGMRGRLWgLWVVQTIGGVLCVVLGa
Sorghum_bicolor vKLsTAGfIAASFGmANIISRPGGGLmSDWLstRFGMRGRLWgLWVVQTIGGVLCVVLGa
Zea_mays vKLsTAGfIAASFGmANIVSRPGGGLlSDWLssRFGMRGRLWgLWVVQTIGGVLCVVLGa
Hordeum_vulgare vnLHTAGLIAASFGmANIISRPGGGLmSDWLsdRFGMRGRLWgLWVVQTIGGiLCIVLGi
Brachypodium_distachyon vnLHTAGLIAASFGmANIVSRPGGGLmSDWLsaRFGMRGRLWgLWVVQTIGGVLCVVLGv
Arabidopsis_thaliana LKLqTAGIIAASFGLANffaRPGGGIfSDFmsRRFGMRGRLWAwWIVQTsGGVLCacLGq
Solanum_tuberosum vnLHTAGIIAASFGLANlfSRPGGGMlSDimAKRFGMRGRLWvLWIVQTIGGlLCVlLGk
Glycine_max-1 LKLHTAGIIAASFGLANffSRPGGGyISDvmAKRFGMRGRLWALWIcQTlaGVfCIILGl
Glycine_max-2 LKLHTAGIIAASFGLANIfSRPGGGyISDvmAKRFGMRGRLWALWIcQTlaGVfCIILGl
Vitis_vinifera LKLHTAGIIAASFGLANlISRPaGGfISDamAKRFGMRGRLWtLWVVQTlGGVLCIILGr
Ricinus_communis LKLHTAGVIAASFGLANIISRPaGGLISDavAKRFGMRGRLWALWIVQTlGGVfCIILGr
Theobroma_cacao LKLHTAGIIAASFGLANlfSRPaGGIISDrmAsRFGMRGRLWALWIIQTlGGVfCIILGq
Populus_trichocarpa-1 LKLHTAGmIAASFGLANIVSRPGGGMISDavgKRFGMRGRLWALWIaQTlGGVfCIILGr
Populus_trichocarpa-2 LKLHTAGmIAASFGLANIVSRPGGGMISDavAKRFGMRGRLWALWIVQTlGGVfCIILGr

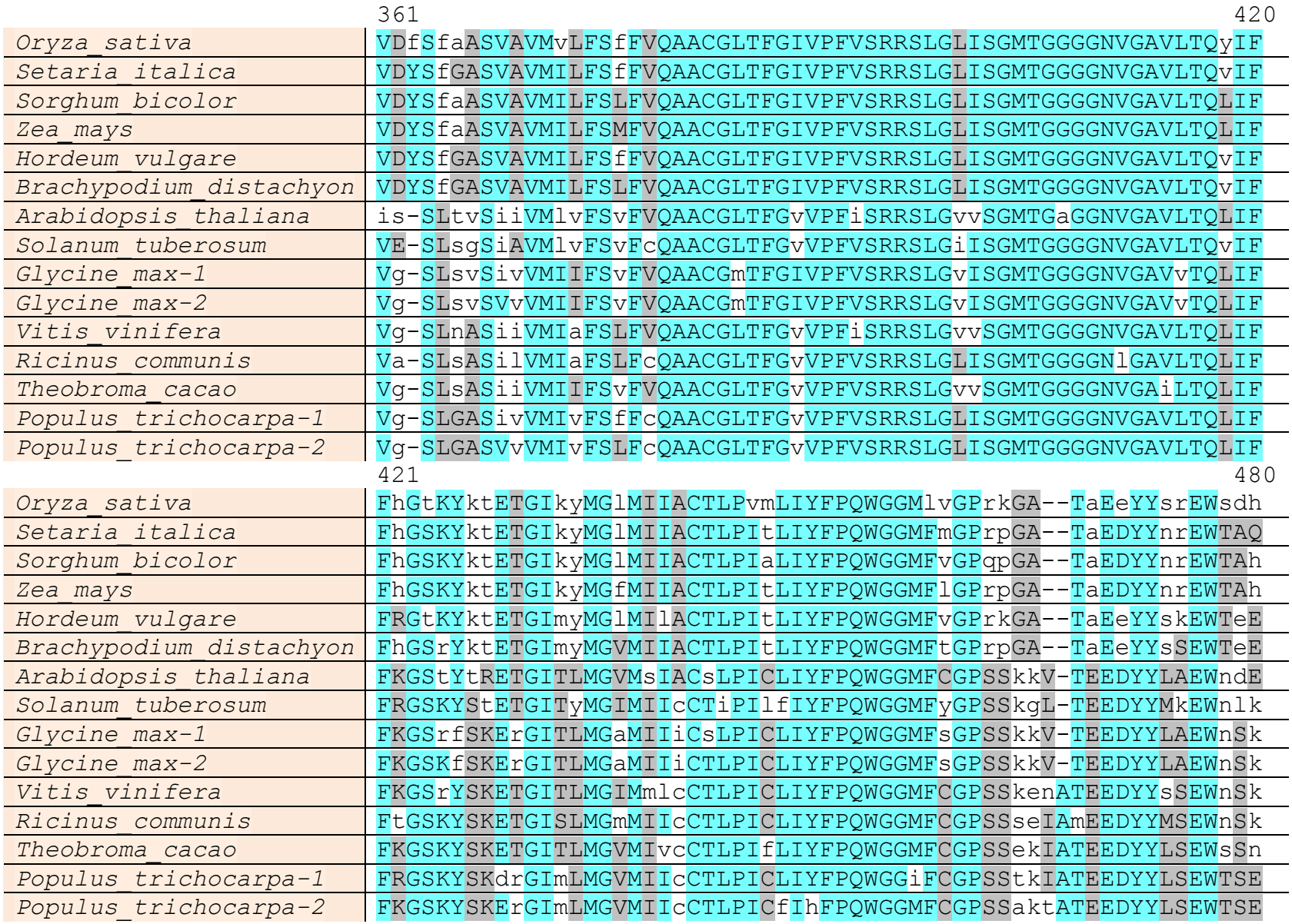
361
420
Oryza_sativa VDfSfaASVAVMvLFSfFVQAACGLTFGIVPFVSRRSLGLISGMTGGGGNVGAVLTQyIF
Setaria_italica VDYSfGASVAVMILFSfFVQAACGLTFGIVPFVSRRSLGLISGMTGGGGNVGAVLTQvIF
Sorghum_bicolor VDYSfaASVAVMILFSLFVQAACGLTFGIVPFVSRRSLGLISGMTGGGGNVGAVLTQLIF
Zea_mays VDYSfaASVAVMILFSMFVQAACGLTFGIVPFVSRRSLGLISGMTGGGGNVGAVLTQLIF
Hordeum_vulgare VDYSfGASVAVMILFSfFVQAACGLTFGIVPFVSRRSLGLISGMTGGGGNVGAVLTQvIF
Brachypodium_distachyon VDYSfGASVAVMILFSLFVQAACGLTFGIVPFVSRRSLGLISGMTGGGGNVGAVLTQvIF
Arabidopsis_thaliana is-SLtvSiiVMlvFSvFVQAACGLTFGvVPFiSRRSLGvvSGMTGaGGNVGAVLTQLIF
Solanum_tuberosum VE-SLsgSiAVMlvFSvFcQAACGLTFGvVPFVSRRSLGiISGMTGGGGNVGAVLTQvIF
Glycine_max-1 Vg-SLsvSivVMIIFSvFVQAACGmTFGIVPFVSRRSLGvISGMTGGGGNVGAVvTQLIF
Glycine_max-2 Vg-SLsvSVvVMIIFSvFVQAACGmTFGIVPFVSRRSLGvISGMTGGGGNVGAVvTQLIF
Vitis_vinifera Vg-SLnASiiVMIaFSLFVQAACGLTFGvVPFiSRRSLGvvSGMTGGGGNVGAVLTQLIF
Ricinus_communis Va-SLsASilVMIaFSLFcQAACGLTFGvVPFVSRRSLGLISGMTGGGGNlGAVLTQLIF
Theobroma_cacao Vg-SLsASiiVMIIFSvFVQAACGLTFGvVPFVSRRSLGvvSGMTGGGGNVGAiLTQLIF
Populus_trichocarpa-1 Vg-SLGASivVMIvFSfFcQAACGLTFGvVPFVSRRSLGLISGMTGGGGNVGAVLTQLIF
Populus_trichocarpa-2 Vg-SLGASVvVMIvFSLFcQAACGLTFGvVPFVSRRSLGLISGMTGGGGNVGAVLTQLIF
421
480
Oryza_sativa FhGtKYktETGIkyMGlMIIACTLPvmLIYFPQWGGMlvGPrkGA--TaEeYYsrEWsdh
Setaria_italica FhGSKYktETGIkyMGlMIIACTLPItLIYFPQWGGMFmGPrpGA--TaEDYYnrEWTAQ
Sorghum_bicolor FhGSKYktETGIkyMGlMIIACTLPIaLIYFPQWGGMFvGPqpGA--TaEDYYnrEWTAh
Zea_mays FhGSKYktETGIkyMGfMIIACTLPItLIYFPQWGGMFlGPrpGA--TaEDYYnrEWTAh
Hordeum_vulgare FRGtKYktETGImyMGlMIlACTLPItLIYFPQWGGMFvGPrkGA--TaEeYYskEWTeE
Brachypodium_distachyon FhGSrYktETGImyMGVMIIACTLPItLIYFPQWGGMFtGPrpGA--TaEeYYsSEWTeE
Arabidopsis_thaliana FKGStYtRETGITLMGVMsIACsLPICLIYFPQWGGMFCGPSSkkV-TEEDYYLAEWndE
Solanum_tuberosum FRGSKYStETGITyMGIMIIcCTiPIlfIYFPQWGGMFyGPSSkgL-TEEDYYMkEWnlk
Glycine_max-1 FKGSrfSKErGITLMGaMIIiCsLPICLIYFPQWGGMFsGPSSkkV-TEEDYYLAEWnSk
Glycine_max-2 FKGSKfSKErGITLMGaMIIiCTLPICLIYFPQWGGMFsGPSSkkV-TEEDYYLAEWnSk
Vitis_vinifera FKGSrYSKETGITLMGIMmlcCTLPICLIYFPQWGGMFCGPSSkenATEEDYYsSEWnSk
Ricinus_communis FtGSKYSKETGISLMGmMIIcCTLPICLIYFPQWGGMFCGPSSseIAmEEDYYMSEWnSk
Theobroma_cacao FKGSKYSKETGITLMGVMIvcCTLPIfLIYFPQWGGMFCGPSSekIATEEDYYLSEWsSn
Populus_trichocarpa-1 FRGSKYSKdrGImLMGVMIIcCTLPICLIYFPQWGGiFCGPSStkIATEEDYYLSEWTSE
Populus_trichocarpa-2 FKGSKYSKErGImLMGVMIIcCTLPICfIhFPQWGGMFCGPSSaktATEEDYYLSEWTSE

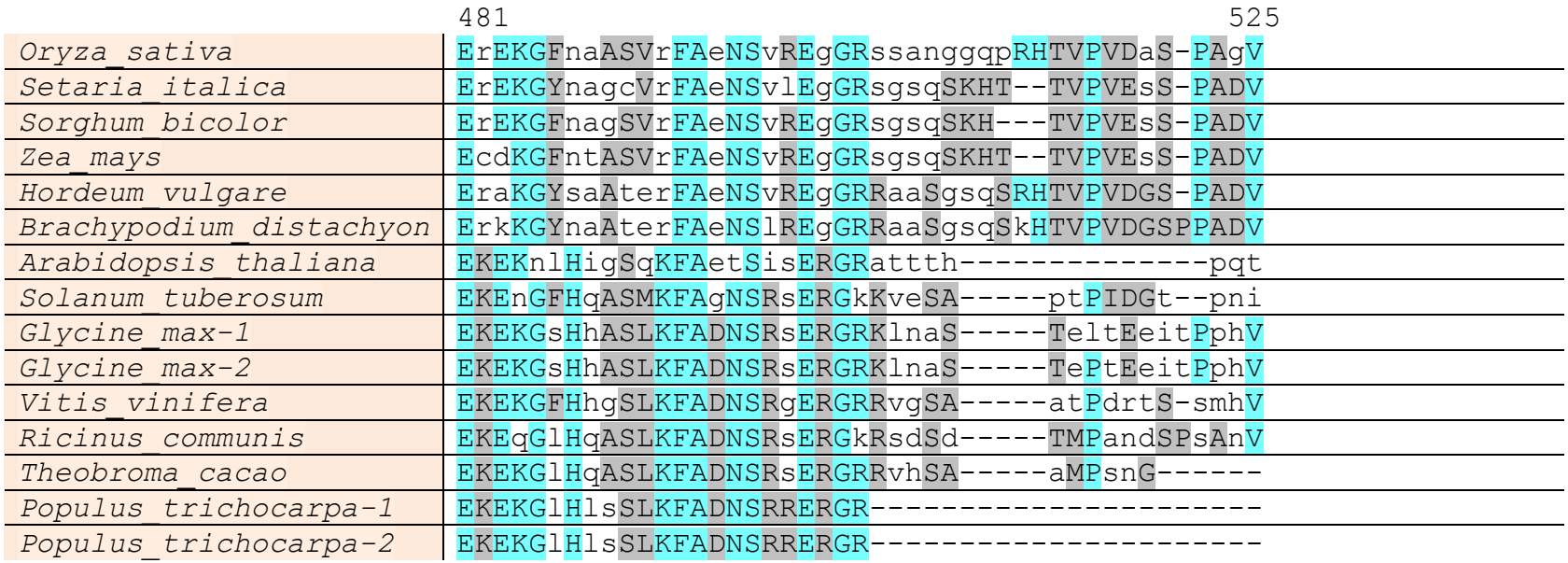

Figure 5-11. Multiple sequence alignment of AtNRT2.5 orthologs using Muscle alignment software (Edgar, 2004). Highly conserved amino acids are highlighted in blue. Gene IDs: ***Oryza_sativa***- OS01G5082; ***Setaria_italica*** - K3XRA3_SETIT; ***Sorghum_bicolor*** - SB03G032310; ***Zea_mays*** - GRMZM2G455124; ***Hordeum_vulgare*** - A0EXC0_HORVD; ***Brachypodium_distachyon***- Bradi2G47640; ***Arabidopsis_thaliana*** - AT1G12940; ***Solanum_tuberosum***- PGSC0003DMP400029708; ***Glycine_max-1*** - Glyma08g39140; ***Glycine_max-2*** - Glyma18g20510; ***Vitis_vinifera*** - F6HHT1_VITVI VIT_01s0127g00070; ***Ricinus_communis*** - 27504.m000614; ***Theobroma_cacao*** - Thecc1EG010451; ***Populus_trichocarpa-1*** - B9IEW2_POPTR; ***Populus_trichocarpa-2*** - B9IEW4_POPTR

Table 5-2. Amino acid identity (blue) and similarity (red) matrix of the *Arabidopsis thaliana* AtNRT2.5 orthologs (sequences and gene IDs given in the Figure 5-11). Values were obtained using SIAS server (Pedro Reche, http://imed.med.ucm.es/Tools/sias.html)

%	Sb	Zm	Si	Hv	Bd	Os	Vv	Tc	Rc	Pt1	Pt2	Gm1	Gm2	At	St
S.bicolor	-	98.01	96.93	93.86	94.22	93.5	81.04	79.78	80.68	80.86	81.40	81.94	81.76	81.04	84.29
Z.mays	93.86	-	96.38	93.32	93.68	92.41	79.60	78.70	79.78	79.96	80.50	81.22	81.04	79.42	83.39
S.italica	93.50	91.33	-	94.58	94.40	92.96	80.68	79.42	80.14	81.04	81.58	81.76	81.76	80.14	84.11
H.vulgare	87.36	85.55	88.98	-	96.75	93.50	80.50	78.88	79.96	80.68	81.22	81.76	81.76	79.24	84.29
B.distachyon	88.26	87	89.35	93.14	-	92.59	81.22	79.96	80.86	81.40	81.94	82.67	82.49	80.32	85.19
O.sativa	85.19	83.21	85.37	85.19	83.57	-	79.78	79.24	80.14	80.14	80.14	81.04	81.04	79.96	84.47
V.vinifera	68.23	66.06	67.68	66.78	67.32	64.80	-	92.59	93.32	90.43	90.79	90.79	90.79	85.37	87.54
T.cacao	66.78	65.16	66.78	65.70	66.60	64.44	85.92	-	92.41	91.51	91.33	90.43	90.43	86.10	88.62
R.communis	68.05	66.24	67.68	67.32	67.87	66.06	84.65	84.65	-	91.33	90.97	90.25	90.25	85.92	88.98
P.trichocarpa1	68.23	66.96	68.41	67.50	68.23	66.24	81.58	84.83	84.83	-	98.91	89.35	89.16	86.10	87
P.trichocarpa 2	69.13	67.68	68.95	67.87	68.95	66.42	82.31	84.65	84.47	96.93	-	89.35	89.16	85.55	86.82
G.max1	66.06	64.98	65.52	65.16	65.88	64.25	80.50	81.22	79.42	79.42	79.42	-	99.09	87.36	88.98
G.max2	66.96	66.42	66.96	66.60	66.60	65.34	80.32	81.94	80.32	79.96	80.50	96.57	-	87.18	88.62
A.thaliana	66.24	64.44	65.70	63.89	64.80	63.53	74.90	75.45	73.10	74.36	74	74.54	74.18	-	85.55
S.tuberosum	68.95	67.68	68.59	69.49	69.85	68.05	74.54	76.35	75.99	73.82	73.82	74.18	74.90	71.66	-

Discussion

It is well documented that nitrate uptake in N-starved plants is increased by exposure to external nitrate, mainly by up-regulation of *AtNRT2.1* and *AtNRT2.2*. The corresponding proteins, in association with AtNAR2.1 constitute the high-affinity nitrate transport system (iHATS). In addition to iHATS, the existence of a constitutive high-affinity transport system in plants that does not require prior exposure to nitrate is supported by ample physiological evidence (Behl *et al*., 1988; Aslam *et al*., 1992; Siddiqi *et al*., 1992; Wang and Crawford, 1996). Behl *et al.* (1988) concluded based on their experimental work with barley that the role of the low-capacity cHATS is to take up nitrate and facilitate up-regulation of the high-capacity inducible system.

AtNRT2.5 is one of 7 members of the *NRT2* transporter family in Arabidopsis. Its importance in the plant-growth response to growth-promoting soil bacterium *Phylliobacterium brassicacearum* has recently been shown (Kechid *et al*., 2013). In Chapter 3, I have demonstrated that AtNRT2.5 interacts with AtNAR2.1 in yeast, and that *Xenopus* oocytes injected with a cRNA mixture of *AtNRT2.5* and *AtNAR2.1* showed the highest levels of nitrate uptake compared to all other AtNRT2 representatives, indicating an important function in nitrate transport for NRT2.5.

AtNRT2.5 is located on chromosome 1 in the forward orientation, on the first half of the chromosome, as are the three most important Arabidopsis transporters involved in nitrate uptake *NRT1.1*, *NRT2.1* and *NRT2.2* (Fig. 5-1a). Two independent T-DNA-insertion mutant alleles of *AtNRT2.5* were characterized (*Atnrt2.5-1* and *Atnrt2.5-2*), and complete loss of *NRT2.5* expression due to exon position of the insertions was demonstrated (Fig. 5.1b and 5-2).

The effect of these mutations on nitrate uptake was examined using $^{13}NO_3^-$. Both mutants showed a consistent reduction of high-affinity nitrate uptake compared to WT (Fig. 5-3, 5-4 and 5.5), the defective nitrate uptake being more pronounced in N-starved (uninduced) plants, prior to re-exposure to nitrate (Fig. 5-3 and 5-5a). Observed $^{13}NO_3^-$ influx in uninduced *Atnrt2.5-1* and *Atnrt2.5-2* mutants was reduced by from 50 to 65% of WT fluxes. Induced influx was always significantly higher than that of uninduced fluxes in both WT and *Atnrt2.5-1* (Fig. 5-3 and 5-5a), similar to earlier findings presented in publications by Cerezo

et al. (2001) and Li *et al.* (2007). *Atnrt2.5-1* exhibited a statistically significant reduction of nitrate influx compared to WT even in 6-h induced plants (Fig. 5-3a). This might be due to slower induction of iHATS influx encoded by AtNRT2.1 as less nitrate is taken up into the mutant roots to promote the induction. This hypothesis is supported by the lower nitrate content measured in roots and shoots of the *Atnrt2.5-1* mutants compared to WT (Fig. 5-8) and the quantitative RT-PCR data indicating lower expression of *AtNRT2.1* in *Atnrt2.5-1* mutant (Fig. 5-10). Similarly, expression of *AtNRT2.1* and *AtNRT1.1* was markedly reduced in the *Atnar2.1-1* mutant compared to WT plants grown on 0.2 mM nitrate (Orsel *et al*., 2006), and induction of *AtNRT2.1* and *AtNRT1.1* by nitrate was hindered in *Atnar2.1-2* mutant (Okamoto *et al*., 2006). Accordingly, Okamoto *et al.* (2006) reported almost five times lower root nitrate concentration in *Atnar2.1-2* mutants compared to WT. Experimental data presented in Chapter 3 indicate that AtNRT2.5 requires co-expression of AtNAR2.1 to exert functional nitrate transport. Lower expression of *AtNRT2.1* observed by Okamoto *et al.* (2006) and Orsel *et al*. (2006) in *nar2.1* mutants might be the result of the absence of a functional AtNRT2.5 transporter in *nar2.1* mutants which is required to take up nitrate for the induction of *AtNRT2.1* and *AtNRT1.1*.

Evaluation of the concentration dependence of the $^{13}NO_3^-$ influx in uninduced WT plants revealed that cHATS (influx in uninduced N-starved plants) conforms to saturable Michaelis–Menten kinetics over the low nitrate concentration range from 10 to 250 µM KNO_3 (Fig. 5-4a and 5-5b). Nitrate uptake in *Atnrt2.5* mutants was reduced at all concentrations, averaging more than 60 % overall. I have calculated kinetic parameters of the difference between WT and *Atnrt2.5-1* $^{13}NO_3^-$ influx as a measure of that due to the AtNRT2.5 transporter. Vmax is estimated to be 2.3 µmol g FW^{-1} h^{-1} and Km to ~11 µM. These results are consistent with findings by Behl *et al*. (1988), Siddiqi *et al*. (1990), Aslam *et al*. (1992) and Kronzucker *et al*. (1995) where cHATS was found to be a low capacity uptake system that exhibits high substrate specificity (low Km).

The reduction of nitrate influx in the *Atnrt2.5-1* mutant was evident only in roots, but not in shoot tissue, indicating that AtNRT2.5 plays an important role in nitrate uptake into roots and not in the transfer of nitrate to shoots of Arabidopsis (Fig. 5-6). This is consistent with patterns of mRNA expression of *AtNRT2.5* that was more abundant in roots than in shoots of

5-week old WT plants (Fig. 5-9a). The same expression profile of *AtNRT2.5* during both vegetative and reproductive growth stage of Arabidopsis was observed previously by Orsel *et al.* (2002) and Okamoto *et al.* (2003). In addition, *AtNRT2.5* gene expression was strongly suppressed by nitrate and ammonium supply to N-starved plants (Fig. 5-9b). After prolonged nitrate exposure, mRNA of *AtNRT2.5* was almost undetectable. Likewise, Okamoto *et al*. (2003) observed that induction of WT Arabidopsis with nitrate repressed expression of AtNRT2.5. Elevated expression of *AtNRT2.5* in roots under N-starvation is consistent with its role as a component of cHATS that has the important function in nitrate uptake to exert full induction of the high capacity iHATS. Repression of its expression by nitrate supply could be beneficial to plants that are investing energy in up-regulating the inducible system genes like *AtNRT2.1* and *AtNRT2.2* (Filleur *et al.*, 2001; Li *et al*., 2007) because iHATS has higher capacity than cHATS and is, therefore, a preferable uptake system. Recently, Garnett and colleagues followed responses of nitrate transporters to nitrogen supply in *Zea mays* over the life cycle and found that *ZmNRT2.5* is only expressed when plants were grown in low nitrate hydroponic solution (Garnett *et al*., 2013). Moreover, while examining the double deletion (*NRT2.1/NRT2.2*) Arabidopsis *nrt2* mutant, defective in iHATS, Cerezo and others found that the remaining high-affinity nitrate uptake in the mutant is not inducible by nitrate, is saturable and most likely the result of cHATS activity (Cerezo *et al*., 2001). Also, Figure 5-9c shows that the expression of *AtNRT2.5* is significantly higher in double mutant *Atnrt2.1-nrt2.2* (mutant described in Li *et al*., 2007) compared with WT plants both under induced and uninduced conditions. Similar observations were presented earlier showing elevated expression of *AtNRT2.5* in *Atnrt2.1-1* mutant disrupted in both NRT2.1 and NRT2.2 compared to WT (Orsel *et al.*, 2004*;* Orsel *et al.*, 2006). It is possible that N starvation is more pronounced in the mutant plants allowing higher expression of the cHATS gene and, in the case of induced plants (Fig. 5-9c), *AtNRT2.5* up-regulation could be a compensatory mechanism mitigating the absence of AtNRT2.1 and AtNRT2.2.

It was clearly demonstrated that the absence of *AtNRT2.1* in Arabidopsis mutant lines has a strong effect on plant growth resulting in smaller plants, especially at low nitrate supply (Li et al., 2007). AtNRT2.1 also has an important role in morphological and physiological responses of the root system to nitrogen-limited conditions, having direct effect on initiation of lateral root primordia (Remans *et al*., 2006). In order to examine the effect of *AtNRT2.5*

mutation on growth, plants were grown on low and high nitrate prior to weight and root length measurements. There were no differences between WT and *Atnrt2.5-1* root weights of 5-week old plants or root length of 2-week old plants (Fig. 5-7a and 5-7c, respectively). The only significant difference between the mutant and WT was observed in shoots of plants grown for 5 weeks under low (250 µM) nitrate (Fig. 5-7b).

The evidence presented in this chapter strongly supports the hypothesis that AtNRT2.5 encodes the cHATS transporter in roots of *A. thaliana*. Even though the *Atnrt2.5-1* mutant lacks expression of *AtNRT2.5* completely, there is a significant nitrate influx of around 40 % of WT left in the mutant. Consequently, an important question arises: where does the remaining influx come from in the mutant? To check for possible up-regulation of other nitrate transporters in the absence of AtNRT2.5, the expression of six NRT2s and also two known LATS NRT1 genes was examined in uninduced *Atnrt2.5-1* and WT plants. The gene with highest expression in WT plants was *AtNRT2.1*, followed by *AtNRT2.2* and *AtNRT2.4*. All other genes showed very low expression (Fig. 5-10a). Genes that are known to be inducible by nitrate (*AtNRT2.1, AtNRT2.2, AtNRT2.4* and *AtNRT1.1*) had significantly lower expression in the *Atnrt2.5-1* (5-10b). The phenomenon could be explained by less nitrate being available for induction due to the absence of the AtNRT2.5 transporter in the mutant. None of the genes examined showed statistically significant increase in their expression in the mutant genotype and they do not seem to be compensating for AtNRT2.5 in the *Atnrt2.5-1* (Fig. 5-10b). A possible source of the remaining nitrate influx in *Atnrt2.5* mutants could be the AtNRT2.1/AtNAR2.1 molecular complex that encodes iHATS (described in Chapter 2). As shown in the Chapter 2, the AtNRT2.1/AtNAR2.1 complex has a long half-life and is present even in uninduced plants, starved of nitrogen for 1 week, the same conditions used to measure constitutive HATS presented in this chapter. Moreover, cHATS was found to be reduced by 30 % in *Atnrt2.1-nrt2.2* mutant compared to WT (Li *et al*., 2007), signifying contribution of AtNRT2.1 and/or AtNRT2.2 to the constitutive nitrate influx under the same conditions used in experimental work presented in this chapter. Also, AtNRT2.4 expressed in roots under N-starvation contributes to nitrate influx in the very low concentration range, below 100 µM (Kiba *et al*., 2012). In addition, there may be some contribution to the constitutive high-affinity nitrate influx by LATS transporters, namely AtNRT1.1 and AtNRT1.2 (Liu *et al*., 1999; Huang *et al*., 1999).

The importance of the NRT2.5 transporter is further substantiated by the existence of highly similar homologs in other plants species (Fig. 5-11). Amino acid sequence identity among the different NRT2.5 orthologs compared here ranges from 64 to 97 % (Table 5-2). Arabidopsis NRT2.5 shares between 79 and 87 % similarity with other species orthologs (Table 5-2), while having only 58-67 % similarity with other Arabidopsis NRT2 family members (Orsel *et al*., 2002; Plett *et al*., 2010).

Conclusion

The work presented in this thesis provides evidence supporting the research hypotheses stated in the Introduction. My experimental results have added novel information about nitrite and nitrate uptake in plants using the model dicot *Arabidopsis thaliana.* I have emphasised the importance of nitrite uptake and shown that plants have nitrite-specific transport (Chapter 1). Furthermore, the molecular complex responsible for iHATS in Arabidopsis has been isolated and characterized (Chapter 2). The importance of AtNAR2.1 for the function of other members of the NRT2 family was demonstrated in Chapter 3. Chapter 4 clearly demonstrated a crucial role of the central cytoplasmic loop of AtNRT2.1 in its interaction with AtNAR2.1. Finally, I have established that *AtNRT2.5* encodes the constitutive high-affinity nitrate transporter in roots of Arabidopsis and has a critical role in induction of *AtNRT2.1*.

Chapter 1

It is well established that plants and fungi are capable of taking up nitrite (Criddle *et al.*, 1988; Brinkhuis *et al.*, 1989; Zsoldos *et al.*, 1993; Wang *et al.*, 2008). Nitrite is a potential source of N, and as such may play an important role under certain environmental conditions that favour its accumulation. Bacterial, algal and fungal nitrite transporters have been characterized (Galvan *et al.*, 1996; Gao-Rubinelli and Marzluf, 2004; Jia and Cole, 2005; Serrani and Berardi, 2005; Wang *et al.*, 2008; Jia *et al.*, 2009; Unkles *et al.*, 2011). For the first time in higher plants, I have provided the following evidence of the existence of a nitrite-specific transporter:

1. The *Atnar2.1-2* mutant, lacking a functional iHATS for nitrate influx, is, nevertheless, still capable of significant nitrite influx (60% of WT) that conforms to Michaelis-Menten kinetics. While the *Atnar2.1-2* plants cannot sustain growth on low nitrate, this nitrite uptake allows them to grow on low nitrite as sole N source.
2. Unlike nitrate influx, this putative nitrite-specific influx is not inducible but constitutive.
3. Nitrite influx by this nitrite-specific transporter is unaffected by nitrate competition, and the putative nitrite transporter is incapable of nitrate uptake.

4. Nitrite influx by means of the nitrite-specific transporter is an active process, and is subject to down-regulation by ammonium.

Isolation of the nitrite-specific transporter is the next most important step in resolving the nitrite uptake in plants. In order to isolate putative plant nitrite transporter, expression of a full length cDNA library from Arabidopsis roots could be performed in *Aspergillus nidulans* triple mutant (ΔnrtA-nrtB-nitA) described in Wang *et al.* (2008). This *A. nidulans* mutant is not capable of growth on minimal media with nitrite as a sole N-source. Successful transformation with Arabidopsis cDNA could recover the *A. nidulans* mutant phenotype, and colonies growing on nitrite media would be selected to isolate DNA and sequence the gene responsible for complementing the mutant phenotype.

Chapter 2

It is now well established that plants have a two-component high-affinity nitrate transporter, more specifically, NRT2.1 transporter requires and interacts with a second smaller protein NAR2 (Quesada *et al.*, 1994; Zhou *et al.*, 2000a; Tong *et al.* 2005; Okamoto *et al*., 2006; Orsel *et al.*, 2006; Wirth *et al*., 2007). By the means of Blue Native PAGE (BN-PAGE) and immunological methods I have successfully identified a PM oligomer (MW ~150 kDa), that was resolved into its component monomers of AtNRT2.1 and AtNAR2.1 (MW's ~ 48 and 26 kDa, respectively) by SDS-PAGE in the second dimension. Localization of the two-component complex consisting of AtNRT2.1 and AtNAR2.1 was confirmed by *in vivo* transient expression of split YFP-labelled AtNRT2.1 and AtNAR2.1 in Arabidopsis protoplasts. This work is at variance with several of the conclusions arrived at by Wirth *et al.* (2007) who used formaldehyde *in vivo* cross-linking and SDS-PAGE separation of proteins and their complexes to examine regulation of nitrite uptake at AtNRT2.1 protein level. In particular I have observed:

1. A novel PM complex that is made up of both AtNRT2.1 and AtNAR2.1 that is completely absent in knockout mutants *Atnrt2.1* and *Atnar2.1*.
2. A complete absence of free AtNRT2.1 in PM preparations from membrane fractions solubilized with dodecyl–β-maltoside, suggesting that AtNRT2.1 is only present in association with AtNAR2.1. As a consequence, we conclude that the 150 kDa

complex and not the monomeric form of AtNRT2.1 is the one involved in high-affinity nitrate transport.

3. No higher molecular weight forms of AtNRT2.1 (at 75 or 120 kDa) were observed when membranes were SDS-solubilized. Neither were these forms observed in the recent barley study by Ishikawa *et al.* (2009).
4. Only when SDS was used to solubilize membrane proteins, a condition that resulted in a complete separation of AtNRT2.1 and AtNAR2.1, was monomeric AtNRT2.1 observed.
5. A molecular mass of ~150 kDa suggests that the observed AtNRT2.1/AtNAR2.1 complex is a tetramer consisting of two units each of AtNRT2.1 and AtNAR2.1.
6. The 150 kDa molecular complex has a long half-life of 35 h, and is subject to posttranslational regulation of its function.

The crucial information needed to complete the story of the higher-order molecular complex of AtNRT2.1 and AtNAR2.1 is the complex structure. It would be necessary to isolate and purify sufficient amounts of the functional complex that could possibly be analyzed by X-ray crystallography. One approach could be expressing the AtNRT2.1 and AtNAR2.1 in a heterologous system such as baculovirus expression system that allows efficient expression of large amounts of polypeptides in relatively small volumes of growth media. However, a possible limitation may be incorrect folding and processing of proteins in the heterologous system which result in a non-functional complex.

Chapter 3

It was demonstrated in Chapter 2 that AtNAR2.1 is critical for the function of AtNRT2.1. The importance of AtNAR2.1 for the function of other members of the NRT2 family has been investigated. The results of the yeast two-hybrid and Arabidopsis protoplast experiments establish that all NRT2s, except AtNRT2.7, interact strongly with AtNAR2.1, while the *Xenopus* oocytes system reveals that all the NRT2 polypeptides, when co-expressed with AtNAR2.1, are capable of nitrate transport. The enhancement of $^{15}NO_3^-$ uptake by oocytes expressing AtNRT2.7 and AtNAR2.1 may appear to be contradictory to the apparent absence of interaction indicated by the yeast two-hybrid and Arabidopsis

protoplast assay. However, it is possible that the nature of the interaction between AtNRT2.7 and AtNAR2.1 precludes recognition by the methods we have presently employed.

AtNRT2.1 and AtNRT2.2 are two well characterized iHATS transporters (Cerezo *et al*., 2001; Filleur *et al*., 2001; Li *et al*., 2007). Interaction of AtNRT2.1 with AtNAR2.1 was confirmed by isolation of their molecular complex from root PM (Chapter 2). AtNRT2.7 has a role in seed nitrate accumulation (Chopin *et al.*, 2007a). Significant contribution of AtNRT2.4 to nitrate uptake in roots of N-starved plants at very low concentrations (10-25 µM nitrate) was shown by Kiba *et al*. (2012). AtNRT2.5 contributes to cHATS root transport as demonstrated in Chapter 5. Further physiological *in planta* characterization of nitrate transport by AtNRT2.3, AtNRT2.4 and AtNRT2.6 is necessary. Arabidopsis insertional mutants and/or RNA silencing of the genes could be useful tools in examining the roles of AtNRT2.3, AtNRT2.4 and AtNRT2.6 in nitrate transport. In addition, interaction of NRT2s with AtNAR2.1 should be confirmed by isolating molecular complexes, similarly to AtNRT2.1/AtNAR2.1 complex in Chapter 2. Some of the NRT2 genes are expressed at very low levels, in different tissues and growth stages, and that might hinder protein detection. To overcome this, the mutant genotypes could be complemented with cDNA of the disrupted gene tagged with an epitope oligopeptide such as V5 or myc to facilitate immuno-detection.

Chapter 4

Strong interaction between AtNRT2.1and AtNAR2.1 has been demonstrated in the yeast-two-hybrid system (Orsel *et al*., 2006; Chapter 3) and by isolation of their molecular complex (Chapter 2). Myc-tagged AtNAR2.1 could not be detected by anti-myc antibody while being associated with NRT2.1 in the complex, possibly as a result of tight interaction with NRT2.1. The exact nature of interaction and importance of certain protein regions is, however, not known. On the other hand, fungal iHATS transporter *A. nidulans* NRTA does not require other proteins to enable nitrate transport. A major difference between the plant's NRT2.1 and AnNRTA is the size of the central cytosolic loop between 6^{th} and 7^{th} TM region, where the fungal loop is 4.3 times larger than the AtNRT2.1 loop. AtNRT2.1 was modified by substituting its central loop with the *A. nidulans* central loop to obtain a chimeric protein AtNRT2.1-AnLoop. Expression of the *AtNRT2.1-AnLoop* in *A. nidulans* mutant defective in nitrate uptake, prompted WT-like nitrate influx without the presence of NAR2.1. This

finding suggests that the presence of the large cytosolic loop in fungi makes NAR2 protein unnecessary. However, when the *AtNRT2.1-AnLoop* was introduced into *Atnar2.1-2* mutant of Arabidopsis, it failed to complement the mutant phenotype and recover HATS nitrate uptake. In addition, the central loop substitution abolished the interaction of AtNRT2.1 with AtNAR2.1 in the yeast-two-hybrid system, implying the importance of the short central cytoplasmic loop of AtNRT2.1 for interaction with AtNAR2.1. A role of NAR2.1 may be to help with AtNRT2.1 folding and stabilization in the PM to realize high-affinity nitrate transport. Nevertheless, a possible direct role of AtNAR2.1 in the 150 kDa-complex for nitrate uptake cannot be excluded. A remaining puzzling question concerns the unsuccessful complementation of the Arabidopsis *nar2.1-2* mutant with *AtNRT2.1-AnLoop.* One hypothesis could be that distinct membrane properties of the examined species influence protein activity and that additional molecules exist in *A. nidulans* that help with expression/function of *AtNRT2.1-AnLoop*; molecules that are absent in Arabidopsis (and *Xenopus* oocytes).

Substitution of the *A. nidulans* NRTA central loop with the smaller AtNRT2.1 loop would help us to further explore hypothesis of the loop importance and provide explanation for the marked differences between fungal and plants central cytosolic loops. Similarly, introducing the hydrophilic portion of AtNAR2.1 instead of the large cytosolic loop of AnNRTA, might answer the question of redundancy of NAR2 in fungi.

Chapter 5

In order to adapt to fluctuating nitrate levels in soil, plants have developed low- and high-affinity transport systems that function at high and low nitrate concentration, respectively. The high affinity transport system has inducible and constitutive components. AtNRT2.1 and AtNRT2.2 are the iHATS nitrate transporters (Cerezo *et al*., 2001; Filleur *et al*., 2001; Li *et al*., 2007). Wang and Crawford (1996) isolated a chlorate-resistant Arabidopsis mutant that has impaired constitutive nitrate uptake. However, the gene coding for that cHATS transporter has not been isolated until now. I have provided evidence that *AtNRT2.5* is the cHATS transporter in roots of Arabidopsis plants that were starved of N. I have used two independent T-DNA-insertion mutants of Arabidopsis that completely lack expression of

AtNRT2.5. By characterizing expression of AtNRT2.5 and $^{13}NO_3^-$ influx in WT and mutant plants, I conclude that:

1. *AtNRT2.5* is predominantly expressed in roots of N-starved WT plants, and within a few hours down-regulated by nitrate and ammonium supply.
2. *Atnrt2.5* mutants exhibit ~60 % reduction of the high-affinity WT nitrate influx into roots of N-starved uninduced plants.
3. cHATS contributed by AtNRT2.5 (influx difference between the WT and *Atnrt2.5*-1 mutant) in uninduced plants is saturable, following a rectangular hyperbola, and has low Vmax and Km kinetics parameters, typical of cHATS transport.
4. Disruption of *AtNRT2.5* does not affect root growth of *Atnrt2.5-1* plants, but under low-N supply results in 23% reduction in shoot growth. This effect might be indirect and a consequence of lower *AtNRT2.1* expression in the *Atnrt2.5-1* mutant.
5. *AtNRT2.1* expression is significantly reduced in *Atnrt2.5-1* mutant compared to WT, and correlates well with the lower nitrate tissue concentration in the mutant. However, it is necessary to futher test the effect of AtNRT2.5 absence on AtNRT2.1 expression during the iHATS induction.
6. The remaining cHATS nitrate influx in *Atnrt2.5* mutants may be the result of contribution by the high-affinity transporters AtNRT2.1, AtNRT2.2 and AtNRT2.4, and low-affinity AtNRT1.1 and AtNRT1.2.

In summary, AtNRT2.5 contributes predominantly to the constitutive HATS and has important role in up-regulation of the inducible HATS.

Creating a double mutant between *Atnrt2.1-nrt2.2* and *Atnrt2.5-1* would provide a genotype that eliminates the contribution of the inducible system to cHATS. In addition, more specific tissue localization of the AtNRT2.5 expression should be examined by expressing a GFP-tagged protein under NRT2.5 native promoter and/or *in situ* hybridization. Similarly to the 150 kDa complex in Chapter 2, a putative molecular complex or AtNRT2.5 and AtNAR2.1 could be isolated from roots of Arabidopsis plants to complete the molecular characterization of AtNRT2.5.

Works cited

Abdel-Basset R, Ali AH (1995) Regulation of the nitrite transport system in *Chlorella fusca* Shih. et Krauss. Acta Hydrobiologica **37:** 183-189

Abramoff MD, Magalhaes PJ, Ram SJ (2004) Image Processing with ImageJ. Biophotonics International **11(7)**: 36-42

Adetunji MT (1994) Nitrogen application and underground water contamination in some agricultural soils of South-Western Nigeria. Fertilizer Res **37:** 159-163

Alonso JM, Stepanova AN, Leisse TJ, Kim SJ, Chen H, Shinn P, Stevenson DK, Zimmerman J, Barajas P, Cheuk R, et al. (2003) Genome-wide insertional mutagenesis of *Arabidopsis thaliana.* Science **301**: 653-656

Amarasinghe BH, de Bruxelles GL, Braddon M, Onyeocha I, Forde BG, Udvardi MK (1998) Regulation of GmNRT2 expression and nitrate transport activity in roots of soybean (*Glycine max*). Planta **206:** 44-52

Ames BN (1966) Assay of inorganic phosphate, total phosphate and phosphatases. In Eds. E Neufeld and V Ginsburg, Methods in Enzymology Vol 8, pp 115-118, Academic Press, New York, USA

Andrews M (1986) The partitioning of nitrate assimilation between root and shoot of higher plants. Plant Cell Environ **9:** 511-519

Araki R, Hasegawa H (2006) Expression of rice (*Oryza sativa* L.) genes involved in high-affinity nitrate transport during the period of nitrate induction. Breed Sci **56:** 295-302

Aslam M, Travis RL, Huffaker RC (1992) Comparative kinetics and reciprocal inhibition of nitrate and nitrite uptake in roots of uninduced and induced barley *Hordeum vulgare* L. seedlings. Plant Phys **99:** 1124-1133

Bancroft K, Grant IF, Alexander M (1979) Toxicity of No2 - Effect of nitrite on microbial activity in an acid soil. Appl Environ Microbiol **38:** 940-944

Behl R, Tischner R, Raschke K (1988) Induction of a high-capacity nitrate-uptake mechanism in barley roots prompted by nitrate uptake through a constitutive low-capacity mechanism. Planta **176:** 235-240

Bhattacharya J, Singh AK, Rai AN (2002) Isolation and characterization of a chlorate-resistant mutant (Clo-R) of the symbiotic cyanobacterium Nostoc ANTH: Heterocyst formation and N_2-fixation in the presence of nitrate, and evidence for separate nitrate and nitrite transport systems. Curr Microbiol **45:** 99-104

Boesch DF, Brinsfield RB, Magnien RE (2001) Chesapeake Bay eutrophication: Scientific understanding, ecosystem restoration, and challenges for agriculture. J Environ Qual **30:** 303-320

Brinkhuis BH, Renzhi L, Chaoyuan W (1989) Nitrite uptake transients and consequences for in-vivo algal nitrate reductase assays. J Phycol **25:** 539-545

Broadbent FE, Clark F (1965) Denitrification. In Eds. WV Bartholomew and FE Clark, Soil nitrogen. Agronomy 10, pp. 344-359, American Society of Agronomy, Madison, Wisconsin, USA

Burns LC, Stevens RJ, Smith RV, Cooper JE (1995) The occurrence and possible sources of nitrite in a grazed, fertilized, grassland soil. Soil Biol Biochem **27:** 47-59

Cai C, Wang J, Zhu Y, Shen Q, Li B, Tong Y, Li Z (2008) Gene structure and expression of the high-affinity nitrate transport system in rice roots. J Integr Plant Biol **50:** 443-451

Cai C, Zhao X, Zhu Y, Li B, Tong Y, Li Z (2007) Regulation of the high-affinity nitrate transport system in wheat roots by exogenous abscisic acid and glutamine. J Integr Plant Biol **49:** 1719-1725

Cameron KC, Di HJ, Moir JL (2013) Nitrogen losses from the soil/plant system: a review. Ann Appl Biol **162:** 145-173

Cataldo DA, Haroon M, Schrader LE, Youngs VL (1975) Rapid colorimetric determination of nitrate in plant tissue by nitration of salicylic acid. Commun Soil Sci Plant Anal **6:** 71-80

Cerezo M, Tillard P, Filleur S, Munos S, Daniel-Vedele F, Gojon A (2001) Major alterations of the regulation of root NO_3^- uptake are associated with the mutation of Nrt2.1 and Nrt2.2 genes in Arabidopsis. Plant Physiol **127**: 262-271

Chapman HD, Liebig GF (1952) Field and laboratory studies of nitrite accumulation in soils. Soil Sci Soc Am Proceedings **16:** 276-282

Chopin F, Orsel M, Dorbe M, Chardon F, Truong H, Miller AJ, Krapp A, Daniel-Vedele F (2007a) The Arabidopsis ATNRT2.7 nitrate transporter controls nitrate content in seeds. Plant Cell **19:** 1590-1602

Chopin F, Wirth J, Dorbe M, Lejay L, Krapp A, Gojon A, Daniel-Vedele F (2007b) The Arabidopsis nitrate transporter AtNRT2.1 is targeted to the root plasma membrane. Plant Physiology and Biochemistry **45:** 630-635

Citovsky V, Lee LY, Vyas S, Glick E, Chen MH, Vainstein A, Gafni Y, Gelvin SB, Tzfira T (2006) Subcellular localization of interacting proteins by bimolecular fluorescence complementation in planta. J Mol Biol **362:** 1120-1131

Clarkson DT, Warner AJ (1979) Relationships between root temperature and the transport of ammonium and nitrate ions by italian and perennial ryegrass (*Lolium multiflorum* and *Lolium perenne*). Plant Physiol **64:** 557-561

Clement CR, Hopper MJ, Jones LHP, Leafe EL (1978) Uptake of nitrate by *Lolium-perenne* from flowing nutrient solution .2. Effect of light, defoliation, and relationship to CO2 flux. J Exp Bot **29:** 1173-1183

Clough SJ, Bent AF (1998) Floral dip: a simplified method for Agrobacterium-mediated transformation of *Arabidopsis thaliana*. Plant J **16:** 735-743

Collos Y (1982) Transient situations in nitrate assimilation by marine diatoms .2. changes in nitrate and nitrite following a nitrate perturbation. Limnol Oceanogr **27:** 528-535

Cooper HD, Clarkson DT (1989) Cycling of amino-nitrogen and other nutrients between shoots and roots in cereals - a possible mechanism integrating shoot and root in the regulation of nutrient-uptake. J Exp Bot **40:** 753-762

Crawford NM (1995) Nitrate: nutrient and signal for plant growth. Plant Cell **7:** 859-868

Crawford NM, Glass ADM (1998) Molecular and physiological aspects of nitrate uptake in plants. Trends Plant Sci **3:** 389-395

Cresswell RC, Syrett PJ (1982) The uptake of nitrite by the diatom Phaeodactylum - interactions between nitrite and nitrate. J Exp Bot **33:** 1111-1121

Criddle RS, Ward MR, Huffaker RC (1988) Nitrogen uptake by wheat seedlings interactive effects of four nitrogen sources nitrate nitrite ammonium and urea. Plant Phys **86:** 166-175

Criscuolo G, Valkov VT, Parlati A, Alves LM, Chiurazzi M (2012) Molecular characterization of the *Lotus japonicus* NRT1(PTR) and NRT2 families. Plant Cell Environ **35:** 1567-1581

De La Haba P, Aguera E, Maldonado JM (1990) Differential effects of ammonium and tungsten on nitrate and nitrite uptake and reduction by sunflower plants. Plant Sci **70:** 21-26

Dechorgnat J, Nguyen CT, Armengaud P, Jossier M, Diatloff E, Filleur S, Daniel-Vedele F (2011) From the soil to the seeds: the long journey of nitrate in plants. J Exp Bot **62:** 1349-1359

Dechorgnat J, Patrit O, Krapp A, Fagard M, Daniel-Vedele F (2012) Characterization of the *Nrt2.6* Gene in *Arabidopsis thaliana*: a link with plant response to biotic and abiotic stress. Plos One **7:** e42491

Delhon P, Gojon A, Tillard P, Passama L (1995) Diurnal regulation of NO_3^- uptake in soybean plants .1. Changes in NO_3^- influx, efflux, and n utilization in the plant during the day-night cycle. J Exp Bot **46:** 1585-1594

Doddema H, Telkamp GP (1979) Uptake of nitrate by mutants of *Arabidopsis thaliana*, disturbed in uptake or reduction of nitrate .2. Kinetics. Physiol Plantarum **45:** 332-338

Edgar RC (2004) MUSCLE: multiple sequence alignment with high accuracy and high throughput. Nucleic Acids Res **32(5)**: 1792-1797

Ezzine M, Debouba M, Ghorbel MH, Gouia H (2011) Ion uptake and structural modifications induced by nitrogen source in tomato (*Solanum lycopersicum* Mill. Cv. Ibiza F1). Comptes Rendus Biologies **334:** 526-534

Fernandez E, Galvan A (2008) Nitrate assimilation in Chlamydomonas. Eukaryot Cell **7:** 555-559

Ferrario-Mery S, Meyer C, Hodges M (2008) Chloroplast nitrite uptake is enhanced in Arabidopsis PII mutant's. FEBS Lett **582:** 1061-1066

Filleur S, Daniel-Vedele F (1999) Expression analysis of a high-affinity nitrate transporter isolated from *Arabidopsis thaliana* by differential display. Planta **207:** 461-469

Filleur S, Dorbe MF, Cerezo M, Orsel M, Granier F, Gojon A, Daniel-Vedele F (2001) An Arabidopsis T-DNA mutant affected in Nrt2 genes is impaired in nitrate uptake. FEBS Lett **489:** 220-224

Forde BG (2000) Nitrate transporters in plants: structure, function and regulation. Biochimica Et Biophysica Acta-Biomembranes **1465:** 219-235

Gabas JM, Macarulla JM, Serra JL (1981) Characterization of nitrite uptake by the diatom *Phaeodactylum tricornutum*. Ciencia Biologica **6:** 223-226

Galvan A, Cordoba F, Cardenas J, Fernandez E (1991) Regulation of nitrite uptake and nitrite reductase expression in *Chlamydomonas reinhardtii.* Biochim Biophys Acta **1074:** 6-11

Galvan A, Quesada A, Fernandez E (1996) Nitrate and nitrite are transported by different specific transport systems and by a bispecific transporter in *Chlamydomonas reinhardtii*. J Biol Chem **271:** 2088-2092

Gansel X, Munos S, Tillard P, Gojon A (2001) Differential regulation of the NO_3^- and NH_4^+ transporter genes AtNrt2.1 and AtAmt1.1 in Arabidopsis: relation with long-distance and local controls by N status of the plant. Plant J **26:** 143-155

Gao-Rubinelli F, Marzluf GA (2004) Identification and characterization of a nitrate transporter gene in *Neurospora crassa*. Biochem Genet **42:** 21-34

Garnett T, Conn V, Plett D, Conn S, Zanghellini J, Mackenzie N, Enju A, Francis K, Holtham L, Roessner U, et al. (2013) The response of the maize nitrate transport system to nitrogen demand and supply across the lifecycle. New Phytol **198:** 82-94

Gems DH, Clutterbuck AJ (1993) Cotransformation with autonomously-replicating helper plasmids facilitates gene cloning from an *Aspergillus nidulans* gene library. Curr Genet **24:** 520-524

Girin T, Lejay L, Wirth J, Widiez T, Palenchar PM, Nazoa P, Touraine B, Gojon A, Lepetit M (2007) Identification of a 150 bp cis-acting element of the AtNRT2.1 promoter involved in the regulation of gene expression by the N and C status of the plant. Plant Cell Environ **30:** 1366-1380

Glass AD, Siddiqi MY, Ruth TJ, Rufty TW (1990) Studies of the uptake of nitrate in barley : II. Energetics. Plant Physiol **93:** 1585-1589

Glass ADM (2003) Nitrogen use efficiency of crop plants: Physiological constraints upon nitrogen absorption. Crit Rev Plant Sci **22:** 453-470

Glass ADM (2009) Nitrate uptake by plant roots. Botany **87:** 659-667

Glass ADM, Erner Y, Hunt T, Kronzucker HJ, Okamoto M, Rawat SR, Silim S, Schjoerring JK, Siddiqi MY, Vidmar JJ, et al. (1999) Inorganic nitrogen absorption by plant roots: physiology and molecular biology. In Eds. G Gissel-Nielsen and A Jensen, Plant Nutrition- Molecular Biology and Genetics, pp. 1-16, Kluwer Academic, Wageningen, Netherlands

Glass ADM, Siddiqi MY (1995) Nitrogen absorption by plant roots. In Eds. HS Srivastava and RP Singh, Nitrogen nutrition in higher plants. pp. 21-56, Associated Publishing Company, New Delhi, India

Gojon A, Nacry P, Davidian J (2009) Root uptake regulation: a central process for NPS homeostasis in plants. Curr Opin Plant Biol **12**: 328-338

Grignon C, Thibaud J-, Lamaze T (2001) Transport of nitrate by roots. In Eds. JF Morot-Gaudry Nitrogen assimilation by plants- physiological, biochemical and molecular aspects. pp. 15-32. Science Publishers INC., Enfield, NH, USA

Guo JK, Zhang ZZ, Bi YR, Yang W, Xu YN, Zhang LX (2005) Decreased stability of photosystem I in dgd1 mutant of *Arabidopsis thaliana*. FEBS Lett **579:** 3619-3624

Guy M, Zabala G, Filner P (1988) The kinetics of chlorate uptake by XD tobacco cells. Plant Physiol **86:** 817-821

Haynes RJ (1986) Mineral nitrogen in the plant-soil system. In Ed.TT Kozlowski, pp. 2-6, Academic Press Inc., Orlando, USA

Hellens R, Mullineaux P, Klee H (2000a) A guide to Agrobacterium binary Ti vectors. Trends Plant Sci **5:** 446-451

Hellens RP, Edwards EA, Leyland NR, Bean S, Mullineaux PM (2000b) pGreen: a versatile and flexible binary Ti vector for Agrobacterium-mediated plant transformation. Plant Mol Biol **42:** 819-832

Henry HAL, Jefferies RL (2002) Free amino acid, ammonium and nitrate concentrations in soil solutions of a grazed coastal marsh in relation to plant growth. Plant Cell Environ **25:** 665-675

Hill WG, Southern NM, MacIver B, Potter E, Apodaca G, Smith CP, Zeidel ML (2005) Isolation and characterization of the Xenopus oocyte plasma membrane: a new method for studying activity of water and solute transporters. Am J Phys **289:** F217-F224

Hofmockel KS, Fierer N, Colman BP, Jackson RB (2010) Amino acid abundance and proteolytic potential in North American soils. Oecologia **163:** 1069-1078

Huang NC, Liu KH, Lo HJ, Tsay YF (1999) Cloning and functional characterization of an Arabidopsis nitrate transporter gene that encodes a constitutive component of low-affinity uptake. Plant Cell **11:** 1381-1392

Ibarlucea JM, Llama MJ, Serra JL, Macarulla JM (1983) Mixed transfer kinetics of nitrite uptake in barley *Hordeum vulgare* cultivar miranda seedlings. Plant Sci Lett **29:** 339-347

Ishii S, Ikeda S, Minamisawa K, Senoo K (2011) Nitrogen cycling in rice paddy environments: past achievements and future challenges. Microbes Environ **26:** 282-292

Ishikawa S, Ito Y, Sato Y, Fukaya Y, Takahashi M, Morikawa H, Ohtake N, Ohyama T, Sueyoshi K (2009) Two-component high-affinity nitrate transport system in barley: Membrane localization, protein expression in roots and a direct protein-protein interaction. Plant Biotech **26:** 197-205

Jackson WA, Johnson RE, Volk RJ (1974a) Nitrite uptake by nitrogen depleted wheat seedlings. Physiol Plantarum **32:** 37-42

Jackson WA, Johnson RE, Volk RJ (1974b) Nitrite uptake patterns in wheat seedlings as influenced by nitrate and ammonium. Physiol Plantarum **32:** 108-114

Jia W, Cole JA (2005) Nitrate and nitrite transport in *Escherichia coli*. Biochem Soc Trans **33:** 159-161

Jia W, Tovell N, Clegg S, Trimmer M, Cole J (2009) A single channel for nitrate uptake, nitrite export and nitrite uptake by *Escherichia coli* NarU and a vole for NirC in nitrite export and uptake. Biochem J **417:** 297-304

Jones RD, Schwab AP (1993) Nitrate leaching and nitrite occurrence in a fine-textured soil. Soil Sci **155:** 272-282

Kawachi T, Sunaga Y, Ebato M, Hatanaka T, Harada H (2006) Repression of nitrate uptake by replacement of Asp105 by asparagine in AtNRT3.1 in *Arabidopsis thaliana* L. Plant Cell Phys **47:** 1437-1441

Kechid M, Desbrosses G, Rokhsi W, Varoquaux F, Djekoun A, Touraine B (2013) The NRT2.5 and NRT2.6 genes are involved in growth promotion of Arabidopsis by the plant growth-promoting rhizobacterium (PGPR) strain *Phyllobacterium brassicacearum* STM196. New Phytol **198:** 514-524

Kersey PJ, Staines DM, Lawson D, Kulesha E, Derwent P, Humphrey JC, Hughes DST, Keenan S, Kerhornou A, Koscielny G, *et al*. (2012) Ensembl Genomes: an integrative resource for genome-scale data from non-vertebrate species. Nucleic Acids Res **40**: D91-D97

Kiba T, Feria-Bourrellier A, Lafouge F, Lezhneva L, Boutet-Mercey S, Orsel M, Brehaut V, Miller A, Daniel-Vedele F, Sakakibara H, Krapp A (2012) The Arabidopsis nitrate transporter NRT2.4 plays a double role in roots and shoots of nitrogen-straved plants. Plant Cell **24:** 245-258

Kleinboelting N, Huep G, Kloetgen A, Viehoever P, Weisshaar B (2012) GABI-Kat SimpleSearch: new features of the Arabidopsis thaliana T-DNA mutant database. Nucleic Acid Res **40**: D1211-D1215

Krapp A, Fraisier V, Scheible WR, Quesada A, Gojon A, Stitt M, Caboche M, Daniel-Vedele F (1998) Expression studies of Nrt2:1Np, a putative high-affinity nitrate transporter: evidence for its role in nitrate uptake. Plant J **14:** 723-731

Kronzucker HJ, Glass ADM, Yaeesh Siddiqi M (1999) Inhibition of nitrate uptake by ammonium in barley. Analysis of component fluxes. Plant Physiol **120:** 283-292

Kronzucker HJ, Siddiqi MY, Glass ADM (1995) Kinetics of NO_3^- influx in spruce. Plant Physiol **109:** 319-326

Krouk G, Mirowski P, LeCun Y, Shasha DE, Coruzzi GM (2010) Predictive network modeling of the high-resolution dynamic plant transcriptome in response to nitrate. Genome Biol **11:** R123

Laine P, Ourry A, Boucaud J, Salette J (1998) Effects of a localized supply of nitrate on NO_3^- uptake rate and growth of roots in *Lolium multiflorum Lam*. Plant Soil **202:** 61-67

Laugier E, Bouguyon E, Mauriès A, Tillard P, Gojon A, Lejay L (2012) Regulation of high-affinity nitrate uptake in roots of Arabidopsis depends predominantly on posttranscriptional control of the NRT2.1-NAR2.1 transport system. Plant Phys **158**: 1067-1078

Law CJ, Maloney PC, Wang D (2008) Ins and Outs of Major Facilitator Superfamily, antiporters. Annu Rev Microbiol **62:** 289-305

Lea PJ, Robinson SA, Stewart GR (1990) The enzymology and metabolism of glutamine, glutamate, and asparagine. In Eds. BJ Miflin and PJ Lea, The Biochemistry of Plants Vol 16: Intermediary Metabolism pp. 121-157, Academic Press, San Diego, USA

Lee RB (1979) Effect of nitrite on root-growth of barley and maize. New Phytol **83:** 615-622

Lee RB, Purves JV, Ratcliffe RG, Saker LR (1992) Nitrogen assimilation and the control of ammonium and nitrate absorption by maize roots. J Exp Bot **43:** 1385-1396

Lee RB, Rudge KA (1986) Effects of nitrogen deficiency on the absorption of nitrate and ammonium by barley plants. Ann Botany **57:** 471-486

Lee R, Drew M (1989) Rapid, Reversible Inhibition of Nitrate Influx in Barley by Ammonium. J Exp Bot **40:** 741-752

Lejay L, Gansel X, Cerezo M, Tillard P, Muller C, Krapp A, von Wiren N, Daniel-Vedele F, Gojon A (2003) Regulation of root ion transporters by photosynthesis: Functional importance and relation with hexokinase. Plant Cell 15: 2218-2232

Lejay L, Tillard P, Lepetit M, Olive FD, Filleur S, Daniel-Vedele F, Gojon A (1999) Molecular and functional regulation of two NO_3^- uptake systems by N- and C-status of Arabidopsis plants. Plant J **18**: 509-519

Leonard RT, Hodges TK (1973) Characterization of plasma membrane-associated adenosine-triphosphatase activity of oat roots. Plant Physiol **52:** 6-12

Li W, Wang Y, Okamoto M, Crawford NM, Siddiqi MY, Glass ADM (2007) Dissection of the AtNRT2.1:AtNRT2.2 inducible high-affinity nitrate transporter gene cluster. Plant Physiol **143:** 425-433

Liman ER, Tytgat J, Hess P (1992) Subunit stoichiometry of a mammalian K+ channel determined by construction of multimeric cDNAs. Neuron **9:** 861-871

Liu KH, Huang CY, Tsay YF (1999) CHL1 is a dual-affinity nitrate transporter of Arabidopsis involved in multiple phases of nitrate uptake. Plant Cell **11**: 865-874

Liu X, Zhang F (2011) Nitrogen fertilizer induced greenhouse gas emissions in China. Curr Opinion Environ Sustainability **3:** 407-413

Lomas MW, Lipschultz F (2006) Forming the primary nitrite maximum: Nitrifiers or phytoplankton? Limnol Oceanogr **51:** 2453-2467

Lopez Pasquali CE, Fernandez Hernando P, Durand Alegria JS (2007) Spectrophotometric simultaneous determination of nitrite, nitrate and ammonium in soils by flow injection analysis. Anal Chim Acta **600:** 177-82

Mariscal V, Rexach J, Fernandez E, Galvan A (2004) The plastidic nitrite transporter NAR1;1 improves nitrate use efficiency for growth in Chlamydomonas. Plant Cell Environ **27:** 1321-1328

Masek T, Vopalensky V, Suchomelova P, Pospisek M (2005) Denaturing RNA electrophoresis in TAE agarose gels. Anal Biochem **336:** 46-50

Mcelfresh MW, Meeks JC, Parks NJ (1979) Synthesis of N-13-labeled nitrite of high specific activity and purity. J Radioanalytical Chem **53:** 337-344

McFarlane HE, Shin JJ, Bird DA, Samuels AL (2010) Arabidopsis ABCG transporters, which are required for export of diverse cuticular lipids, dimerize in different combinations. Plant Cell **22**: 3066-3075

Meeder E, Mackey KRM, Paytan A, Shaked Y, Iluz D, Stambler N, Rivlin T, Post AF, Lazar B (2012) Nitrite dynamics in the open ocean - clues from seasonal and diurnal variations. Mar Ecol Prog Ser **453:** 11-26

Meijering E, Jacob M, Sarria JCF, Steiner P, Hirling H, Unser M (2004) Design and validation of a tool for neurite tracing and analysis in fluorescence microscopy images. Cytometry **58A:** 167-176

Metcalfe RJ, Nault J, Hawkins BJ (2011) Adaptations to nitrogen form: comparing inorganic nitrogen and amino acid availability and uptake by four temperate forest plants. Canadian J Forest Res **41:** 1626-1637

Miller A, Smith S, Fan X, Shen Q (2007) Expression and functional analysis of rice NRT2 nitrate transporters. Comparative Biochemistry and Physiology A-Molecular & Integrative Physiology **146:** S241-S241

Miller AJ, Shen Q, Xu G (2009) Freeways in the plant: transporters for N, P and S and their regulation. Curr Opin Plant Biol **12:** 284-290

Morard P, Silvestre J, Lacoste L, Caumes E, Lamaze T (2004) Nitrate uptake and nitrite release by tomato roots in response to anoxia. J Plant Physiol **161:** 855-865

Muller B, Touraine B (1992) Inhibition of NO_3^- uptake by various phloem-translocated amino-acids in soybean seedlings. J Exp Bot **43:** 617-623

Nadelhoffer KJ, Giblin AE, Shaver GR, Linkins AE (1992) Microbial Processes and Plant Nutrient Availability in Arctic Soils. In Eds. FS Chapin, RL Jefferies, JF Reynolds, GR Shaver and J Svoboda, Arctic Ecosystems in a Changing Climate. An Ecophysiological Perspective. pp 281-300, Academic Press Inc., San Diego, CA, USA

Navarro FJ, Machin F, Martin Y, Siverio JM (2006) Down-regulation of eukaryotic nitrate transporter by nitrogen-dependent ubiquitinylation. J Biol Chem **281:** 13268-13274

Nazoa P, Vidmar JJ, Tranbarger TJ, Mouline K, Damiani I, Tillard P, Zhuo D, Glass ADM, Touraine B (2003) Regulation of the nitrate transporter gene AtNRT2.1 in *Arabidopsis thaliana*: responses to nitrate, amino acids and developmental stage. Plant Mol Biol **52:** 689-703

Okamoto M, Kumar A, Li W, Wang Y, Siddiqi MY, Crawford NM, Glass ADM (2006) High-affinity nitrate transport in roots of Arabidopsis depends on expression of the NAR2-like gene AtNRT3.1. Plant Physiol **140:** 1036-1046

Okamoto M, Vidmar JJ, Glass ADM (2003) Regulation of NRT1 and NRT2 gene families of *Arabidopsis thaliana:* responses to nitrate provision. Plant Cell Physiol **44:** 304-317

Ono F, Frommer WB, von Wiren N (2000) Coordinated diurnal regulation of low- and high-affinity nitrate transporters in tomato. Plant Biol **2:** 17-23

Orsel M, Chopin F, Leleu O, Smith SJ, Krapp A, Daniel-Vedele F, Miller AJ (2006) Characterization of a two-component high-affinity nitrate uptake system in Arabidopsis. Physiology and protein-protein interaction. Plant Physiol **142:** 1304-1317

Orsel M, Eulenburg K, Krapp A, Daniel-Vedele F (2004) Disruption of the nitrate transporter genes AtNRT2.1 and AtNRT2.2 restricts growth at low external nitrate concentration. Planta **219:** 714-721

Orsel M, Krapp A, Daniel-Vedele F (2002) Analysis of the NRT2 nitrate transporter family in Arabidopsis. Structure and gene expression. Plant Physiol **129:** 886-896

Pfaffl MW (2001) A new mathematical model for relative quantification in real-time RT-PCR. Nucleic Acids Res **29:** 2003-2007

Phipps RH, Cornforth IS (1970) Factors Effecting the Toxicity of Nitrite Nitrogen to Tomatoes-D. Plant Soil **33:** 457-466

Plett D, Toubia J, Garnett T, Tester M, Kaiser BN, Baumann U (2010) Dichotomy in the nrt gene families of dicots and grass species. Plos One **5 (12):** e15289

Punt P, Greaves P, Kuyvenhoven A, Vandeutekom J, Kinghorn J, Pouwels P, Vandenhondel C (1991) A Twin-reporter vector for simultaneous analysis of expression signals of divergently transcribed, contiguous genes in filamentous fungi. Gene **104:** 119-122

Quesada A, Galvan A, Fernandez E (1994) Identification of nitrate transporter genes in *Chlamydomonas reinhardtii*. Plant J **5:** 407-419

Quesada A, Krapp A, Trueman LJ, Daniel-Vedele F, Fernandez E, Forde BG, Caboche M (1997) PCR-identification of a *Nicotiana plumbaginifolia* cDNA homologous to the high-affinity nitrate transporters of the crnA family. Plant Mol Biol **34:** 265-274

Rasmussen R (2001) Quantification on the LightCycler. In Eds. S Meuer, C Wittwer and KI Nakagawara Rapid cycle real-time PCR: methods and applications. pp. 21-34, Springer-Verlag, Berlin, Germany

Remans T, Nacry P, Pervent M, Girin T, Tillard P, Lepetit M, Gojon A (2006) A central role for the nitrate transporter NRT2.1 in the integrated morphological and physiological responses of the root system to nitrogen limitation in Arabidopsis. Plant Physiol **140**: 909-921

Rexach J, Fernandez E, Galvan A (2000) The *Chlamydomonas reinhardtii* Nar1 gene encodes a chloroplast membrane protein involved in nitrite transport. Plant Cell **12:** 1441-1453

Rexach J, Montero B, Fernandez E, Galvan A (1999) Differential regulation of the high affinity nitrite transport systems III and IV in *Chlamydomonas reinhardtii*. J Biol Chem **274:** 27801-27806

Riach MBR, Kinghorn JR (1996) Genetic transformation and vector developments in filamentous fungi. In Eds. JB Cees Fungal genetics: principles and practice vol. 13. pp. 209-233, Marcel Dekker INC., New York, USA

Riley WJ, Ortiz-Monasterio I, Matson PA (2001) Nitrogen leaching and soil nitrate, nitrite, and ammonium levels under irrigated wheat in Northern Mexico. Nutr Cycling Agroecosyst **61:** 223-236

Rodgers CO, Barneix AJ (1993) The effect of amino-acids and amides on the regulation of nitrate uptake by wheat seedlings. J Plant Nutr **16:** 337-348

Rouse JD, Bishop CA, Struger J (1999) Nitrogen pollution: An assessment of its threat to amphibian survival. Environ Health Perspect **107:** 799-803

Sahrawat KL (2005) Fertility and organic matter in submerged rice soils. Curr Sci **88:** 735-739

Saier MH,Jr, Beatty JT, Goffeau A, Harley KT, Heijne WH, Huang SC, Jack DL, Jahn PS, Lew K, Liu J, Pao SS, Paulsen IT, Tseng TT, Virk PS (1999) The major facilitator superfamily. J Mol Microbiol Biotechnol **1:** 257-279

Samater AH, Van Cleemput O, Ertebo T (1998) Influence of the presence of nitrite and nitrate in soil on maize biomass production, nitrogen immobilization and nitrogen recovery. Biol Fertility Soils **27:** 211-218

Santoni, V (2007) Plant plasma membrane protein extraction and solubilization for proteomic analysis. In Eds. H Thiellement, M Zivy C, Damerval and V Méchin, Methods in Molecular Biology, Vol 335, pp. 93-109, Humana Press Inc., Totowa, NJ,USA

Schagger H, Cramer WA, Vonjagow G (1994) Analysis of molecular masses and oligomeric states of protein complexes by blue native electrophoresis and isolation of membrane-protein complexes by 2-dimensional native electrophoresis. Anal Biochem **217:** 220-230

Schimel JP, Chapin FS (1996) Tundra plant uptake of amino acid and NH_4^+ nitrogen in situ: Plants compete well for amino acid N. Ecology **77:** 2142-2147

Schloemer RH, Garrett RH (1974) Uptake of nitrite by *Neurospora-crassa*. J Bacteriol **118:** 270-274

Scholl RL, May ST, Ware DH (2000) Seed and molecular resources for Arabidopsis. Plant Physiol **124(4)**: 1477-80

Serrani F, Berardi E (2005) The NII2 gene of *Hansenula polymorpha* is involved in nitrite assimilation. Fems Yeast Research **5:** 999-1007

Siddiqi MY, Glass ADM, Ruth TJ, Fernando M (1989) Studies of the regulation of nitrate influx by barley seedlings using NO(3). Plant Physiol **90:** 806-813

Siddiqi MY, Glass ADM, Ruth TJ, Rufty TW (1990) Studies of the uptake of nitrate in barley: I. Kinetics of NO(3) influx. Plant Physiol **93:** 1426-1432

Siddiqi MY, King BJ, Glass ADM (1992) Effects of nitrite, chlorate, and chlorite on nitrate uptake and nitrate reductase activity. Plant Phys **100:** 644-650

Sivasubramanian V, Rao VNR (1988) Uptake and assimilation of nitrogen by marine diatoms i. kinetics of nitrogen uptake. Proceedings of the Indian Academy of Sciences **98:** 71-88

Spyropoulos IC, Liakopoulos TD, Bagos PG, Hamodrakas SJ (2004) TMRPres2D: high quality visual representation of transmembrane protein models. Bioinformatics **20:** 3258-3260

Sugiura M, Georgescu MN, Takahashi M (2007) A nitrite transporter associated with nitrite uptake by higher plant chloroplasts. Plant Cell Phys **48:** 1022-1035

Sustiprijatno, Sugiura M, Ogawa K, Takahashi M (2006) Improvement of nitrate- and nitrite-dependent growth of rice by the introduction of a constitutively expressing chloroplastic nitrite transporter. Plant Biotech J **23**: 47-54

Tiwari S, Wang S, Hagen G, Guilfoyle TJ (2006) Transfection assays with protoplasts containing integrated reporter genes. Methods Mol Biol **323:** 237-244

Tong Y, Zhou JJ, Li Z, Miller AJ (2005) A two-component high-affinity nitrate uptake system in barley. Plant J **41:** 442-450

Touraine B, Gojon A (2001) Integration of nitrate uptake in the whole plant. In Eds. JF Morot-Gaudry Nitrogen assimilation by plants- physiological, biochemical and molecular aspects. pp. 95-114. Science Publishers INC., Enfield, NH, USA

Touraine B, Glass ADM (1997) NO_3^- and ClO_3^- fluxes in the chl1-5 mutant of *Arabidopsis thaliana*. Does the CHL1-5 gene encode a low-affinity NO_3^- transporter? Plant Phys **114:** 137-144

Trueman LJ, Richardson A, Forde BG (1996) Molecular cloning of higher plant homologues of the high-affinity nitrate transporters of *Chlamydomonas reinhardtii* and *Aspergillus nidulans.* Gene **175:** 223-231

Tsay YF, Schroeder JI, Feldmann KA, Crawford NM (1993) The herbicide sensitivity gene CHL1 of Arabidopsis encodes a nitrate-inducible nitrate transporter. Cell **72:** 705-713

Tsujimoto R, Yamazaki H, Maeda S, Omata T (2007) Distinct roles of nitrate and nitrite in regulation of expression of the nitrate transport genes in the moss *Physcomitrella patens.* Plant Cell Physiol **48:** 484-497

Tusnady GE, Simon I (2001) The HMMTOP transmembrane topology prediction server. Bioinformatics **17:** 849-850

Tusnady GE, Simon I (1998) Principles governing amino acid composition of integral membrane proteins: Application to topology prediction. J Mol Biol **283:** 489-506

Unkles SE, Hawker KL, Grieve C, Campbell EI, Montague P, Kinghorn JR (1991) crnA encodes a nitrate transporter in *Aspergillus nidulans*. Proc Natl Acad Sci **88:** 204-208

Unkles SE, Rouch DA, Wang Y, Siddiqi MY, Okamoto M, Stephenson RM, Kinghorn JR, Glass ADM (2005) Determination of the essentiality of the eight cysteine residues of the NrtA protein for high-affinity nitrate transport and the generation of a functional cysteine-less transporter. Biochemistry **44:** 5471-5477

Unkles SE, Wang R, Wang Y, Glass ADM, Crawford NM, Kinghorn JR (2004) Nitrate reductase activity is required for nitrate uptake into fungal but not plant cells. J Biol Chem **279:** 28182-28186

Unkles SE, Zhou D, Siddiqi MY, Kinghorn JR, Glass ADM (2001) Apparent genetic redundancy facilitates ecological plasticity for nitrate transport. EMBO J **20:** 6246-6255

Unkles SE, Symington VF, Kotur Z, Wang Y, Siddiqi MY, Kinghorn JR, Glass ADM (2011) Physiological and biochemical characterization of AnNitA, the *Aspergillus nidulans* high-affinity nitrite transporter. Eukaryot Cell **10:** 1724-1732

Uwah EI, Ndahi NP, Abdulrahaman FI, Ogugbuaja VO (2009) Measurement of nitrate and nitrite contents in soils and some leguminous vegetables cultivated in Maiduguri, Nigeria. World J Agricultural Sci **5:** 881-887

Vidmar JJ, Zhuo D, Siddiqi MY, Schjoerring JK, Touraine B, Glass ADM (2000) Regulation of high-affinity nitrate transporter genes and high-affinity nitrate influx by nitrogen pools in roots of barley. Plant Physiol **123:** 307-318

Wang RC, Crawford NM (1996) Genetic identification of a gene involved in constitutive, high-affinity nitrate transport in higher plants. Proc Natl Acad Sci **93:** 9297-9301

Wang R, Xing X, Crawford N (2007) Nitrite acts as a transcriptome signal at micromolar concentrations in Arabidopsis roots. Plant Physiol **145:** 1735-1745

Wang Y, Li W, Siddiqi Y, Kinghorn JR, Unkles SE, Glass ADM (2007) Evidence for post-translational regulation of NrtA, the *Aspergillus nidulans* high-affinity nitrate transporter. New Phytol **175:** 699-706

Wang Y, Li W, Siddiqi Y, Symington VF, Kinghorn JR, Unkles SE, Glass ADM (2008) Nitrite transport is mediated by the nitrite-specific high-affinity NitA transporter and by nitrate transporters NrtA, NrtB in *Aspergillus nidulans*. Fungal Genet Biol **45:** 94-102

Wang Y, Hsu P, Tsay Y (2012) Uptake, allocation and signaling of nitrate. Trends Plant Sci **17:** 458-467

Warrens A, Jones M, Lechler R (1997) Splicing by overlap extension by PCR using asymmetric amplification: An improved technique for the generation of hybrid proteins of immunological interest. Gene **186:** 29-35

Wirth J, Chopin F, Santoni V, Viennois G, Tillard P, Krapp A, Lejay L, Daniel-Vedele F, Gojon A (2007) Regulation of root nitrate uptake at the NRT2.1 protein level in *Arabidopsis thaliana*. J Biol Chem **282:** 23541-23552

Wolt JD (1994) Soil solution chemistry: applications to environmental science and agriculture. Wiley, New York, USA

Yamaoka T (1998) Pore gradient gel electrophoresis: theory, practice, and applications. Anal Chim Acta **372:** 91-98

Yamaoka T, Yamashita K, Itakura M (1993) Determination of the number and relative molecular mass of subunits in an oligomeric protein by 2-dimensional electrophoresis - application to the subunit structure-analysis of rat-liver amidophosphoribosyltransferase. J Chromatogr **630:** 345-351

Yan M, Fan X, Feng H, Miller AJ, Shen Q, Xu G (2011) Rice OsNAR2.1 interacts with OsNRT2.1, OsNRT2.2 and OsNRT2.3a nitrate transporters to provide uptake over high and low concentration ranges. Plant Cell Environ **34:** 1360-1372

Yang YY, Li XH, Ratcliffe RG, Ruan JY (2013) Characterization of ammonium and nitrate uptake and assimilation in roots of tea plants. Russ J Plant Phys **60:** 91-99

Yin L, Li P, Wen B, Taylor D, Berry JO (2007) Characterization and expression of a high-affinity nitrate system transporter gene (TaNRT2.1) from wheat roots, and its evolutionary relationship to other NTR2 genes. Plant Sci **172:** 621-631

Zentmyer G, Bingham F (1956) The Influence of nitrite on the development of phytophthora root rot of avocado. Phytopathology **46:** 121-124

Zhao XQ, Li YJ, Liu JZ, Li B, Liu QY, Tong YP, Li JY, Li ZS (2004) Isolation and expression analysis of a high-affinity nitrate transporter TaNRT2.3 from roots of wheat. Acta Botanica Sinica **46:** 347-354

Zhou JJ, Fernandez E, Galvan A, Miller AJ (2000a) A high affinity nitrate transport system from Chlamydomonas requires two gene products. FEBS Lett **466:** 225-227

Zhou JJ, Trueman LJ, Boorer KJ, Theodoulou FL, Forde BG, Miller AJ (2000b) A high affinity fungal nitrate carrier with two transport mechanisms. J Biol Chem **275:** 39894-39899

Zhuo D, Okamoto M, Vidmar JJ, Glass ADM (1999) Regulation of a putative high-affinity nitrate transporter (Nrt2;1At) in roots of *Arabidopsis thaliana*. Plant J **17:** 563-568

Zsoldos F, Vashegyi A, Pecsvaradi A, Haunold E, Herger P (1995) Effects of nitrite and nitrate on potassium uptake of rice and wheat seedlings at different pH values. Acta Phytopathol Entomol Hung **30:** 93-97

Zsoldos F, Vashegyi A, Pecsvaradi A, Bona L (2001) Growth and potassium transport in common and durum wheat as affected by aluminum and nitrite stress. J Plant Nutr **24:** 345-356

Zsoldos F, Haunold E, Vashegyi A, Herger P (1993) Nitrite in the root zone and its effects on ion uptake and growth of wheat seedlings. Physiol Plantarum **89:** 626-631

Appendices

Appendix A

Primer sequences

Table 1A. Oligonucleotide primer sequences with gene-specific sequences underlined, used for cloning into split-YFP expression vectors.

Primer Name	**Primer Sequence (5' → 3' direction)**
AtNAR2.1 Forward	ATTCTAGAAAAAATGGCGATCCAGAAGATCC
AtNAR2.1 Reverse	GTAGGCCTGTTTTGCTTTGCTCTATCTTGGC
AtNRT2.1 Forward	CTGGATCCATGGGTGATTCTACTGGTGAGC
AtNRT2.1 Reverse	ATGAATTCTCAAACATTGTTGGGTGTGTTC

Table 2A. Oligonucleotide primer sequences used in real-time PCR reactions.

Primer Name	**Primer Sequence (5' → 3' direction)**
AtNRT2.1 Forward	TAACGCAGTTGCTCATGCCCATTG
AtNRT2.1 Reverse	TTTGTCTTTGGCAACTTCTCCGCGC
AtNAR2.1 Forward	AGATCCTCTTTGCTTCACTTCTC
AtNAR2.1 Reverse	GCGTCCATGTAATGTTCAACG
ACTIN 2 Forward	ACACTGTGCCAATCTACGAGGGTT
ACTIN 2 Reverse	ACAATTTCCCGCTCTGCTGTTGTG

Table 3A. Oligonucleotide primer sequences with gene-specific sequences highlighted in gray used for cloning into Y-2-H bait and prey vectors.

Primer Name	**Primer Sequence (5' → 3' direction)**
AtNAR2.1 Forward	ATTCTAGAAAAAATGGCGATCCAGAAGATCC
AtNAR2.1 Reverse	GTAGGCCTGTTTTGCTTTGCTCTATCTTGGC
AtNRT2.1 Forward	CTGGATCCATGGGTGATTCTACTGGTGAGC
AtNRT2.1 Reverse	ATGAATTCTCAAACATTGTTGGGTGTGTTC
AtNRT2.2 Forward	ATGGATCCATGGGTTCTACTGATGAGCCC
AtNRT2.2 Reverse	ACGAATTCAAAGCAAATGATGAAAGAAATGGT
AtNRT2.3 Forward	ATGGATCCATGACTCACAACCATTCTAATGAAGA
AtNRT2.3 Reverse	ACGAATTCTCAAACATGACTTGGAGTTCCG
AtNRT2.4 Forward	ATGGATCCATGGCCGATGGTTTTGGT
AtNRT2.4 Reverse	ACGAATTCTTAAACGTGTTCCGGCGG
AtNRT2.5 Forward	ATGGATCCATGGAGGTCGAAGGCAAAG
AtNRT2.5 Reverse	ACGAATTCTCAAGTTTGGGGATGAGTCG
AtNRT2.6 Forward	ATGGATCCATGGCTCACAACCATTCTAATGA
AtNRT2.6 Reverse	ACGAATTCCTAGACATGAGCCGGAGATCC
AtNRT2.7 Forward	ATGGATCCATGGAGCCATCTCAACGC
AtNRT2.7 Reverse	ATATCGATACAAACGGGACGTAGACTACC

Table 4A. Oligonucleotide primer sequences containing attB1/attB2 Gateway® recombination sites and gene-specific sequences highlighted in gray, used for cloning into Gateway® pDONR221 donor vector.

Primer Name	**Primer Sequence (5' → 3' direction)**
AtNAR2.1 F	GGGGACAAGTTTGTACAAAAAAGCAGGCTAGATTCAAGGATATATCCATGGC
AtNAR2.1 R	GGGGACCACTTTGTACAAGAAAGCTGGGTGTTCCATATCAATGGCTTAATTGTAC
AtNRT2.1 F	GGGGACAAGTTTGTACAAAAAAGCAGGCTCAATGGGTGATTCTACTGGTGA
AtNRT2.1 R	GGGGACCACTTTGTACAAGAAAGCTGGGTCTTATATGCGATCATCCTTCACC
AtNRT2.2 F	GGGGACAAGTTTGTACAAAAAAGCAGGCTCTTGAATTTTCTCAAAGGAACTTGA
AtNRT2.2 R	GGGGACCACTTTGTACAAGAAAGCTGGGTAAAGCAAATGATGAAAGAAATGGT
AtNRT2.3 F	GGGGACAAGTTTGTACAAAAAAGCAGGCTATGACTCACAACCATTCTAATGAAG
AtNRT2.3 R	GGGGACCACTTTGTACAAGAAAGCTGGGTTCAAACATGACTTGGAGTTCC
AtNRT2.4 F	GGGGACAAGTTTGTACAAAAAAGCAGGCTATGGCCGATGGTTTTGGT
AtNRT2.4 R	GGGGACCACTTTGTACAAGAAAGCTGGGTTTAAACGTGTTCCGGCGG
AtNRT2.5 F	GGGGACAAGTTTGTACAAAAAAGCAGGCTATGGAGGTCGAAGGCAAAG
AtNRT2.5 R	GGGGACCACTTTGTACAAGAAAGCTGGGTATACGTTTGTTCATTCCATGATGA
AtNRT2.6 F	GGGGACAAGTTTGTACAAAAAAGCAGGCTCAAAGGCCACAAAGAAGAAGA
AtNRT2.6 R	GGGGACCACTTTGTACAAGAAAGCTGGGTAGGATCTTACTCGGTACATCTCTCA
AtNRT2.7 F	GGGGACAAGTTTGTACAAAAAAGCAGGCTGATAATGTTCATTGATTGGGTGG
AtNRT2.7 R	GGGGACCACTTTGTACAAGAAAGCTGGGTTGGGCCAGCAGTTCAAAT

Table 5A. Oligonucleotide primer sequences with gene-specific sequences underlined, used for cloning into split-YFP expression vectors.

Primer Name	**Primer Sequence (5' → 3' direction)**
AtNRT2.2 Forward	ATCTCGAGATGGGTTCTACTGATGAGCCC
AtNRT2.2 Reverse	ATGGATCCCAGCATTGTTGGTTGCGTTC
AtNRT2.3 Forward	ATCTCGAGATGACTCACAACCATTCTAATGAAG
AtNRT2.3 Reverse	ATGGATCCCAACATGACTTGGAGTTCCGTTC
AtNRT2.4 Forward	ACGAATTCATGGCCGATGGTTTTGGT
AtNRT2.4 Reverse	ATGGTACCCAACGTGTTCCGGCGGAG
AtNRT2.5 Forward	ATCTCGAGATGGAGGTCGAAGGCAAAG
AtNRT2.5 Reverse	ATGGATCCCAGTTTGGGGATGAGTCGTTG
AtNRT2.6 Forward	ACGAATTCATGGCTCACAACCATTCTAATG
AtNRT2.6 Reverse	ATGGTACCCGACATGAGCCGGAGATCC
AtNRT2.7 Forward	ACCTCGAGATGGAGCCATCTCAACGC
AtNRT2.7 Reverse	ATGGATCCCACAAACGGGACGTAGACTACCA

Table 6A. Oligonucleotide primer sequences used in the real-time PCR reactions

Primer Name	**Primer Sequence (5' → 3' direction)**
AtNRT2.2 Forward	TCATGGGAATCTTGGTGCTC
AtNRT2.2 Reverse	GTCCTGTAATTTGTAACGGCG
AtNRT2.3 Forward	ACTATCAACAACGTTATCTCCGG
AtNRT2.3 Reverse	GCTACATCAGAAGCGTAACCA
AtNRT2.4 Forward	AGCTCACAACCGATAACGTC
AtNRT2.4 Reverse	AATATCTGAGGCCCAACCAC
AtNRT2.5 Forward	TCATGCCCATCGTGTTCTC
AtNRT2.5 Reverse	CCACATCATCTTTCTCCCTCTC
AtNRT2.6 Forward	CTTCATCCCCGGCATTCTT
AtNRT2.6 Reverse	CACAGCGAACCAAAAGACC
AtNRT2.7 Forward	AGAGATTCGGTATGAGAGGGAG
AtNRT2.7 Reverse	GCAGCTTGAACGAAAACAGAG
AtNRT1.1 Forward	CGGAAGGTTCGATGAAGGG
AtNRT1.1 Reverse	TGTTAGTGTTGAGAGTGTCCAC
AtNRT1.2 Forward	CTTCCTCATCTCAGCTTCCATC
AtNRT1.2 Reverse	ACAACCCCACGAATAGCATC

Appendix B

Chapter 2- Solution/ buffer recipes for protoplast isolation and transfection

Cellulase-macerozyme solution: 1% w/v Cellulase R10, 0.25% w/v Macerozyme R10, 400 mM mannitol, 10 mM $CaCl_2$, 5 mM MES (2-[N-morpholino]ethanesulfonic acid). Adjust to pH 5.7 with 1 M KOH; filter-sterilize (0.45 µm cellulose acetate). Store at 4°C.

Mg-mannitol solution: 400 mM mannitol, 15 mM $MgCl_2$, 4 mM MES. Adjust to pH 5.7 with 1 M KOH; filter-sterilize (0.22 µm cellulose acetate). Store at 4°C.

W5 solution: 154 mM NaCl, 5 mM KCl, 125 mM $CaCl_2$, 5 mM glucose. Filter-sterilize (0.22 µm cellulose acetate) and store at room temperature.

40% PEG (polyethylene glycol) solution: Make 500 mL Ca-mannitol solution (100 mM $CaNO_3$, 400 mM mannitol). Add 160 g of PEG (avg. mol. wt. 3350) to 280 mL of Ca-mannitol solution. Warm the solution on a stirring plate until the solution is clear. Adjust the pH to 10.0 by 1 M KOH. Make up volume to 400 mL with Ca-mannitol solution. Filter-sterilize (0.45 µm membrane); store at –20°C.

WI solution: 500 mM mannitol, 20 mM KCl, 4 mM MES. Adjust to pH 5.7 with 1 M KOH. Filter-sterilize (0.22 µm cellulose acetate). Store at 4°C.

Chapter 4- *Aspergillus* medium recipes

Complete medium (1 litre)

Glucose	10 g
Peptone	2g
Yeast extract	1g
1000X Vitamin stock (pppb)	1ml
1000X Trace elements stock	1ml
KCl	1.3g
$MgSO_4$ $7H_2O$	1.3g

KH_2PO_4 3.8g

Casamino acids 1g

Adjust pH 6.5 with 5M KOH, autoclave (for solid medium, add 1.2% agar)

Minimal Medium (1 litre)

Glucose 10g

1000X Trace elements 1ml

KCl 1.3g

$MgSO_4$ $7H_2O$ 1.3g

KH_2PO_4 3.8g

Adjust pH 6.5 with 5M KOH, autoclave (for solid medium, add 1.2% agar)

1000 X Trace elements

$MnCl_4$ H_2O 0.4g

$ZnSO_4$ 1.0g

$CuSO_4$ x $5H_2O$ 0.5g

Na_2MoO_4 x $2H_2O$ 1.1g

$CoCl_2$ x $6H_2O$ 0.5g

$FeSO_4$ x $7H_2O$ 0.5

HBO_3 1.0g

Citric acid 3.72g

Adjust pH to 6.5 with 5M KOH, make up to 1 liter, store in dark bottle at 4^oC

1000X Vitamin Stock (pppb)

P-aminobenzoic acid 100mg

Pyrodoxin HCl 500mg

Pantothenic acid 200mg

Biotin 200mg

Make up to 1 litre, store in dark bottle at 4^oC. Shake well before use, filter sterilize before adding to sterile medium.

Chapter 4- *Aspergillus* transformation solutions and buffers recipes

OSMO

1.2 M $MgSO_4$

10 mM sodium phosphate pH 7.0

Adjust to pH 5.8 with 0.2. M Na_2HPO_4, filter sterilize, and store in 100-ml aliquots.

STC

1.2 M sorbitol

10 mM Tris-HCl pH 7.5

10 mM $CaCl_{2.}$ Sterilize by autoclaving.

Trapping buffer

0.6 M sorbitol

100 mM Tris-Hcl pH 7.0. Sterilize by autoclaving.

Appendix C

Real-time PCR cycling conditions

1. Incubate at 95°C for 00:03:00
2. Incubate at 94°C for 00:00:10
3. Incubate at 56°C for 00:00:10
4. Incubate at 72°C for 00:00:20
5. Plate read
6. Repeat 39 more cycles
7. Melting Curve from 55°C to 95°C, read every 0.3°C, hold 00:00:01
8. END